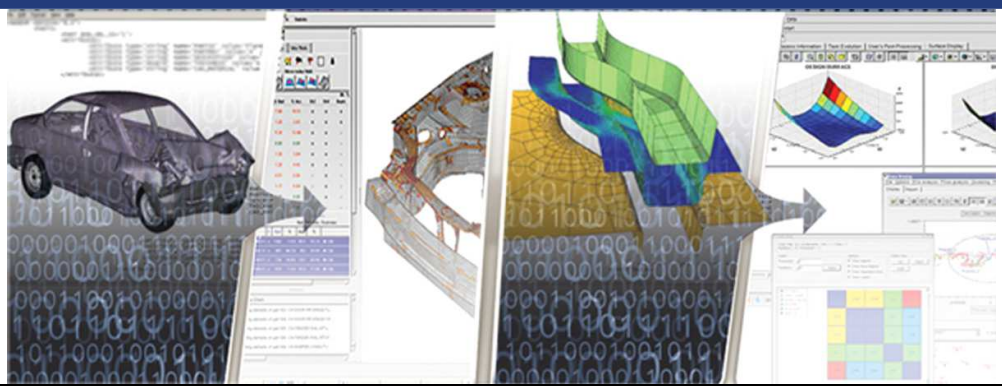

RADIOSS THEORY MANUAL

Version 2017 – January 2017

Large Displacement Finite Element Analysis

PART 2

F

Altair Engineering, Inc., World Headquarters: 1820 E. Big Beaver Rd., Troy MI 48083-2031 USA
Phone: +1.248.614.2400 • Fax: +1.248.614.2411 • www.altair.com • info@altair.com

CONTENTS

Chapter 9

MATERIALS

9.0 MATERIAL LAWS

A large variety of materials is used in the structural components and must be modeled in stress analysis problems. For any kind of these materials a range of constitutive laws is available to describe by a mathematical approach the behavior of the material. The choice of a constitutive law for a given material depends at first to desired quality of the model. For example, for standard steel, the constitutive law may take into account the plasticity, anisotropic hardening, the strain rate, and temperature dependence. However, for a routine design maybe a simple linear elastic law without strain rate and temperature dependence is sufficient to obtain the needed quality of the model. This is the analyst design choice. On the other hand, the software must provide a large constitutive library to provide models for the more commonly encountered materials in practical applications.

RADIOSS material library contains several distinct material laws. The constitutive laws may be used by the analyst for general applications or a particular type of analysis. You can also program a new material law in RADIOSS. This is a powerful resource for the analyst to code a complex material model.

Theoretical aspects of the material models that are provided in RADIOSS are described in this chapter. The available material laws are classified in Table 9.0.1. This classification is in complementary with those of RADIOSS input manual. The reader is invited to consult that one for all technical information related to the definition of input data.

Table 9.0.1 Material law description

Group	Model description	Law number in RADIOSS (MID)
Elasto-plasticity Materials	Johnson-Cook	(2)
	Zerilli-Armstrong	(2)
	von Mises isotropic hardening with polynomial pressure	(3)
	Johnson-Cook	(4)
	Gray model	(16)
	Ductile damage for solids and shells	(22)
	Ductile damage for solids	(23)
	Aluminum, glass, etc.	(27)
	Hill	(32)
	Tabulated piecewise linear	(36)
	Cowper-Symonds	(44)
	Zhao	(48)
	Steinberg-Guinan	(49)
	Ductile damage for porous materials, Gurson	(52)
	Foam model	(53)
	3-Parameter Barlat	(57)
	Tabulated quadratic in strain rate	(60)
	Hänsel model	(63)
	Ugine and ALZ approach	(64)
	Elastomer	(65)
	Visco-elastic	(66)
	Anisotropic Hill	(72)
	Thermal Hill Orthotropic	(73)
	Thermal Hill Orthotropic 3D	(74)
	Semi-analytical elasto-plastic	(76)
	Yoshida-Uemori	(78)
	Brittle Metal and Glass	(79)
	High strength steel	(80)
	Swift and Voce elastio-plastic Material	(84)
	Barlat YLD2000	(87)
Hyper and Visco-elastic	Closed cell, elasto-plastic foam	(33)
	Boltzman	(34)
	Generalized Kelvin-Voigt	(35)
	Tabulated law	(38)

Group	Model description	Law number in RADIOSS (MID)
	Generalized Maxwell-Kelvin	(40)
	Ogden-Mooney-Rivlin	(42)
	Hyper visco-elastic	(62)
	Tabulated input for Hyper-elastic	(69)
	Tabulated law - hyper visco-elastic	(70)
	Tabulated law - visco-elastic foam	(77)
	Ogden material	(82)
	Arruda-Boyce Hyperelastic Material	(92)
Composite and Fabric	Tsai-Wu formula for solid	(12)
	Composite Solid	(14)
	Composite Shell Chang-Chang	(15)
	Fabric	(19)
	Composite Shell	(25)
	Fabric	(58)
Concrete and Rock	Drucker-Prager for rock or concrete by polynominal	(10)
	Drucker-Prager for rock or concrete	(21)
	Reinforced concrete	(24)
	Drücker-Prager with cap	(81)
Honeycomb	Honeycomb	(28)
	Crushable foam	(50)
	Cosserat Medium	(68)
Multi-Material, Fluid and Explosive Material	Jones Wilkins Lee model	(5)
	Hydrodynamic viscous	(6)
	Hydrodynamic viscous with k-ε	(6)
	Boundary element	(11)
	Boundary element with k-ε	(11)
	ALE and Euler formulation	(20)
	Hydrodynamic bi-material liquid gas material	(37)
	Lee-Tarver material	(41)
	Viscous fluid with LES subgrid scale viscosity	(46)
	Solid, liquid, gas and explosives	(51)
Connections Materials	Predit rivets	(54)
	Connection material	(59)
	Advanced connection material	(83)
Other Materials	Fictitious	(0)

Group	Model description	Law number in RADIOSS (MID)
	Hooke	(1)
	Purely thermal material	(18)
	SESAM tabular EOS, used with a Johnson-Cook yield criterion	(26)
	Superelastic Law for Shape Memory Alloy	(71)
	Porous material	(75)
	GAS material	GAS (-)
	User material	(29~31)

9.1 Isotropic Elastic Material

Two kinds of isotropic elastic materials are considered:

- Hooke's law for linear elastic materials,
- Ogden and Mooney-Rivlin laws for nonlinear elastic materials.

These material laws are used to model purely elastic materials, or materials that remain in the elastic range. The Hooke's law requires only two values to be defined; the Young's or elastic modulus E, and Poisson's ratio, υ. The law represents a linear relation between stress and strain.

The Ogden's law is applied to slightly compressible materials as rubber or elastomer foams undergoing large deformation with an elastic behavior [34]. The strain energy W is expressed in a general form as a function of $W(\lambda_1, \lambda_2, \lambda_3)$:

$$W(\lambda_1,\lambda_2,\lambda_3)=\sum_p \frac{\mu_p}{\alpha_p}\left(\bar{\lambda}_1^{\alpha_p}+\bar{\lambda}_2^{\alpha_p}+\bar{\lambda}_3^{\alpha_p}-3\right)+\frac{K}{2}(J-1)^2 \qquad \text{EQ. 9.1.0.1}$$

where λ_i, i_{th} principal stretch ($\lambda_i = 1+\varepsilon_i$, ε_i being the i_{th} principal engineering strain), $J = \lambda_1 \cdot \lambda_2 \cdot \lambda_3$, relative volume: $J = \frac{\rho_0}{\rho}$, $\bar{\lambda}_i = J^{-\frac{1}{3}}\lambda_i$ is the deviatoric stretch, and α_p and μ_p material constants.

This law is very general due to the choice of coefficient α_p and μ_p.

For an incompressible material, we have J=1. For uniform dilatation:

$$\lambda_1 = \lambda_2 = \lambda_3 = \lambda \qquad \text{EQ. 9.1.0.2}$$

The strain energy function can be decomposed into deviatoric and spherical parts:

$$W = \bar{W}(\bar{\lambda}_1,\bar{\lambda}_2,\bar{\lambda}_3)+U(J) \qquad \text{EQ. 9.1.0.3}$$

With:

$$\bar{W}(\bar{\lambda}_1,\bar{\lambda}_2,\bar{\lambda}_3)=\sum_p \frac{\mu_p}{\alpha_p}\left(\bar{\lambda}_1^{\alpha_p}+\bar{\lambda}_2^{\alpha_p}+\bar{\lambda}_3^{\alpha_p}-3\right)$$

$$U(J)=\frac{K}{2}(J-1)^2$$

The stress corresponding to this strain energy is given by:

$$\sigma_i = \frac{\lambda_i}{J}\frac{\partial W}{\partial \lambda_i}$$ EQ. 9.1.0.4

which can be written as:

$$\sigma_i = \frac{\lambda_i}{J}\frac{\partial W}{\partial \lambda_i} = \frac{\lambda_i}{J}\left(\sum_{j=1}^{3}\frac{\partial \overline{W}}{\partial \overline{\lambda}_j}\frac{\partial \overline{\lambda}_j}{\partial \lambda_i} + \frac{\partial U}{\partial J}\frac{\partial J}{\partial \lambda_i}\right)$$ EQ. 9.1.0.5

Since $\lambda_i \frac{\partial J}{\partial \lambda_i} = J$ and $\frac{\partial \overline{\lambda}_j}{\partial \lambda_i} = \frac{2}{3} J^{-\frac{1}{3}}$ for i=j and $\frac{\partial \overline{\lambda}_j}{\partial \lambda_i} = \frac{1}{3} J^{-\frac{1}{3}} \frac{\lambda_j}{\lambda_i}$ for i≠j, EQ. 9.1.0.5 is simplified to:

$$\sigma_i = \frac{1}{J}\left(\overline{\lambda}_i \frac{\partial \overline{W}}{\partial \overline{\lambda}_i} - \left(\frac{1}{3}\sum_{j=1}^{3}\overline{\lambda}_j \frac{\partial \overline{W}}{\partial \overline{\lambda}_j} - J\frac{\partial U}{\partial J}\right)\right)$$ EQ. 9.1.0.6

For which the deviator of the Cauchy stress tensor, and the pressure would be:

$$s_i = \frac{1}{J}\left(\overline{\lambda}_i \frac{\partial \overline{W}}{\partial \overline{\lambda}_i} - \frac{1}{3}\sum_{j=1}^{3}\overline{\lambda}_j \frac{\partial \overline{W}}{\partial \overline{\lambda}_j}\right)$$ EQ. 9.1.0.7

$$p = -\frac{1}{3}\sum_{j=1}^{3}\sigma_j = -\frac{\partial U}{\partial J}$$ EQ. 9.1.0.8

The only deviatoric stress above is retained, and the pressure is computed independently as follows:

$$p = K\ f_{bulk}(J)\,(J-1)$$ EQ. 9.1.0.9

where f_{bulk} a user-defined function related to the bulk modulus *K*:

$$K = \mu \cdot \frac{2(1+\upsilon)}{3(1-2\upsilon)}$$ EQ. 9.1.0.10

$$\mu = \frac{\sum_p \mu_p \cdot \alpha_p}{2}$$ EQ. 9.1.0.11

μ being the ground shear modulus, and υ the Poisson's ratio.

Note: For an incompressible material you have $\upsilon \approx 0.5$. However, $\upsilon = 0.495$ is a good compromise to avoid too small time steps in explicit codes.

Mooney-Rivlin material law admits two basic assumptions:

- The rubber is incompressible and isotropic in unstrained state,
- The strain energy expression depends on the invariants of Cauchy tensor.

The three invariants of the Cauchy-Green tensor are:

$$I_1 = \lambda_1^2 + \lambda_2^2 + \lambda_3^2$$

$$I_2 = \lambda_1^2\lambda_2^2 + \lambda_2^2\lambda_3^2 + \lambda_3^2\lambda_1^2 \qquad \text{EQ. 9.1.0.14}$$

$$I_3 = \lambda_1^2\lambda_2^2\lambda_3^2 = 1 \text{ for incompressible material}$$

The Mooney-Rivlin law gives the closed expression of strain energy as:

$$W = C_{10}(I_1 - 3) + C_{01}(I_2 - 3) \qquad \text{EQ. 9.1.0.15}$$

with:

$$\mu_1 = 2 \cdot C_{10}$$
$$\mu_2 = -2 \cdot C_{01} \qquad \text{EQ. 9.1.0.16}$$
$$\alpha_1 = 2$$
$$\alpha_2 = -2$$

The model can be generalized for a compressible material.

Viscous effects are modeled through the Maxwell model:

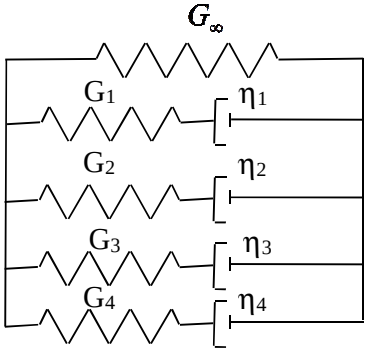

Maxwell model

Where, the shear modulus of the hyper-elastic law μ is exactly the long-term shear modulus G_∞.

τ_i are relaxation times: $\tau_i = \dfrac{\eta_i}{G_i}$

Rate effects are modeled through visco-elasticity using convolution integral using Prony series. This corresponds to extension of small deformation theory to finite deformation.

This viscous stress is added to the elastic one.

The visco-Kirchoff stress is given by:

$$\tau^v = \sum_{i=1}^{m} G_i \int_0^t e^{-\frac{t-s}{\tau_i}} \frac{d}{ds}\left[dev(\overline{F}\overline{F}^T)\right] ds \qquad \text{EQ. 9.1.0.17}$$

Where, m is the order of the Maxwell model, F is the deformation gradient matrix, , $\overline{F} = J^{-\frac{1}{3}} F$ and $dev(\overline{F}\overline{F}^T)$ denotes the deviatoric part of tensor $\overline{F}\overline{F}^T$.

The viscous-Cauchy stress is written as:

$$\sigma^v(t) = \frac{1}{J}\tau^v(t) \qquad \text{EQ. 9.1.0.18}$$

9.2 Composite and Anisotropic Materials

The orthotropic materials can be classified into following cases:

- Linear elastic orthotropic shells as fabric
- Nonlinear orthotropic pseudo-plastic solids as honeycomb materials
- Elastic-plastic orthotropic shells
- Elastic-plastic orthotropic composites

The purpose of this section is to describe the mathematical models related to composite and orthotropic materials.

9.2.1 Fabric law for elastic orthotropic shells (laws 19 and 58)

Two elastic linear models and a nonlinear model exist in RADIOSS.

9.2.1.1 Fabric linear law for elastic orthotropic shells (law 19)

A material is orthotropic if its behavior is symmetrical with respect to two orthogonal plans. The fabric law enables to model this kind of behavior. This law is only available for shell elements and can be used to model an airbag fabric. Many of the concepts for this law are the same as for law 14 which is appropriate for composite solids. If axes 1 and 2 represent the orthotropy directions, the constitutive matrix *C* is defined in terms of material properties:

$$C^{-1} = \begin{bmatrix} \frac{1}{E_{11}} & -\frac{\upsilon_{21}}{E_{22}} & 0 & 0 & 0 \\ -\frac{\upsilon_{12}}{E_{11}} & \frac{1}{E_{22}} & 0 & 0 & 0 \\ 0 & 0 & \frac{1}{G_{12}} & 0 & 0 \\ 0 & 0 & 0 & \frac{1}{G_{23}} & 0 \\ 0 & 0 & 0 & 0 & \frac{1}{G_{31}} \end{bmatrix} \qquad \text{EQ. 9.2.1.1}$$

where the subscripts denote the orthotropy axes. As the matrix *C* is symmetric:

$$\frac{\upsilon_{12}}{E_{11}} = \frac{\upsilon_{21}}{E_{22}} \qquad \text{EQ. 9.2.1.2}$$

Therefore, six independent material properties are the input of the material:

E_{11} = Young's modulus in direction 1

E_{22} = Young's modulus in direction 2

υ_{12} = Poisson's ratio

G_{12}, G_{23}, G_{31} = Shear moduli for each direction

The coordinates of a global vector $\vec{V}$ is used to define direction 1 of the local coordinate system of orthotropy.

The angle Φ is the angle between the local direction 1 (fiber direction) and the projection of the global vector $\vec{V}$ as shown in Figure 9.2.1.

Figure 9.2.1 Fiber Direction Orientation

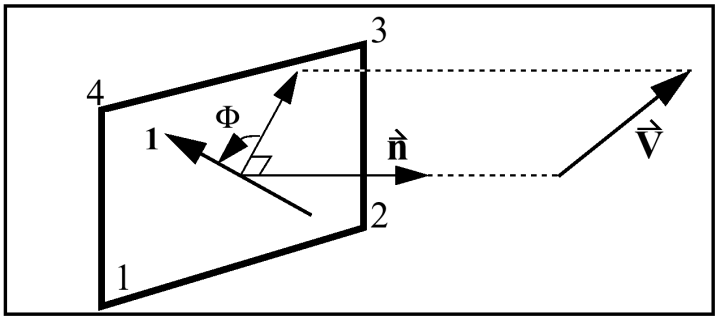

The shell normal defines the positive direction for Φ. Since fabrics have different compression and tension behavior, an elastic modulus reduction factor, R_E, is defined that changes the elastic properties of compression. The formulation for the fabric law has a σ_{11} reduction if $\sigma_{11} < 0$ as shown in Figure 9.2.2.

Figure 9.2.2 Elastic Compression Modulus Reduction

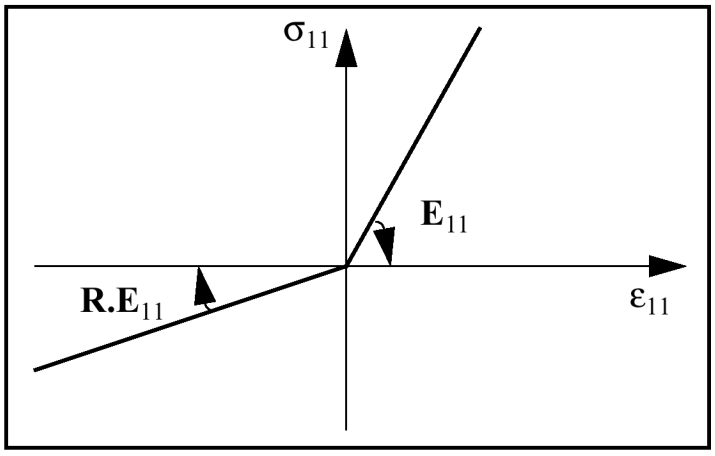

9.2.1.2 Fabric nonlinear law for elastic anisotropic shells (law 58)

This law is used with RADIOSS standard shell elements and anisotropic layered property (type 16). The fiber directions (warp and weft) define the local axes of anisotropy. Material characteristics are determined independently in these axes. Fibers are nonlinear elastic and follow the equation:

$$\sigma_{ii} = E_i\varepsilon_{ii} - \frac{(B_i\varepsilon_{ii}^{\ 2})}{2} \quad \text{with} \quad \frac{d\sigma}{d\varepsilon} > 0$$
$$\sigma_{ii} = \max_{\varepsilon_{ii}}\left(E_i\varepsilon_{ii} - \frac{(B_i\varepsilon_{ii}^{\ 2})}{2}\right) \quad \frac{d\sigma}{d\varepsilon} \le 0 \quad \text{and } i=1,2 \qquad \text{EQ. 9.2.1.3}$$

The shear in fabric material is only supposed to be function of the angle between current fiber directions (axes of anisotropy):

$$\tau = G_0\tan(\alpha) - \tau_0 \quad \text{if} \quad \alpha \le \alpha_T \qquad \text{EQ. 9.2.1.4}$$

$$\tau = G\tan(\alpha) + G_A - \tau_0 \quad \text{if} \quad \alpha > \alpha_T$$

and

$$G_A = (G_0 - G)\tan(\alpha_T), \qquad G = \frac{G_T}{1+\tan^2(\alpha_T)} \qquad \text{with} \qquad \tau_0 = G_0\tan(\alpha_0)$$

Where α_T is a shear lock angle, G_T is a tangent shear modulus at α_T, and G_0 is a shear modulus at α = 0. If G_0 = 0, the default value is calculated to avoid shear modulus discontinuity at α_T: $G_0 = G$.

Figure 9.2.4 Elastic Compression Modulus Reduction

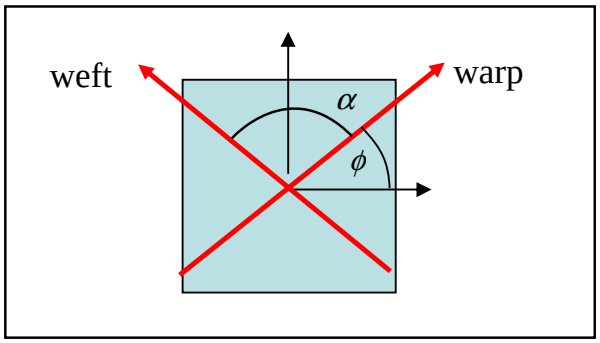

α_0 is an initial angle between fibers defined in the shell property (type 16).

The warp and weft fiber are coupled in tension and uncoupled in compression. But there is no discontinuity between tension and compression. In compression only fiber bending generates global stresses. Figure 9.2.5 illustrates the mechanical behavior of the structure.

Figure 9.2.5 Local frame definition

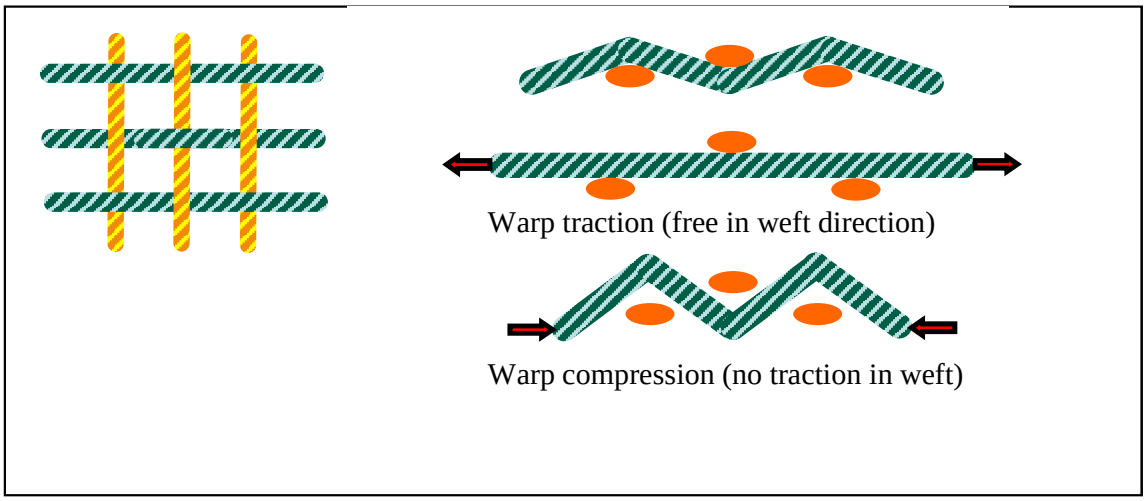

A local micro model describes the material behavior (Figure 9.2.6). This model represents just ¼ of a warp fiber wave length and ¼ of the weft one. Each fiber is described as a nonlinear beam and the two fibers are connected with a contacting spring. These local nonlinear equations are solved with Newton iterations at membrane integration point.

Figure 9.2.6 Local frame definition

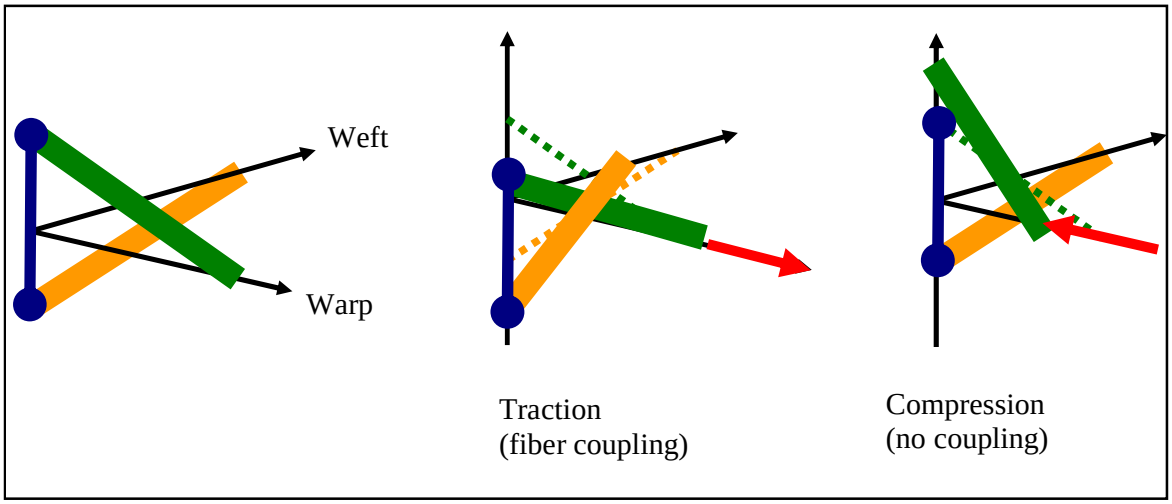

9.2.2 Nonlinear pseudo-plastic orthotropic solids (laws 28, 50 and 68)

9.2.2.1 Conventional nonlinear pseudo-plastic orthotropic solids (laws 28 and 50)

These laws are generally used to model honeycomb material structures as crushable foams. The microscopic behavior of this kind of materials can be considered as a system of three independent orthogonal springs. The nonlinear behavior in orthogonal directions can then be determined by experimental tests. The behavior curves are injected directly in the definition of law. Therefore, the physical behavior of the material can be obtained by a simple law. However, the microscopic elasto-plastic behavior of a material point cannot be represented by decoupled unidirectional curves. This is the major drawback of the constitutive laws based on this approach. The cell direction is defined for each element by a local frame in the orthotropic solid property. If no property set is given, the global frame is used.

Figure 9.2.7 Local frame definition

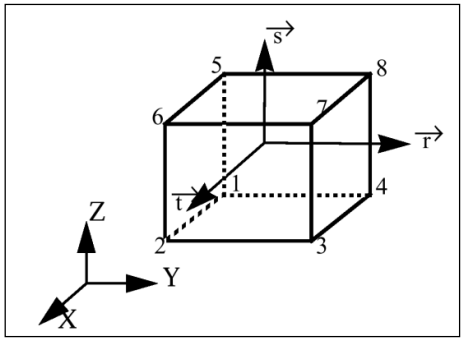

The Hooke matrix defining the relation between the stress and strain tensors is diagonal, as there is no Poisson's effect:

$$\begin{bmatrix} \sigma_{11} \\ \sigma_{22} \\ \sigma_{33} \\ \sigma_{12} \\ \sigma_{23} \\ \sigma_{31} \end{bmatrix} = \begin{bmatrix} E_{11} & 0 & 0 & 0 & 0 & 0 \\ 0 & E_{22} & 0 & 0 & 0 & 0 \\ 0 & 0 & E_{33} & 0 & 0 & 0 \\ 0 & 0 & 0 & G_{12} & 0 & 0 \\ 0 & 0 & 0 & 0 & G_{23} & 0 \\ 0 & 0 & 0 & 0 & 0 & G_{31} \end{bmatrix} \begin{bmatrix} \varepsilon_{11} \\ \varepsilon_{22} \\ \varepsilon_{33} \\ \varepsilon_{12} \\ \varepsilon_{23} \\ \varepsilon_{31} \end{bmatrix} \qquad \text{EQ. 9.2.2.1}$$

An isotropic material may be obtained if:

$$E_{11} = E_{22} = E_{33} \text{ and } G_{12} = G_{23} = G_{31} = \frac{E_{11}}{2} \qquad \text{EQ. 9.2.2.2}$$

Plasticity may be defined by a volumic strain or strain dependent yield curve (Figure 9.2.8). The input yield stress function is always positive. If the material undergoes plastic deformation, its behavior is always orthotropic, as all curves are independent to each other.

Figure 9.2.8 Honeycomb typical constitutive curve

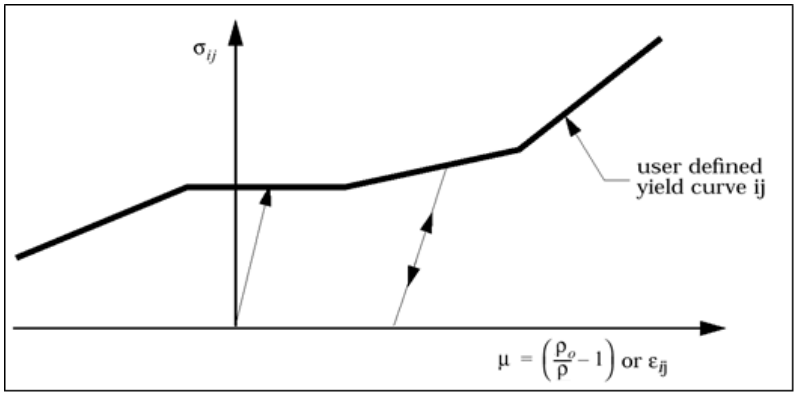

The failure plastic strain may be input for each direction. If the failure plastic strain is reached in one direction, the element is deleted. The material law may include strain rate effects (law 50) or may not (law 28).

9.2.2.2 Cosserat medium for nonlinear pseudo-plastic orthotropic solids (law 68)

Conventional continuum mechanics approaches cannot incorporate any material component length scale. However, a number of important length scales as grains, particles, fibers, and cellular structures must be taken into account in a realistic model of some kinds of materials. To this end, the study of a microstructure material having translational and rotational degrees-of-freedom is underlying. The idea of introducing couple stresses in the continuum modelling of solids is known as Cosserat theory which returns back to the works of brothers Cosserat in the beginning of 20th century [110]. A recent renewal of Cosserat mechanics is presented in several works of Forest et al [111], [112], [113], and [114]. A short summary of these publications is presented in this section.

Cosserat effects can arise only if the material is subjected to non-homogeneous straining conditions. A Cosserat medium is a continuous collection of particles that behave like rigid bodies. It is assumed that the transfer of the interaction between two volume elements through surface element dS occurs not only by means of a traction and shear forces, but also by moment vector as shown in Figure 9.2.9.

Figure 9.2.9 Equilibrium of Cosserat volume element

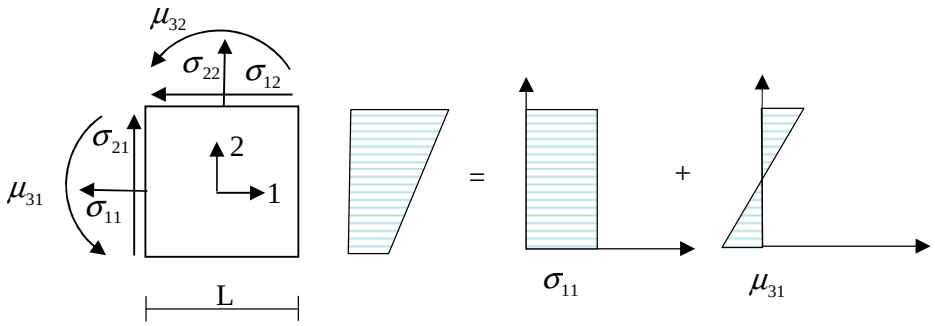

Surface forces and couples are then represented by the generally non-symmetrical force-stress and couple-stress tensors σ_{ij} and μ_{ij} (units MPA and MPa-m):

$$t_i = \sigma_{ij} n_j \quad ; \quad m_i = \mu_{ij} n_j \qquad \text{EQ. 9.2.2.3}$$

The force and couple stress tensors must satisfy the equilibrium of momentums:

$$\sigma_{ij,j} + f_i = \rho \ddot{u}_i$$

$$\mu_{ij,j} - \varepsilon_{ikl}\sigma_{kl} + c_i = I\ddot{\phi}_i \qquad \text{EQ. 9.2.2.4}$$

Where, f_i are the volume forces, c_i volume couples, ρ mass density, *I* the isotropic rotational inertia and ε_{ikl} the signature of the perturbation (i,k,l).

In the often used couple-stress, the Cosserat micro-rotation is constrained to follow the material rotation given by the skew-symmetric part of the deformation gradient:

$$\phi_i = -\frac{1}{2}\varepsilon_{ijk} u_{j,k} \qquad \text{EQ. 9.2.2.5}$$

The associated torsion-curvature and couple stress tensors are then traceless. If a Timoshenko beam is regarded as a one-dimensional Cosserat medium, constraint EQ. 9.2.2.5 is then the counterpart of the Euler-Bernoulli conditions.

The resolution of the previous boundary value problem requires constitutive relations linking the deformation and torsion-curvature tensors to the force- and couple-stresses. In the case of linear isotropic elasticity, we have:

$$\sigma_{ij} = \lambda e_{kk}\delta_{ij} + 2\mu e_{ij}^{Symm.} + 2\mu_c e_{ij}^{Skew\,Symm.}$$
$$\mu_{ij} = \alpha k_{kk}\delta_{ij} + 2\beta \kappa_{ij}^{Symm.} + 2\gamma \kappa_{ij}^{Skew\,Symm.} \qquad \text{EQ. 9.2.2.6}$$

Where $e_{ij}^{Symm.}$ and $e_{ij}^{SkewSymm.}$ are respectively the symmetric and skew-symmetric part of the Cosserat deformation tensor. Four additional elasticity moduli appear in addition to the classical Lamé constants.

Cosserat elastoplasticity theory is also well-established. von Mises classical plasticity can be extended to micropolar continua in a straightforward manner. The yield criterion depends on both force- and couple-stresses:

$$f(\sigma,\mu) = \sqrt{\frac{3}{2}\left(a_1 s_{ij}s_{ij} + a_2 s_{ij}s_{ji} + b_1\mu_{ij}\mu_{ij} + b_2\mu_{ij}\mu_{ji}\right)} - R \qquad \text{EQ. 9.2.2.7}$$

Where, *s* denotes the stress deviator and a_i, and b_i are the material constants.

Cosserat continuum theory can be applied to several classes of materials with microstructures as honeycombs, liquid crystals, rocks and granular media, cellular solids and dislocated crystals.

9.2.3 Hill's Law for Orthotropic Plastic Shells

Hill's law models an anisotropic yield behavior. It can be considered as a generalization of von Mises yield criteria for anisotropic yield behavior. The yield surface defined by Hill can be written in a general form:

$$F(\sigma_{22}-\sigma_{33})^2 + G(\sigma_{33}-\sigma_{11})^2 + H(\sigma_{11}-\sigma_{22})^2 + 2L\sigma_{23}^2 + 2M\sigma_{31}^2 + 2N\sigma_{12}^2 - 1 = 0 \qquad \text{EQ. 9.2.3.1}$$

Where, the coefficients F, G, H, L, M and N are the constants obtained by the material tests in different orientations. The stress components σ_{ij} are expressed in the Cartesian reference parallel to the three planes of anisotropy. EQ.9.2.3.1 is equivalent to von Mises yield criteria if the material is isotropic.

In a general case, the loading direction is not the orthotropic direction. In addition, we are concerned with the plane stress assumption for shell structures. In planar anisotropy, the anisotropy is characterized by different strengths in different directions in the plane of the sheet. The plane stress assumption will enable to simplify EQ. 9.2.3.1, and write the expression of equivalent stress σ_{eq} as:

$$\sigma_{eq} = \sqrt{A_1\sigma_{11}{}^2 + A_2\sigma_{22}{}^2 - A_3\sigma_{11}\sigma_{22} + A_{12}\sigma_{12}{}^2} \qquad \text{EQ. 9.2.3.2}$$

The coefficients A_i are determined using Lankford's anisotropy parameter r_α:

$$R = \frac{r_{00} + 2r_{45} + r_{90}}{4}; \quad H = \frac{R}{1+R}; \quad A_1 = H\left(1 + \frac{1}{r_{00}}\right) \qquad \text{EQ. 9.2.3.3}$$

$$A_2 = H\left(1 + \frac{1}{r_{90}}\right); \quad A_3 = 2H; \quad A_{12} = 2H(r_{45} + 0.5)\left(\frac{1}{r_{00}} + \frac{1}{r_{90}}\right)$$

Where the Lankford's anisotropy parameters r_α are determined by performing a simple tension test at angle α to orthotropic direction 1:

$$r_\alpha = \frac{d\varepsilon_{\alpha+\frac{\pi}{2}}}{d\varepsilon_{33}} = \frac{H + (2N - F - G - 4H) Sin^2\alpha \; Cos^2\alpha}{F \; Sin^2\alpha + G \; Cos^2\alpha} \qquad \text{EQ. 9.2.3.4}$$

The equivalent stress σ_{eq} is compared to the yield stress σ_y which varies in function of plastic strain ε_p and the strain rate $\dot{\varepsilon}$ (law 32):

$$\sigma_y = a\left(\varepsilon_0 + \varepsilon_p\right)^n . \max\left(\dot{\varepsilon}, \dot{\varepsilon}_0\right)^m \qquad \text{EQ. 9.2.3.5}$$

Therefore, the elastic limit is obtained by:

$$\sigma_0 = a\left(\varepsilon_0\right)^n . \left(\dot{\varepsilon}_0\right)^m \qquad \text{EQ. 9.2.3.6}$$

The yield stress variation is shown in Figure 9.2.10.

Figure 9.2.10 Yield stress variation

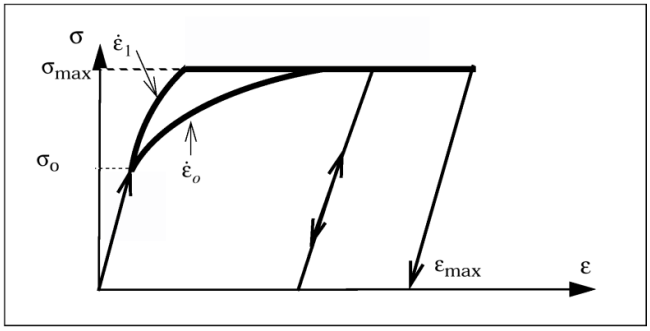

The strain rates are defined at integration points. The maximum value is taken into account:

$$\frac{d\varepsilon}{dt} = \max\left(\frac{d\varepsilon_x}{dt}, \frac{d\varepsilon_y}{dt}, 2\frac{d}{dt}\left(\varepsilon_{xy}\right)\right) \qquad \text{EQ. 9.2.3.7}$$

In RADIOSS, it is also possible to introduce the yield stress variation by a user-defined function (law 43). Then, several curves are defined to take into account the strain rate effect.

It should be noted that as Hill's law is an orthotropic law, it must be used for elements with orthotropy properties as Type 9 and Type 10 in RADIOSS.

9.2.3.1 Anistropic Hill Material Law with MMC Fracture Model (Law 72)

This material law uses an anistropic Hill yield function along with an associated flow rule. A simple isotropic hardening model is used coupled with a modified Mohr fracture criteria. The yield condition is written as

$$\phi(\sigma, \sigma_y) = \sigma_{Hill} - \sigma_y = 0$$

Where, σ_{Hill} is the Equivalent Hill stress given as:

- For 3D model (Solid)

$$\sigma_{Hill} = \sqrt{F(\sigma_{yy} - \sigma_{zz})^2 + G(\sigma_{zz} - \sigma_{xx})^2 + H(\sigma_{xx} - \sigma_{yy})^2 + 2L\sigma_{yz}^2 + 2M\sigma_{zx}^2 + 2N\sigma_{xy}^2}$$

- For Shell

$$\sigma_{hill} = \sqrt{F\sigma_{yy}{}^2 + G\sigma_{xx}{}^2 + H(\sigma_{xx} - \sigma_{yy})^2 + 2N\sigma_{xy}^2}$$

Where, *F, G, H, N, M,* and *L* are Six Hill anisotropic parameters.

For the yield surface a modified swift law is employed to describe the isotropic hardening in the application of the plasticity models :

$$\sigma_y = \sigma_y^0 (\varepsilon_p^0 + \varepsilon_p)^n$$

with σ_y^0 is the initial yield stress, ε_p^0 is the initial equivalent plastic strain, ε_p is the equivalent plastic strain and n is a material constant.

Modified Mohr fracture criteria:

A damage accumulation is computed as:

$$D = \int_0^{\varepsilon_p} \frac{d\varepsilon_p}{\varepsilon_f(\theta,\eta)}$$

Where, ε_f is a plastic strain fracture for the modified Mohr fracture criteria is given by :

- Anisotropic 3D model

$$\varepsilon_f = \left\{ \frac{\sigma_y^0}{C_2} \left[C_3 + \frac{\sqrt{3}}{2-\sqrt{3}}(1-C_3)\left(\sec(\frac{\theta\pi}{6}) - 1 \right) \right] \left[\sqrt{\frac{1+C_1^2}{3}} \cos(\frac{\theta\pi}{6}) + C_1 \left(\eta + \frac{1}{3}\sin(\frac{\theta\pi}{6}) \right) \right] \right\}^{-\frac{1}{n}}$$

with:

$$\begin{cases} \theta = 1 - \dfrac{2}{\pi}\arccos\xi \\ \xi = \dfrac{27}{2}\dfrac{J_3}{\sigma_{VM}^3} \\ \eta = \dfrac{\frac{1}{3}(\sigma_{xx} + \sigma_{yy} + \sigma_{zz})}{\sigma_{VM}} \end{cases}$$

Where, J_3 is the third invariant of the deviatoric stress.

- 2D Anisotropic Model

$$\varepsilon_f = \left\{ \frac{\sigma_y^0}{C_2} f_3 \left[\left(\sqrt{\frac{1+C_1^2}{3}} f_1 \right) + C_1 \left(\eta + \frac{f_2}{3} \right) \right] \right\}^{-\frac{1}{n}}$$

With:

$$\begin{cases} f_1 = \cos\left\{\frac{1}{3}\arcsin\left[-\frac{27}{2}\eta\left(\eta^2-\frac{1}{3}\right)\right]\right\} \\ f_2 = \sin\left\{\frac{1}{3}\arcsin\left[-\frac{27}{2}\eta\left(\eta^2-\frac{1}{3}\right)\right]\right\} \\ f_3 = C_3 + \frac{\sqrt{3}}{2-\sqrt{3}}(1-C_3)\left(\frac{1}{f_1}-1\right) \end{cases}$$

Where, C_1, C_2 and C_3 are parameters for MMC fracture model.

The fracture initiates when D = 1.

In order to represent realistic process of an element, a softening function β is introduced to reduce the deformation resistance. The yield surface is modified as:

$$\sigma_y = \beta\sigma_y^0\left(\varepsilon_p^0 + \varepsilon_p\right)^n$$

with $\beta = \left(\frac{D_c - D}{D_c - 1}\right)^m$

Where, Dc is Critical damage.

We have crack propagation when $1 < D < D_C$ in this case $0<\beta<1$ is considered to reduce the yield surface otherwise the β =1.

The element is deleted if $D \geq D_c$.

9.2.4 Elastic-Plastic Orthotropic Composite Shells

Two kinds of composite shells may be considered in the modeling:

- Composite shells with isotropic layers
- Composite shells with at least one orthotropic layer

The first case can be modeled by an isotropic material where the composite property is defined in element property definition as explained in Chapter 5. However, in the case of composite shell with orthotropic layers the definition of a convenient material law is needed. Two dedicated material laws for composite orthotropic shells exist in RADIOSS:

- Material law COMPSH (25) with orthotropic elasticity, two plasticity models and brittle tensile failure,
- Material law CHANG (15) with orthotropic elasticity, fully coupled plasticity and failure models.

These laws are described here. The description of elastic-plastic orthotropic composite laws for solids is presented in the next section.

9.2.4.1 Tensile behavior

The tensile behavior is shown in Figure 9.2.12. The behavior starts with an elastic phase. Then, reached to the yield state, the material may undergo an elastic-plastic work hardening with anisotropic Tsai-Wu yield criteria. It is possible to take into account the material damage. The failure can occur in the elastic stage or after plastification. It is started by a damage phase then conducted by the formation of a crack. The maximum damage factor will allow these two phases to separate. The unloading can happen during the elastic, elastic-plastic or damage phase. The damage factor *d* varies during deformation as in the case of isotropic material laws (law 27). However, three

damage factors are computed; two damage factors d_1 and d_2 for orthotropy directions and the other d_3 for delamination:

$$\sigma_{11} = E_{11}(1-d_1)\varepsilon_{11}$$
$$\sigma_{22} = E_{22}(1-d_2)\varepsilon_{22} \qquad \text{EQ. 9.2.4.1}$$
$$\sigma_{12} = G_{12}(1-d_1)(1-d_2)\gamma_{12}$$

Figure 9.2.11 Shear strain

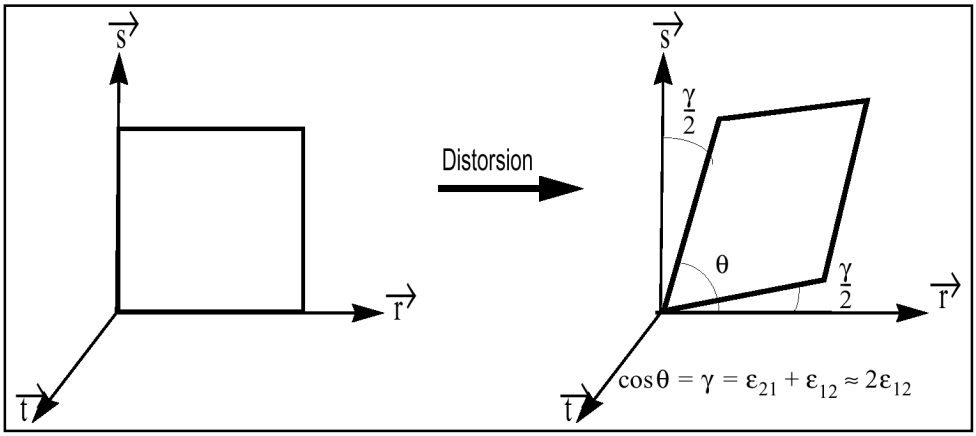

where d_1 and d_2 are the tensile damages factors. The damage and failure behavior is defined by introduction of the following input parameters:

ε_{t1} = Tensile failure strain in direction 1

ε_{m1} = Maximum strain in direction 1

ε_{t2} = Tensile failure strain in direction 2

ε_{m2} = Maximum strain in direction 2

$d_{\max}$ = Maximum damage (residual stiffness after failure)

Figure 9.2.12 Tensile behavior of composite shells

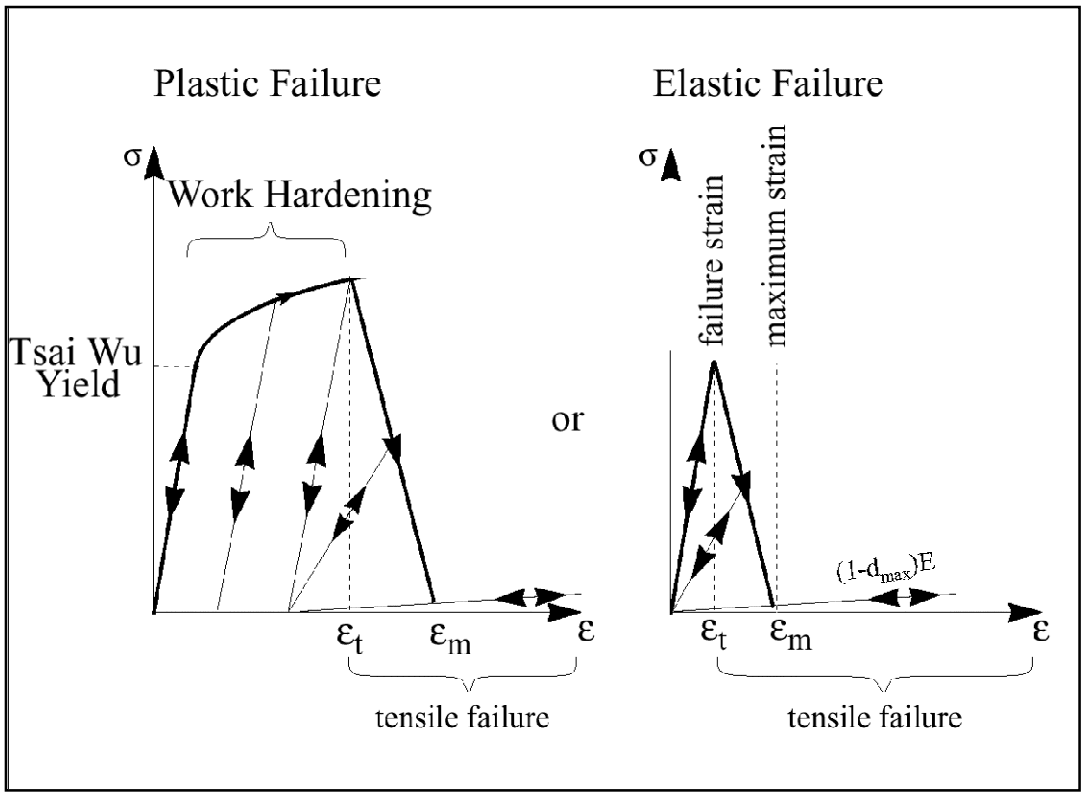

9.2.4.2 Delamination

The delamination equations are:

$$\sigma_{31} = G_{31}(1-d_3)\gamma_{31} \qquad \text{EQ. 9.2.4.2}$$

$$\sigma_{23} = G_{23}(1-d_3)\gamma_{23} \qquad \text{EQ. 9.2.4.3}$$

where d_3 is the delamination damage factor. The damage evolution law is linear with respect to the shear strain.

Let $\gamma = \sqrt{\gamma_{31}^2 + \gamma_{23}^2}$ then:

for $d_3 = 0 \implies \gamma = \gamma_{ini}$

for $d_3 = 1 \implies \gamma = \gamma_{\max}$ EQ. 9.2.4.4

9.2.4.3 Plastic behavior

The plasticity model is based on the Tsai-Wu criterion, which enable to model the yield and failure phases. The criteria are given by [57]:

$$F(\sigma) = F_1\sigma_1 + F_2\sigma_2 + F_{11}\sigma_1^2 + F_{22}\sigma_2^2 + F_{44}\sigma_{12}^2 + 2F_{12}\sigma_1\sigma_2 \qquad \text{EQ. 9.2.4.5}$$

Where $F_1 = -\frac{1}{\sigma_{1y}^c} + \frac{1}{\sigma_{1y}^t}$; $F_2 = -\frac{1}{\sigma_{2y}^c} + \frac{1}{\sigma_{2y}^t}$

$F_{11} = \frac{1}{\sigma_{1y}^c \sigma_{1y}^t}$; $F_{22} = \frac{1}{\sigma_{2y}^c \sigma_{2y}^t}$

$F_{44} = \frac{1}{\sigma_{12y}^c \sigma_{12y}^t}$; $F_{12} = -\frac{\alpha}{2}\sqrt{F_{11}F_{22}}$

Where, α is the reduction factor. The six other parameters are the yield stresses in tension and compression for the orthotropy directions which can be obtained uniaxial loading tests:

$\sigma_{1y}^{\ t}$ = Tension in direction 1 of orthotropy

$\sigma_{2y}^{\ t}$ = Tension in direction 2 of orthotropy

$\sigma_{1y}^{\ c}$ = Compression in direction 1 of orthotropy

$\sigma_{2y}^{\ c}$ = Compression in direction 2 of orthotropy

$\sigma_{12y}^{\ c}$ = Compression in direction 12 of orthotropy

$\sigma_{12y}^{\ t}$ = Tension in direction 12 of orthotropy

The Tsai-Wu criteria are used to determine the material behavior:

- $F(\sigma) < 1$: elastic state
- $F(\sigma) = 1$: plastic admissible state EQ. 9.2.4.6
- $F(\sigma) > 1$: plastically inadmissible stresses

For $F(\sigma) = 1$ the cross-sections of Tsai-Wu function with the planes of stresses in orthotropic directions is shown in Figure 9.2.13.

Figure 9.2.13 Cross-sections of Tsai-Wu yield surface for $F(\sigma)=1$

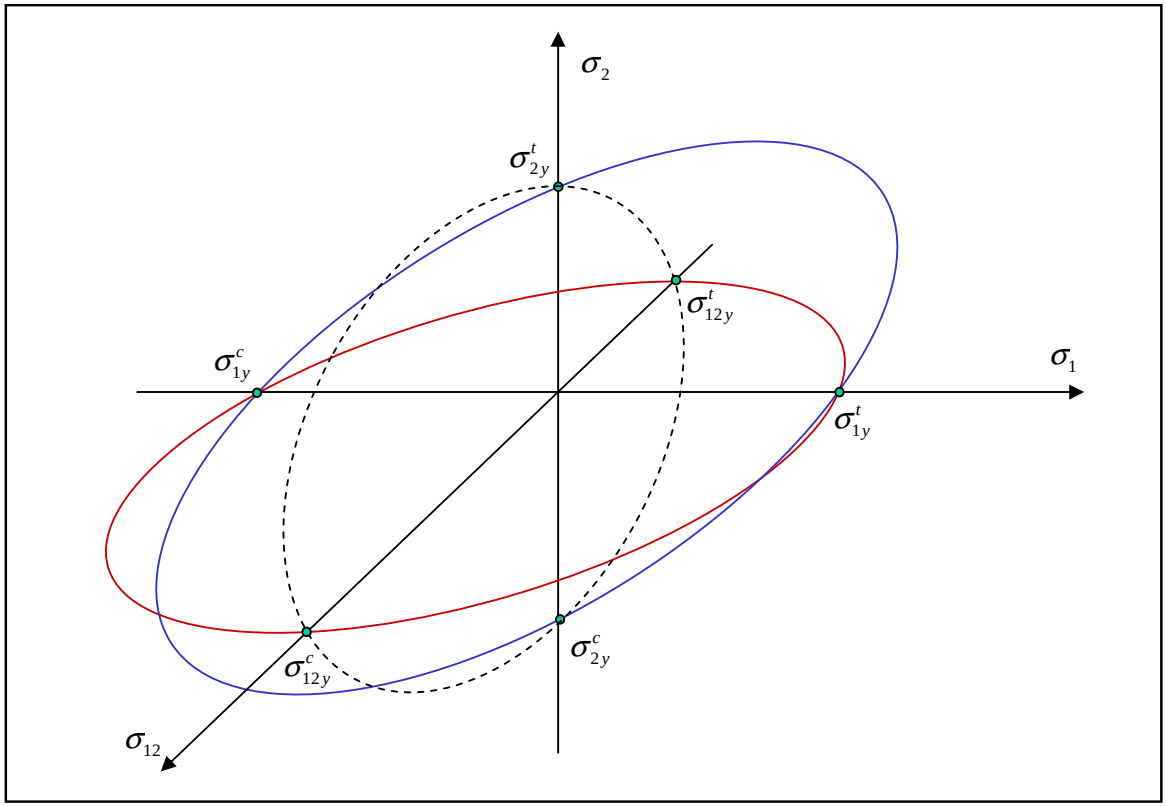

If $F(\sigma)>1$, the stresses must be projected on the yield surface to satisfy the flow rule. $F(\sigma)$ is compared to a maximum value $F(W_p)$ varying in function of the plastic work W_p during work hardening phase:

$$F(\sigma)=F(W_p)=1+bW_p^n \qquad \text{EQ. 9.2.4.7}$$

Where, *b* is the hardening parameter and *n* is the hardening exponent.

Therefore, the plasticity hardening is isotropic as illustrated in Figure 9.2.14.

Figure 9.2.14 Isotropic plasticity hardening

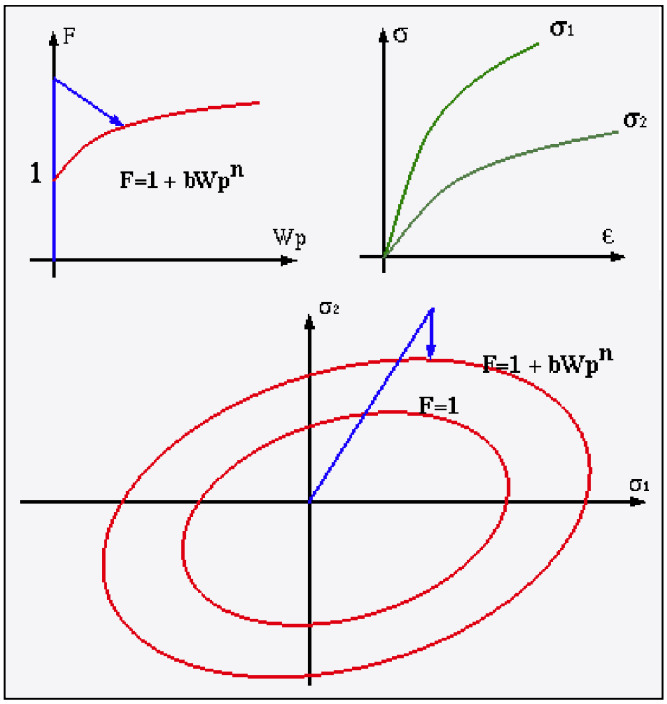

9.2.4.4 Failure behavior

The Tsai-Wu flow surface is also used to estimate the material rupture by means of two variables:

- plastic work limit $W_p^{\max}$,
- maximum value of yield function $F_{\max}$.

If one of the two conditions is satisfied, the material is ruptured. The evolution of yield surface during work hardening of the material is shown in Figure 9.2.15.

Figure 9.2.15 Evolution of Tsai-Wu yield surface

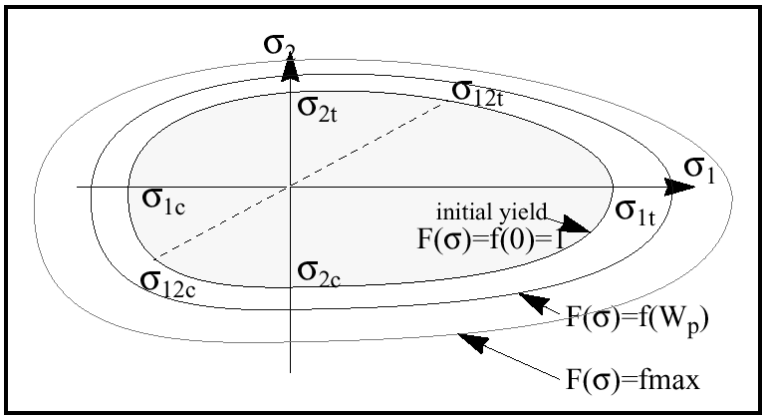

The model will allow the simulation of the brittle failure by formation of cracks. The cracks can either be oriented parallel or perpendicular to the orthotropic reference frame (or fiber direction), as shown in Figure 9.2.16. For plastic failure, if the plastic work W_P is larger than the maximum value $W_P^{\max}$ for a given element, then the element is considered to be ruptured. However, for a multi-layer shell, several criteria may be considered to model a total failure. The failure may happen:

- If $W_P > W_P^{\max}$ for one layer,
- If $W_P > W_P^{\max}$ for all layers,
- If $W_P > W_P^{\max}$ or tensile failure in direction 1 for each layer,
- If $W_P > W_P^{\max}$ or tensile failure in direction 2 for each layer,
- If $W_P > W_P^{\max}$ or tensile failure in directions 1 and 2 for each layer,
- If $W_P > W_P^{\max}$ or tensile failure in direction 1 for all layers,
- If $W_P > W_P^{\max}$ or tensile failure in direction 2 for all layers,
- If $W_P > W_P^{\max}$ or tensile failure in directions 1 and 2 for each layer.

The last two cases are the most physical behaviors; but the use of failure criteria depends, at first, to the analyst's choice. In RADIOSS the flag I_{OFF} defines the used failure criteria in the computation.

Figure 9.2.16 Crack orientation

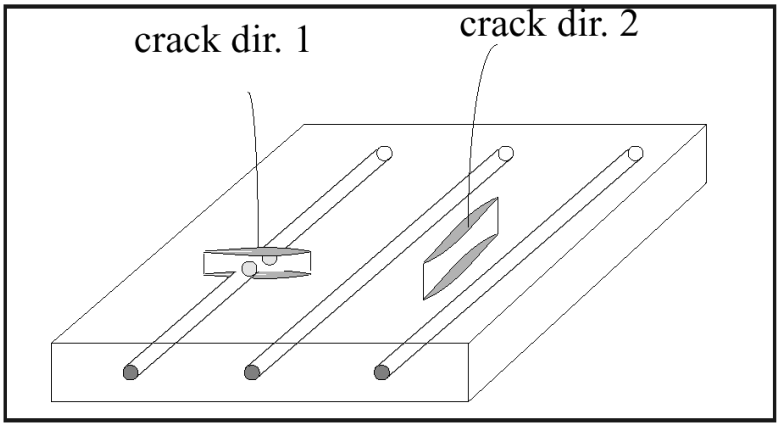

In practice, the use of brittle failure model allows to estimate correctly the physical behavior of a large rang of composites. But on the other hand, some numerical oscillations may be generated due to the high sensibility of the model. In this case, the introduction of an artificial material viscosity is recommended to stabilize results. In addition, in brittle failure model, only tension stresses are considered in cracking procedure.

The ductile failure model allows plasticity to absorb energy during a large deformation phase. Therefore, the model is numerically more stable. This is represented by CRASURV model in RADIOSS. The model makes also possible to take into account the failure in tension, compression and shear directions as described in the following.

9.2.4.5 Strain rate effect

The strain rate is taken into account within the modification of EQ. 9.2.4.7 which acts through a scale factor:

$$F\left(W_p, \dot{\varepsilon}\right) = \left(1 + b\left(\frac{W_p}{W_p^{ref}}\right)^n\right) * \left(1 + c\ln\left(\frac{\dot{\varepsilon}}{\dot{\varepsilon}_0}\right)\right) \qquad \text{EQ. 9.2.4.8}$$

Where,

W_p : plastic work

W_p^{ref} : reference plastic work

b : plastic hardening parameter

n : plastic hardening exponent

c : strain rate coefficient (equal to zero for static loading).

The last equation implies the growing of the Tsai-Wu yield surface when the dynamic effects are increasing. The effects of strain rate are illustrated in Figure 9.2.17.

Figure 9.2.17 Strain rate effect in work hardening

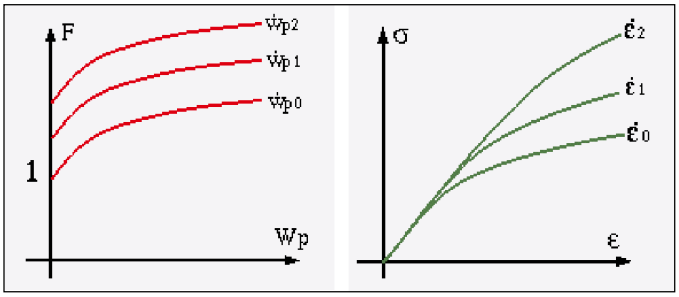

9.2.4.6 CRASURV model

The CRASURV model is an improved version of the former law based on the standard Tsai-Wu criteria. The main changes concern the expression of the yield surface before plastification and during work hardening. First, in CRASURV model the coefficient F_{44} in EQ. 9.2.4.5 depends only on one input parameter:

$$F_{44} = \frac{1}{(\sigma_{12y})^2} \qquad \text{EQ. 9.2.4.9}$$

Another modification concerns the parameters F_{ij} in EQ. 9.2.4.5 which are expressed now in function of plastic work and plastic work rate as in EQ. 9.2.4.8:

$$F(W_p) = 1 = F_1(W_p)\sigma_1 + F_2(W_p)\sigma_2 + F_{11}(W_p)\sigma_1^2 + F_{22}(W_p)\sigma_2^2 + F_{44}(W_p)\sigma_{12}^2 + 2F_{12}(W_p)\sigma_1\sigma_2$$

$$\sigma_{1y}^c = \sigma_{10}^c\left(1 + b_1^c\left(W_p^{1c}\right)^n\right)\left(1 + c_1^c Ln\left(\frac{\dot{\varepsilon}}{\dot{\varepsilon}_o}\right)\right)$$

$$\sigma_{2y}^c = \sigma_{20}^c\left(1 + b_2^c\left(W_p^{2c}\right)^n\right)\left(1 + c_2^c Ln\left(\frac{\dot{\varepsilon}}{\dot{\varepsilon}_o}\right)\right)$$

$$\sigma_{1y}^t = \sigma_{10}^t\left(1 + b_1^t\left(W_p^{1t}\right)^n\right)\left(1 + c_1^t Ln\left(\frac{\dot{\varepsilon}}{\dot{\varepsilon}_o}\right)\right) \qquad \text{EQ. 9.2.4.10}$$

$$\sigma_{2y}^t = \sigma_{20}^t\left(1 + b_2^t\left(W_p^{2t}\right)^n\right)\left(1 + c_2^t Ln\left(\frac{\dot{\varepsilon}}{\dot{\varepsilon}_o}\right)\right)$$

$$\sigma_{12y} = \sigma_{120}\left(1 + b_{12}\left(W_p^{12}\right)^n\right)\left(1 + c_{12} Ln\left(\frac{\dot{\varepsilon}}{\dot{\varepsilon}_o}\right)\right)$$

where the five sets of coefficients *b*, *n* and *c* should be obtained by experience. The work hardening is shown in Figure 9.2.18.

Figure 9.2.18 CRASURV plasticity hardening

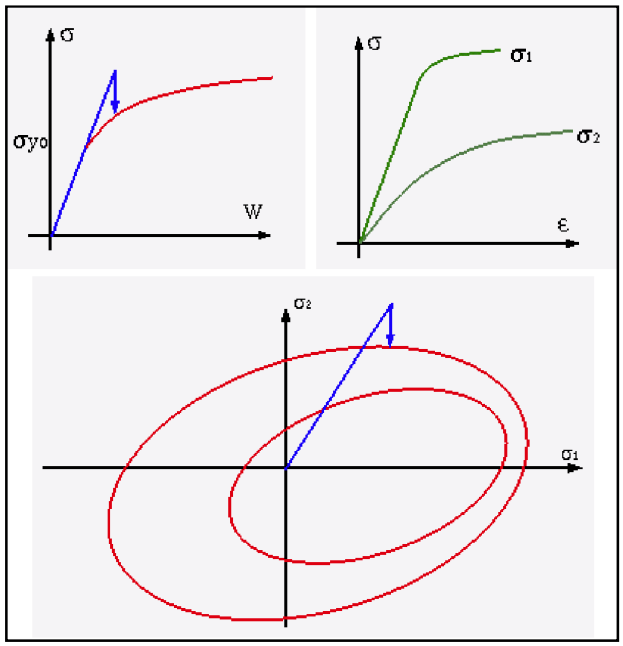

The CRASURV model will allow the simulation of the ductile failure of orthotropic shells. The plastic and failure behaviors are different in tension and in compression. The stress softening may also be introduced in the model to take into account the residual Tsai-Wu stresses. The evolution of CRASURV criteria with hardening and softening works is illustrated in Figure 9.2.19.

Figure 9.2.19 Flow surface in CRASURV model

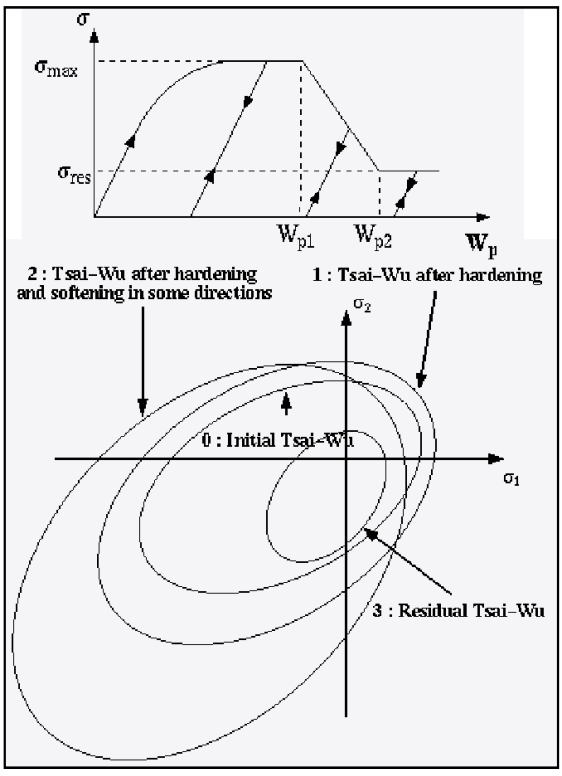

9.2.4.7 Chang-Chang model

Chang-Chang law [58], [59] incorporated in RADIOSS is a combination of the standard Tsai-Wu elastic-plastic law and a modified Chang-Chang failure criteria [60]. The affects of damage are taken into account by decreasing stress components using a relaxation technique to avoid numerical instabilities.

Six material parameters are used in the failure criteria:

$S_1 =$ Longitudinal tensile strength

$S_2 =$ Transverse tensile strength

$S_{12} =$ Shear strength

$C_1 =$ Longitudinal compressive strength

$C_2 =$ Transverse compressive strength

$\beta =$ Shear scaling factor.

Where, *1* is the fiber direction.

The failure criterion for fiber breakage is written as:

- Tensile fiber mode: $\sigma_{11} > 0$

$$e_f^2 = \left(\frac{\sigma_{11}}{S_1}\right)^2 + \beta\left(\frac{\sigma_{12}}{S_{12}}\right)^2 - 1.0 \qquad \begin{cases} \geq 0 & failed \\ < 0 & elastic-plastic \end{cases} \qquad \text{EQ. 9.2.4.11}$$

- Compressive fiber mode: $\sigma_{11} < 0$

$$e_c^2 = \left(\frac{\sigma_{11}}{C_1}\right)^2 - 1.0 \qquad \begin{cases} \geq 0 & failed \\ < 0 & elastic-plastic \end{cases} \qquad \text{EQ. 9.2.4.12}$$

For matrix cracking, the failure criterion is:

- Tensile matrix mode: $\sigma_{22} > 0$

$$e_m^2 = \left(\frac{\sigma_{22}}{S_2}\right)^2 + \beta\left(\frac{\sigma_{12}}{S_{12}}\right)^2 - 1.0 \qquad \begin{cases} \geq 0 & failed \\ < 0 & elastic-plastic \end{cases} \qquad \text{EQ. 9.2.4.13}$$

- Compressive matrix mode: $\sigma_{22} < 0$

$$e_d^2 = \left(\frac{\sigma_{22}}{2S_{12}}\right)^2 + \left[\left(\frac{C_2}{2S_{12}}\right)^2 - 1\right]\frac{\sigma_{22}}{C_2} + \left(\frac{\sigma_{12}}{S_{12}}\right)^2 - 1.0 \qquad \begin{cases} \geq 0 & failed \\ < 0 & elastic-plastic \end{cases} \qquad \text{EQ. 9.2.4.14}$$

If the damage parameter is equal to or greater than 1.0, the stresses are decreased by using an exponential function to avoid numerical instabilities. A relaxation technique is used by gradually decreasing the stress:

$$[\sigma(t)] = f(t) * [\sigma_d(t_r)] \qquad \text{EQ. 9.2.4.15}$$

With: $f(t) = \exp\left(-\frac{t-t_r}{T}\right)$ and $t \geq t_r$ where:

t is the time

$t_r =$ is the start time of relaxation when the damage criteria are assumed

$T =$ $_{IS}$ the time of dynamic relaxation

$[\sigma_d(t_r)]$ is the stress components at the beginning of damage (for matrix cracking $[\sigma_d(t_r)] = \begin{pmatrix} \sigma_{d22} \\ \sigma_{d12} \end{pmatrix}$)

9.2.5 Elastic-Plastic Orthotropic Composite Solids

The material law COMPSO (14) in RADIOSS allows to simulate orthotropic elasticity, Tsai-Wu plasticity with damage, brittle rupture and strain rate effects. The constitutive law applies to only one layer of lamina. Therefore, each layer needs to be modeled by a solid mesh. A layer is characterized by one direction of the fiber or material. The overall behavior is assumed to be elasto-plastic orthotropic.

Direction 1 is the fiber direction, defined with respect to the local reference frame $(\vec{r}, \vec{s}, \vec{t})$ as shown in Figure 9.2.20.

Figure 9.2.20 Local reference frame

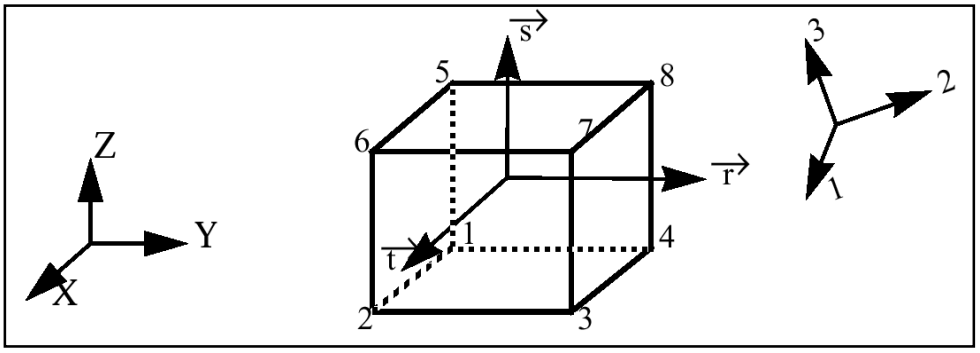

For the case of unidirectional orthotropy (i.e. $E_{33} = E_{22}$ and $G_{31} = G_{12}$) the material law (53) in RADIOSS allows to simulate an orthotropic elastic-plastic behavior by using a modified Tsai-Wu criteria.

9.2.5.1 Linear elasticity

When the lamina has a purely linear elastic behavior, the stress calculation algorithm is as follows:

1. Transform the lamina stress, $\sigma_{ij}(t)$, and strain rate, d_{ij}, from global reference frame to fiber reference frame.

2. Compute lamina stress at time $t + \Delta t$ by explicit time integration:

$$\sigma_{ij}(t + \Delta t) = \sigma_{ij}(t) + D_{ijkl} d_{kl} \Delta t \qquad \text{EQ. 9.2.5.1}$$

3. Transform the lamina stress, $\sigma_{ij}(t + \Delta t)$, back to global reference frame.

The elastic constitutive matrix *C* of the lamina relates the non-null components of the stress tensor to those of strain tensor:

$$\{\sigma\} = [D]\{\varepsilon\} \qquad \text{EQ. 9.2.5.2}$$

The inverse relation is generally developed in term of the local material axes and nine independent elastic constants:

$$\begin{Bmatrix} \varepsilon_{11} \\ \varepsilon_{22} \\ \varepsilon_{33} \\ \gamma_{12} \\ \gamma_{23} \\ \gamma_{31} \end{Bmatrix} = \begin{bmatrix} \frac{1}{E_{11}} & -\frac{\nu_{21}}{E_{22}} & -\frac{\nu_{31}}{E_{33}} & 0 & 0 & 0 \\ & \frac{1}{E_{22}} & -\frac{\nu_{32}}{E_{33}} & 0 & 0 & 0 \\ & & \frac{1}{E_{33}} & 0 & 0 & 0 \\ & & & \frac{1}{2G_{12}} & 0 & 0 \\ & \textit{Symm.} & & & \frac{1}{2G_{23}} & 0 \\ & & & & & \frac{1}{2G_{31}} \end{bmatrix} \begin{Bmatrix} \sigma_{11} \\ \sigma_{22} \\ \sigma_{33} \\ \sigma_{12} \\ \sigma_{23} \\ \sigma_{31} \end{Bmatrix} \qquad \text{EQ. 9.2.5.3}$$

where E_{ij} are the Young's modulus, G_{ij} shear modulus and ν_{ij} Poisson's ratios. γ_{ij} is the strain components due to the distortion.

Figure 9.2.21 Strain components and distortion

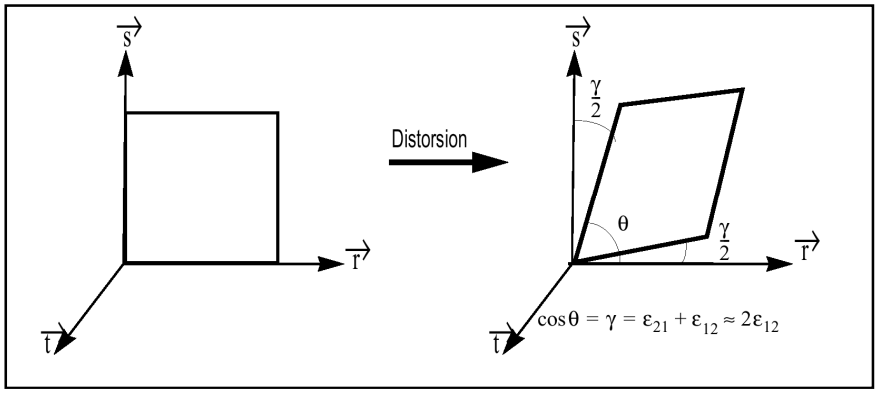

9.2.5.2 Orthotropic plasticity

Lamina yield surface defined by Tsai-Wu yield criteria is used for each layer:

$$F = f(W_p) = F_1\sigma_1 + F_2\sigma_2 + F_3\sigma_3 + F_{11}\sigma_1^2 + F_{22}\sigma_2^2 + F_{33}\sigma_3^2 + F_{44}\sigma_{12}^2 + F_{55}\sigma_{23}^2 + F_{66}\sigma_{31}^2$$

$$+ 2F_{12}\sigma_1\sigma_2 + 2F_{23}\sigma_2\sigma_3 + 2F_{13}\sigma_1\sigma_3 \qquad \text{EQ. 9.2.5.4}$$

with:

$F_i = -\frac{1}{\sigma_{iy}^c} + \frac{1}{\sigma_{iy}^t}$ (i=1,2,3);

$F_{11} = \frac{1}{\sigma_{1y}^c \sigma_{1y}^t}$ $F_{22} = \frac{1}{\sigma_{2y}^c \sigma_{2y}^t}$ $F_{33} = \frac{1}{\sigma_{3y}^c \sigma_{3y}^t}$;

$$F_{44} = \frac{1}{\sigma_{12y}^{c}\sigma_{12y}^{t}} \qquad F_{55} = \frac{1}{\sigma_{23y}^{c}\sigma_{23y}^{t}} \qquad F_{66} = \frac{1}{\sigma_{31y}^{c}\sigma_{31y}^{t}} \quad ;$$

$$F_{12} = -\frac{1}{2}\sqrt{(F_{11}F_{22})} \quad ; \qquad F_{23} = -\frac{1}{2}F_{22}$$

where σ_i is the yield stress in direction *i*, *c* and *t* denote respectively for compression and tension. $f(W_p)$ represents the yield envelope evolution during work hardening with respect to strain rate effects:

$$f(W_p) = \left(1 + B \cdot W_p^{n}\right)\left(1 + c.\ln\left(\frac{\dot{\varepsilon}}{\dot{\varepsilon}_0}\right)\right) \qquad \text{EQ. 9.2.5.5}$$

where W_p is the plastic work, *B* the hardening parameter, *n* the hardening exponent and *c* strain rate coefficient. $f(W_p)$ is limited by a maximum value $f_{\max}$:

$$f(W_p) \le f_{\max} = \left(\frac{\sigma_{\max}}{\sigma_y}\right)^2 \qquad \text{EQ. 9.2.5.6}$$

If the maximum value is reached the material is failed.

In EQ. 9.2.5.5, the strain rate effects on the evolution of yield envelope. However, it is also possible to take into account the strain rate $\dot{\varepsilon}$ effects on the maximum stress $\sigma_{\max}$ as shown in Figure 9.2.22.

Figure 9.2.22 Strain rate dependency

(a) Strain rate effect on $\sigma_{\max}$

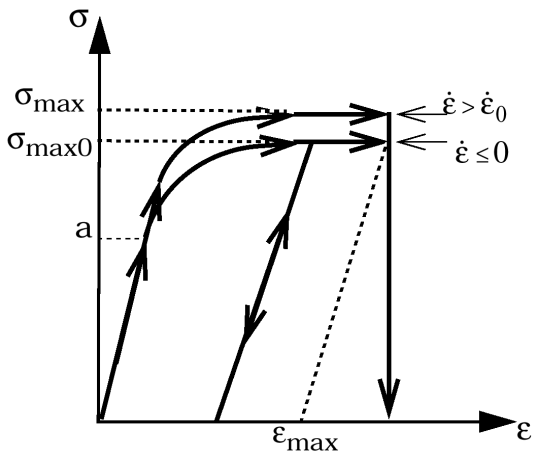

$$\sigma = \sigma_y\left(1 + c.\ln\left(\frac{\dot{\varepsilon}}{\dot{\varepsilon}_0}\right)\right)$$

$$\sigma_{\max} = \sigma_{\max}^{0}\left(1 + c.\ln\left(\frac{\dot{\varepsilon}}{\dot{\varepsilon}_0}\right)\right)$$

$$f_{\max} = \left(\frac{\sigma_{\max}}{\sigma_y}\right)^2$$

(b) No strain rate effect on $\sigma_{\max}$

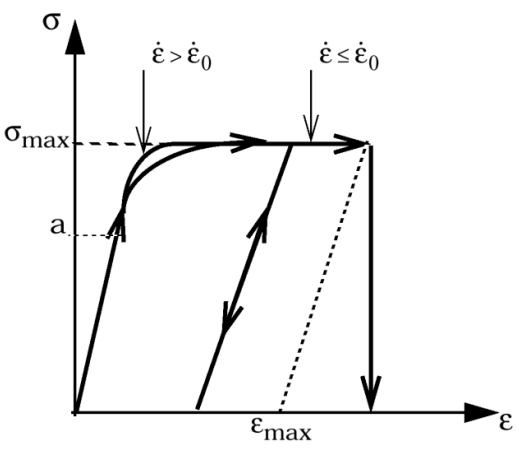

$$\sigma = \sigma_y\left(1 + c.\ln\left(\frac{\dot{\varepsilon}}{\dot{\varepsilon}_0}\right)\right)$$

$$\sigma_{\max} = \sigma_{\max}^{0}$$

9.2.5.3 Unidirectional Orthotropy

Law (53) in RADIOSS provides a simple model for unidirectional orthotropic solids with plasticity. The unidirectional orthotropy condition implies:

$$E_{33} = E_{22} \qquad \text{EQ. 9.2.5.7}$$

$$G_{31} = G_{12}$$

The orthotropic plasticity behavior is modeled by a modified Tsai-Wu criterion (EQ. 9.2.5.4) in which:

$$F_{12} = \frac{2}{\left(\sigma^{45^c}_{y}\right)^2} - \frac{1}{2}\left(F_{11} + F_{22} + F_{44}\right) + \frac{F_1 + F_2}{\sigma^{45^c}_{y}} \qquad \text{EQ. 9.2.5.8}$$

where $\sigma^{45^c}_{y}$ is yield stress in 45° unidirectional test. The yield stresses in direction 11, 22, 12, 13 and 45° are defined by independent curves obtained by unidirectional tests (Figure 9.2.23). The curves give the stress variation in function of a so-called strain ε_v :

$$\varepsilon_v = 1 - \exp\left(Trace\left[\varepsilon\right]\right) \qquad \text{EQ. 9.2.5.9}$$

Figure 9.2.23 Yield stress curve for a unidirectional orthotropic material

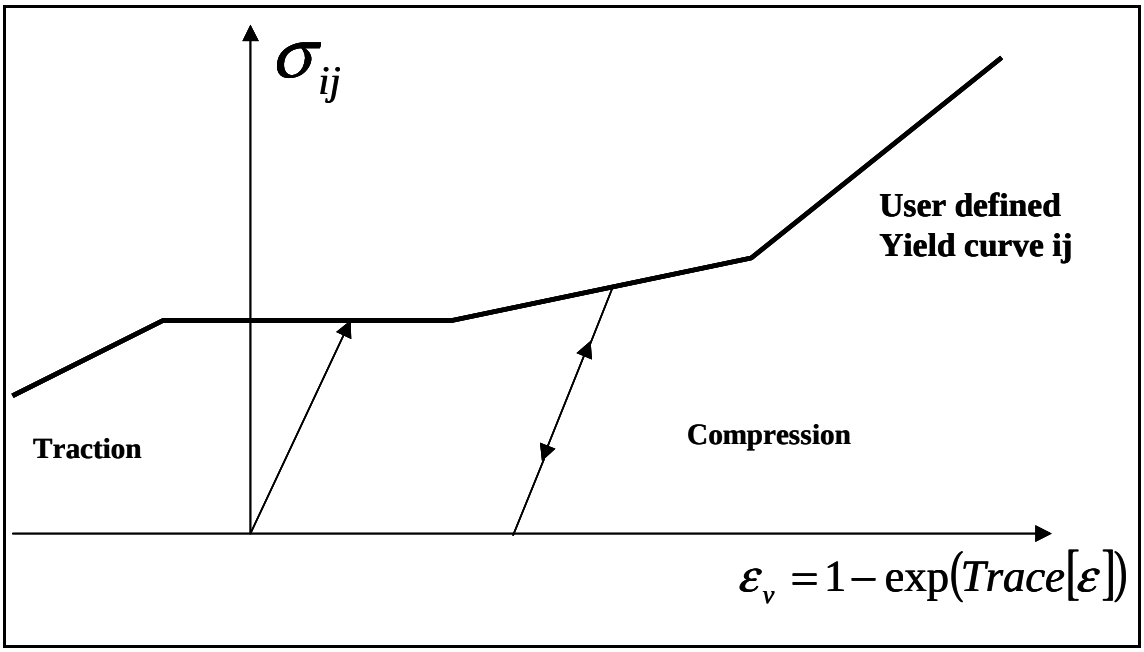

9.2.6 Elastic-plastic anisotropic shells (Barlat's law)

Barlat's 3- parameter plasticity model is developed in [100] for modelling of sheet under plane stress assumption with an anisotropic plasticity model. The anisotropic yield stress criterion for plane stress is defined as:

$$F = a\left|K_1 + K_2\right|^m + a\left|K_1 - K_2\right|^m + c\left|2K_2\right|^m - 2\left(\sigma_e\right)^m \qquad \text{EQ. 9.2.6.1}$$

where σ_e is the yield stress, *a* and *c* are anisotropic material constants, *m* Barlat's exponent and K_1 and K_2 are defined by:

$$K_1 = \frac{\sigma_{xx} - h\sigma_{yy}}{2} \qquad \text{EQ. 9.2.6.2}$$

$$K_2 = \sqrt{\left(\frac{\sigma_{xx} - h\sigma_{yy}}{2}\right)^2 + p^2(\sigma_{xy})^2}$$

where *h* and *p* are additional anisotropic material constants. All anisotropic material constants, except for *p* which is obtained implicitly, are determined from Barlat width to thickness strain ratio *R* from:

$$a = 2 - 2\sqrt{\left(\frac{R_{00}}{1+R_{00}}\right)\left(\frac{R_{90}}{1+R_{90}}\right)} \qquad \text{EQ. 9.2.6.3}$$

$$c = 2 - a$$

$$h = \sqrt{\left(\frac{R_{00}}{1+R_{00}}\right)\left(\frac{1+R_{90}}{R_{90}}\right)}$$

The width to thickness ratio for any angle φ can be calculated according to [100] by:

$$R_\varphi = \frac{2m(\sigma_e)^m}{\left(\frac{\partial F}{\partial \sigma_{xx}} + \frac{\partial F}{\partial \sigma_{yy}}\right)\sigma_\varphi} - 1 \qquad \text{EQ. 9.2.6.4}$$

where σ_φ is the uniaxial tension in the φ direction. Let φ = 45°, EQ. 9.2.6.4 gives an equation from which the anisotropy parameter *p* can be computed implicitly by using an iterative procedure:

$$\frac{2m(\sigma_e)^m}{\left(\frac{\partial F}{\partial \sigma_{xx}} + \frac{\partial F}{\partial \sigma_{yy}}\right)\sigma_{45}} - 1 - R_{45} = 0 \qquad \text{EQ. 9.2.6.5}$$

It is worthwhile to note that Barlat's law reduces to Hill's law when using m=2.

9.3 Elasto-Plasticity of Isotropic Materials

The strain hardening behavior of materials is a major factor in structural response as metal working processes or plastic instability problems. A proper description of strain hardening at large plastic strains is generally imperative. For many plasticity problems, the hardening behavior of the material is simply characterized by the strain-stress curve of the material. For the proportional loading this is generally true. However, if the loading path is combined, the characterization by a simple strain-stress curve is no longer adequate.

The incremental plasticity theory is generally used in computational methods. Plasticity models are written as rate-dependent or independent. A rate-dependent model is a one in which the strain rate does affect the constitutive law. This is true for a large range of metals at low temperature relative to their melting temperature.

Most isotropic elastic-plastic material laws in RADIOSS use von Mises yield criteria as given in section 2.7.2. Several kinds of models are integrated. The models involve damage for ductile or brittle failures with or without dislocation. The cumulative damage law can be used to access failure. The next few paragraphs describe theoretical bases of the integrated models.

9.3.1 Johnson-Cook plasticity model (law 2)

In this law the material behaves as linear elastic when the equivalent stress is lower than the yield stress. For higher value of stress, the material behavior is plastic. This law is valid for brick, shell, truss and beam elements. The relation between describing stress during plastic deformation is given in a closed form:

$$\sigma = \left(a + b\varepsilon_p^n \right)\left(1 + c\ln\frac{\dot{\varepsilon}}{\dot{\varepsilon}_0} \right)\left(1 - \mathrm{T}^{*m} \right) \qquad \text{EQ. 9.3.1.1}$$

where:

σ = Flow stress (Elastic + Plastic Components)

ε_p = Plastic Strain (True strain)

a = Yield Stress

b = Hardening Modulus

n = Hardening Exponent

c = Strain Rate Coefficient

$\dot{\varepsilon}$ = Strain Rate

$\dot{\varepsilon}_0$ = Reference Strain Rate

m = Temperature exponent

$$\mathrm{T}^* = \frac{\mathrm{T} - 298}{\mathrm{T}_{melt} - 298}$$

T_{melt} is the melting temperature in Kelvin degrees. The adiabatic conditions are assumed for temperature computation:

$$\mathrm{T} = \mathrm{T}_i + \frac{E_{\mathrm{int}}}{\rho C_\rho (Volume)} \qquad \text{EQ. 9.3.1.2}$$

Where, ρC_p is the specific heat per unit of volume, T_i is the initial temperature (in degrees Kelvin), and E_{int} is the internal energy.

Two optional additional inputs are:

$\sigma_{\max 0}$ = Maximum flow stress

$\varepsilon_{\max}$ = Plastic strain at rupture

Figure 9.3.1 shows a typical stress-strain curve in the plastic region. When the maximum stress is reached during computation, the stress remains constant and material undergoes deformation until the maximum plastic strain. Element rupture occurs if the plastic strain is larger than $\varepsilon_{\max}$. If the element is a shell, the ruptured element is deleted. If the element is a solid element, the ruptured element has its deviatoric stress tensor permanently set to zero, but the element is not deleted. Therefore, the material rupture is modeled without any damage effect.

Figure 9.3.1 Stress - Plastic Strain Curve

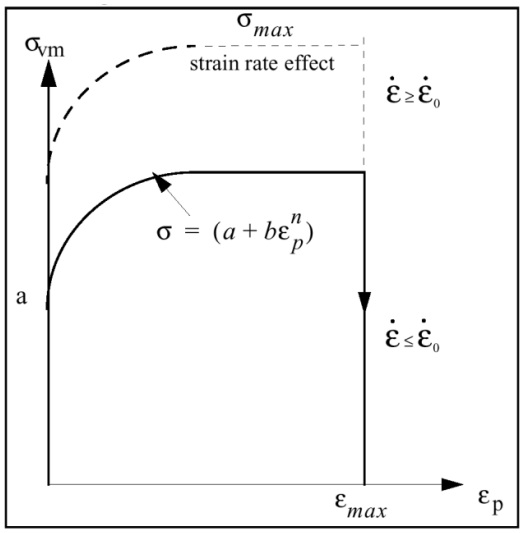

Chard in this material law is same like in /MAT/LAW44. More detail for Chard see 9.3.3.

9.3.1.1 Strain rate definition

Regarding to the plastification method used, the strain rate expression is different. If the progressive plastification method is used (i.e. integration points through the thickness for thin-walled structured), the strain rate is:

$$\frac{d\varepsilon}{dt} = \max\left(\frac{d\varepsilon_x}{dt}, \frac{d\varepsilon_y}{dt}, 2\frac{d}{dt}\left(\varepsilon_{xy}\right)\right) \quad \text{EQ. 9.3.1.3}$$

$$\varepsilon_{xy} = \frac{1}{2}\gamma_{xy} \quad \text{EQ. 9.3.1.4}$$

With global plastification method, we have:

$$\frac{d\varepsilon}{dt} = \left(\frac{dE_i / dt}{\sigma_{VM}}\right) \quad \text{EQ. 9.3.1.5}$$

where E_i is the internal energy.

For solid elements, the maximum value of the strain rate components is used:

$$\dot{\varepsilon} = \max\left(\dot{\varepsilon}_x, \dot{\varepsilon}_y, \dot{\varepsilon}_z, 2\dot{\varepsilon}_{xy}, 2\dot{\varepsilon}_{yz}, 2\dot{\varepsilon}_{xz}\right) \quad \text{EQ. 9.3.1.6}$$

9.3.1.2 Strain rate filtering

The strain rates exhibit very high frequency vibrations which are not physical. The strain rate filtering option will enable to damp those oscillations and; therefore obtain more physical strain rate values.

If there is no strain rate filtering, the equivalent strain rate is the maximum value of the strain rate components:

$$\dot{\varepsilon}_{eq} = \max\left(\dot{\varepsilon}_x, \dot{\varepsilon}_y, \dot{\varepsilon}_z, 2\dot{\varepsilon}_{xy}, 2\dot{\varepsilon}_{yz}, 2\dot{\varepsilon}_{xz}\right) \quad \text{EQ. 9.3.1.7}$$

For thin-walled structures, the equivalent strain is computed by the following approach. If ε is the main component of strain tensor, the kinematic assumptions of thin-walled structures allows to decompose the in-plane strain into membrane and flexural deformations:

$$\varepsilon = \kappa z + \varepsilon_m \quad \text{EQ. 9.3.1.8}$$

Then, the expression of internal energy can by written as:

$$E_i = \int_{-\frac{t}{2}}^{\frac{t}{2}} \sigma\varepsilon \, dz = \int_{-\frac{t}{2}}^{\frac{t}{2}} E\varepsilon^2 dz = \int_{-\frac{t}{2}}^{\frac{t}{2}} E(\kappa z + \varepsilon_m)^2 dz \quad \text{EQ. 9.3.1.9}$$

Therefore:

$$E_i = \int_{-\frac{t}{2}}^{\frac{t}{2}} E(\kappa^2 z^2 + \varepsilon_m^2 + 2\kappa\varepsilon_m z)\, dz = E\left(\frac{1}{3}\kappa^2 z^3 + \varepsilon_m^2 z + \kappa\varepsilon_m z^2\right)_{-\frac{t}{2}}^{\frac{t}{2}} \quad \text{EQ. 9.3.1.10}$$

The expression can be simplified to:

$$E_i = E\left[\frac{1}{12}\kappa^2 t^3 + \varepsilon_m^2 t\right] = E\varepsilon_{eq}^2 t \quad \text{EQ. 9.3.1.11}$$

$$\varepsilon_{eq} = \sqrt{\frac{1}{12}\kappa^2 t^2 + \varepsilon_m^2} \quad \text{EQ. 9.3.1.12}$$

The expression of the strain rate is derived from EQ. 9.3.1.8:

$$\dot{\varepsilon} = \dot{\kappa} z + \dot{\varepsilon}_m \quad \text{EQ. 9.3.1.13}$$

Admitting the assumption that the strain rate is proportional to the strain, i.e.:

$$\dot{\varepsilon}_m = \alpha \varepsilon_m \quad \text{EQ. 9.3.1.14}$$

$$\dot{\kappa} = \alpha \kappa \quad \text{EQ. 9.3.1.15}$$

Therefore:

$$\dot{\varepsilon} = \alpha\varepsilon \quad \text{EQ. 9.3.1.16}$$

Referring to EQ. 9.3.1.12, it can be seen that an equivalent strain rate can be defined using a similar expression to the equivalent strain:

$$\dot{\varepsilon}_{eq} = \alpha\varepsilon_{eq} \quad \text{EQ. 9.3.1.17}$$

$$\dot{\varepsilon}_{eq} = \sqrt{\frac{1}{12}\dot{k}^2 t^2 + \dot{\varepsilon}_m^2} \quad \text{EQ. 9.3.1.18}$$

For solid elements, the strain rate is computed using the maximum element stretch:

$$\dot{\varepsilon}_{eq} = \dot{\lambda}_{\max} \qquad \text{EQ. 9.3.1.19}$$

The strain rate at integration point, *i* in /ANIM/TENS/EPSDOT/i (1<i<n) is calculated by the following expression:

$$\dot{\varepsilon}_i = \dot{\varepsilon}_m - \frac{1}{2}\left(\frac{(2i-1)}{n} - 1\right) t\dot{\varepsilon}_b \qquad \text{EQ. 9.3.1.20}$$

Where $\dot{\varepsilon}_m$ is the membrane strain rate /ANIM/TENS/EPSDOT/MEMB and $\dot{\varepsilon}_b$ is the bending strain rate /ANIM/TENS/EPSDOT/BEND.

The strain rate in upper and lower layers is computed by:

$$\dot{\varepsilon}_u = \dot{\varepsilon}_m + \frac{1}{2} t\dot{\varepsilon}_b \qquad \text{/ANIM/TENS/EPSDOT/UPPER} \qquad \text{EQ. 9.3.1.21}$$

$$\dot{\varepsilon}_l = \dot{\varepsilon}_m - \frac{1}{2} t\dot{\varepsilon}_b \qquad \text{/ANIM/TENS/EPSDOT/LOWER} \qquad \text{EQ. 9.3.1.22}$$

The strain rate is filtered by using the following equation:

$$\dot{\varepsilon}_f(t) = a\dot{\varepsilon}(t) + (1-a)\dot{\varepsilon}_f(t-1) \qquad \text{EQ. 9.3.1.23}$$

where:

$$a = 2\pi\ dt\ F_{cut}$$

Where, dt is the time interval, F_{cut} is the cutting frequency, and $\dot{\varepsilon}_f$ is the filtered strain rate.

9.3.1.3 Example: Strain rate filtering

An example of material characterization for a simple tensile test is given in *RADIOSS Example Manual.* For the same example a strain rate filtering allows to remove high frequency vibrations and obtain smoothed the results. This is shown in Figures 9.3.2 and 9.3.3 where the cut frequency F_{cut} = 10 KHz is used.

Figure 9.3.2 Force comparison in example 9.3.1.3

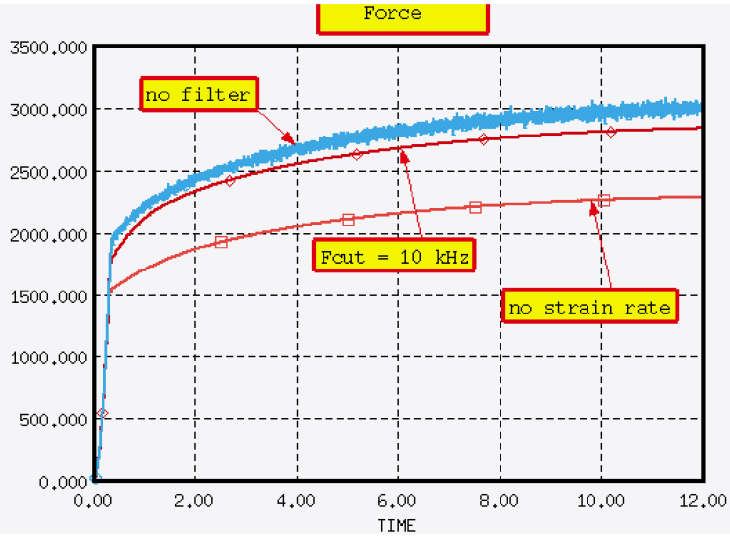

Figure 9.3.3 First principal strain rate comparison (max = 10%)

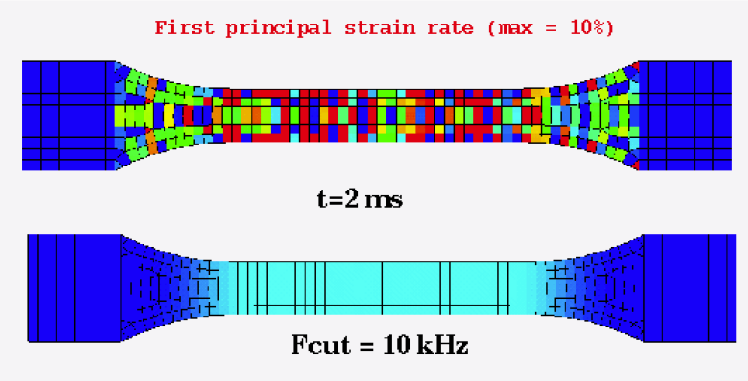

9.3.2 Zerilli-Armstrong plasticity model (law 2)

This law is similar to the Johnson-Cook plasticity model. The same parameters are used to define the work hardening curve. However, the equation that describes stress during plastic deformation is:

$$\sigma = C_0 + \left(C_1 \exp\left(\left(-C_3 \mathrm{T} + C_4 \mathrm{T} \ln\left(\frac{\dot{\varepsilon}}{\dot{\varepsilon}_0} \right) \right) \right) \right) + C_5 \varepsilon_p^n \qquad \text{EQ. 9.3.2.1}$$

where:

σ = Stress (Elastic + Plastic Components)

ε_p = Plastic Strain

T = Temperature (computed as in Johnson Cook plasticity)

C_0 = Yield Stress

n = Hardening Exponent

$\dot{\varepsilon}$ = Strain Rate, must be 1 s^{-1} converted into user's time unit

$\dot{\varepsilon}_0$ = Reference Strain Rate

Additional inputs are:

$\sigma_{\max 0}$ = Maximum flow stress

$\varepsilon_{\max}$ = Plastic strain at rupture

The $\varepsilon_{\max}$ enables to define element rupture as in the former law. The theoretical aspects related to strain rate computation and filtering are also the same.

9.3.3 Cowper-Symonds plasticity model (law 44)

This law models an elasto-plastic material with:

- isotropic and kinematic hardening
- tensile rupture criteria

The damage is neglected in the model. The work hardening model is similar to the Johnson Cook model (law 2) without temperature effect where the only difference is in the strain rate dependent formulation. The equation that describes the stress during plastic deformation is:

$$\sigma = \left(a + b\varepsilon_p^n\right)\left(1 + \frac{1}{c}\dot{\varepsilon}^{\frac{1}{p}}\right) \qquad \text{EQ. 9.3.3.1}$$

where, σ = Flow stress (Elastic + Plastic Components)

ε_p = Plastic Strain (True strain)

a = Yield Stress

b = Hardening Modulus

n = Hardening Exponent

c = Strain Rate Coefficient

$\dot{\varepsilon}$ = Strain Rate

1/p = strain rate exponent

The implanted model in RADIOSS allows the cyclic hardening with a combined isotropic-kinematic approach.

The coefficient C_{hard} varying between zero and unity is introduced to regulate the weight between isotropic and kinematic hardening models.

In isotropic hardening model, the yield surface inflates without moving in the space of principle stresses. The evolution of the equivalent stress defines the size of the yield surface, as a function of the equivalent plastic strain. The model can be represented in one dimensional case as shown in Figure 9.3.4. When the loading direction is changed, the material is unloaded and the strain reduces. A new hardening starts when the absolute value of the stress reaches the last maximum value (Figure 9.3.4(a)).

Figure 9.3.4 Isotropic and Kinematic hardening models for deformation decrease

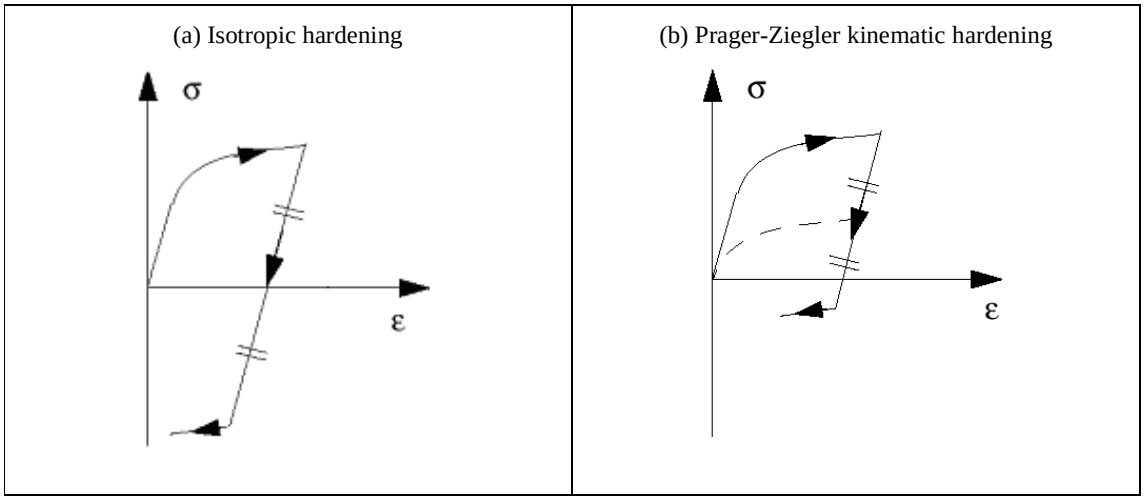

This law is available for solids and shells. Refer to the *RADIOSS Input Manual* for more information about element/material compatibilities.

9.3.4 Zhao plasticity model (law 48)

The elasto-plastic behavior of material with strain rate dependence is given by Zhao formula [61], [62]:

$$\sigma = (A + B\varepsilon_p^n) + (C - D\varepsilon_p^m).\ln\frac{\dot{\varepsilon}}{\dot{\varepsilon}_0} + E\dot{\varepsilon}^k \qquad \text{EQ. 9.3.4.1}$$

where: ε_p = plastic strain

$\dot{\varepsilon}$ = strain rate
A = Yield stress
B = hardening parameter
n = hardening exponent
C = relative strain rate coefficient
D = strain rate plasticity factor
m = Relative strain rate exponent
E = strain rate coefficient
k = strain rate exponent

In the case of material without strain rate effect, the hardening curve given by EQ. 9.3.4.1 is identical to those of Johnson-Cook. However, Zhao law allows a better approximation of strain rate dependent materials by introducing a nonlinear dependency.

As described for Johnson-Cook law, a strain rate filtering can be introduced to smooth the results. The plastic flow with isotropic or kinematic hardening can be modeled as described in section 9.3.3. The material failure happens when the plastic strain reaches a maximum value as in Johnson-Cook model. However, two tensile strain limits are defined to reduce stress when rupture starts:

$$\sigma_{n+1} = \sigma_n\left(\frac{\varepsilon_{t2} - \varepsilon_1}{\varepsilon_{t2} - \varepsilon_{t1}}\right) \qquad \text{EQ. 9.3.4.2}$$

Where, ε_1 is the largest principal strain, and ε_{t1} and ε_{t2} are rupture strain limits.

If $\varepsilon_1 > \varepsilon_{t1}$, the stress is reduced by EQ. 9.3.4.2. When $\varepsilon_1 > \varepsilon_{t2}$ the stress is reduced to zero.

9.3.5 Tabulated piecewise linear and quadratic elasto-plastic laws (laws 36 and 60)

The elastic-plastic behavior of isotropic material is modeled with user-defined functions for work hardening curve. The elastic portion of the material stress-strain curve is modeled using the elastic modulus, E, and Poisson's ratio, υ. The hardening behavior of the material is defined in function of plastic strain for a given strain rate (Figure 9.3.5). An arbitrary number of material plasticity curves can be defined for different strain rates. For a given strain rate, a linear interpolation of stress for plastic strain change, can be used. This is the case of law 36 in RADIOSS. However, in law 60 a quadratic interpolation of the functions allows to better simulate the strain rate effects on the behavior of material as it is developed in law 60. For a given plastic strain, a linear interpolation of stress for strain rate change is used. Compared to Johnson-Cook model (law 2), there is no maximum value for the stress. The curves are extrapolated if the plastic deformation is larger than the maximum plastic strain. The hardening model may be isotropic, kinematic or a combination of the two models as described in section 9.3.3. The material failure model is the same as in Zhao law.

For some kinds of steels the yield stress dependence to pressure has to be incorporated especially for massive structures. The yield stress variation is then given by:

$$\sigma_y = \sigma_y^{\,0}(\varepsilon_p) \times f(p) \qquad \text{EQ. 9.3.5.1}$$

Where, *p* is the pressure defined by EQ. 2.7.2.1. Drucker-Prager model described in section 9.3.6 gives a nonlinear function for $f(p)$. However, for steel type materials where the dependence to pressure is low, a simple linear function may be considered:

$$\sigma_y = \sigma_y{}^0(\varepsilon_p) \times C \times p(\varepsilon_p) \qquad \text{EQ. 9.3.5.2}$$

Where, *C* is user-defined constant and *p* the computed pressure for a given deformed configuration.
Chard in /MAT/LAW36 is same like in /MAT/LAW44. For more detail on Chard, see 9.3.3.

Figure 9.3.5 Piecewise linear stress-strain curves

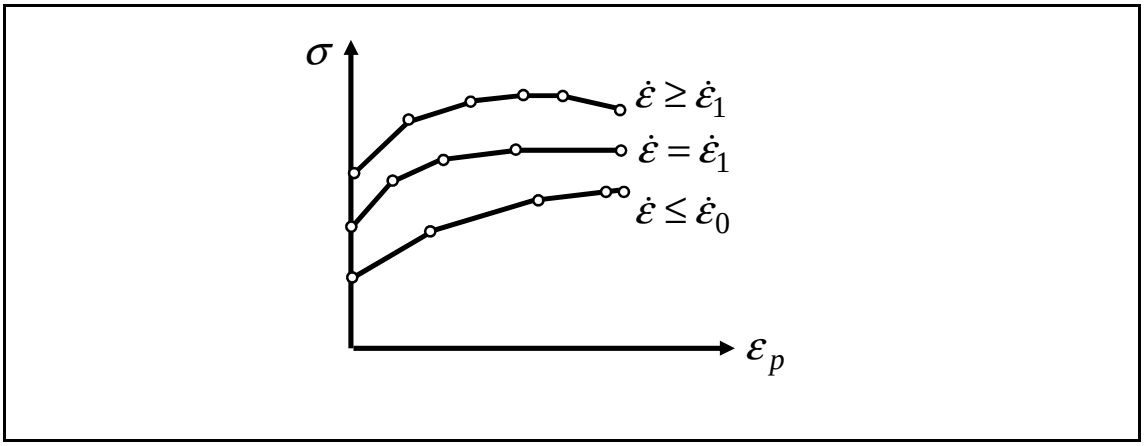

The principal strain rate is used for the strain rate definition:

$$\frac{d\varepsilon}{dt} = \frac{1}{2}\left(\frac{d\varepsilon_x}{dt} + \frac{d\varepsilon_y}{dt} + \sqrt{\left(\frac{d\varepsilon_x}{dt} - \frac{d\varepsilon_y}{dt}\right)^2 + \left(\frac{d\gamma_{xy}}{dt}\right)^2}\right) \qquad \text{EQ. 9.3.5.3}$$

For strain rate filtering, refer to section 9.3.1.2.

9.3.6 Drucker-Prager constitutive model (laws 10 & 21)

For materials like soils and rocks the frictional and dilatational effects are significant. In these materials, the plastic behavior depends on the pressure as the internal friction is proportional to the normal force. Furthermore, for frictional materials, associative plasticity laws, in which the plastic flow is normal to the yield surface, are often inappropriate. Drucker-Prager [63] yield criterion uses a modified von Mises yield criteria to incorporate the effects of pressure for massive structures:

$$F = J_2 - \left(A_0 + A_1 P + A_2 P^2\right) \qquad \text{EQ. 9.3.6.1}$$

where:

J_2 = second invariant of deviatoric stress $J_2 = \frac{1}{2} s_{ij} s_{ij}$

P = pressure

A_0 , A_1, A_2 = material coefficients

Figure 9.3.6 shows EQ. 9.3.6.1 in the plane of $\sqrt{J_2}$ and *P*. The criterion expressed in the space of principal stresses represents a revolutionary surface with an axis parallel to the trisecting of the space as shown in Figure 9.3.7. This representation is in contrast with the von Mises criteria where yield criterion has a cylindrical shape. Drucker-Prager criterion is a simple approach to model the materials with internal friction because of the symmetry of the revolution surface and the continuity in variation of normal to the yield surface.

The pressure in the material is determined in function of volumetric strain for loading phase:

$$P = f(\mu) \qquad \text{for loading } d\mu > 0 \qquad \text{EQ. 9.3.6.2}$$

Where, f is a user-defined (law 21) or a cubic polynomial function (law 10). For unloading phase, if the volumetric strain has a negative value, a linear relation is defined as:

$$P = C_1\mu \qquad \text{for unloading } d\mu < 0 \text{ and } \mu < 0 \qquad \text{EQ. 9.3.6.3}$$

For unloading with a positive volumetric strain, another linear function may be used:

$$P = B\mu \qquad \text{for unloading } d\mu < 0 \text{ and } \mu > 0 \qquad \text{EQ. 9.3.6.4}$$

In RADIOSS Drucker-Prager model is used in laws 21 and 2. Neither of these laws can reproduce the mono-dimensional behavior. In addition, no viscous effect is taken into account.

Figure 9.3.6 Yield Criteria in the plane of $\sqrt{J_2}$ and P.

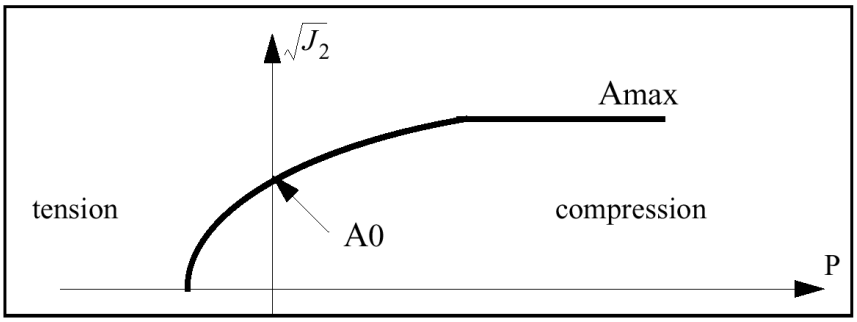

Figure 9.3.7 Drucker-Prager yield criteria in space of principal stresses

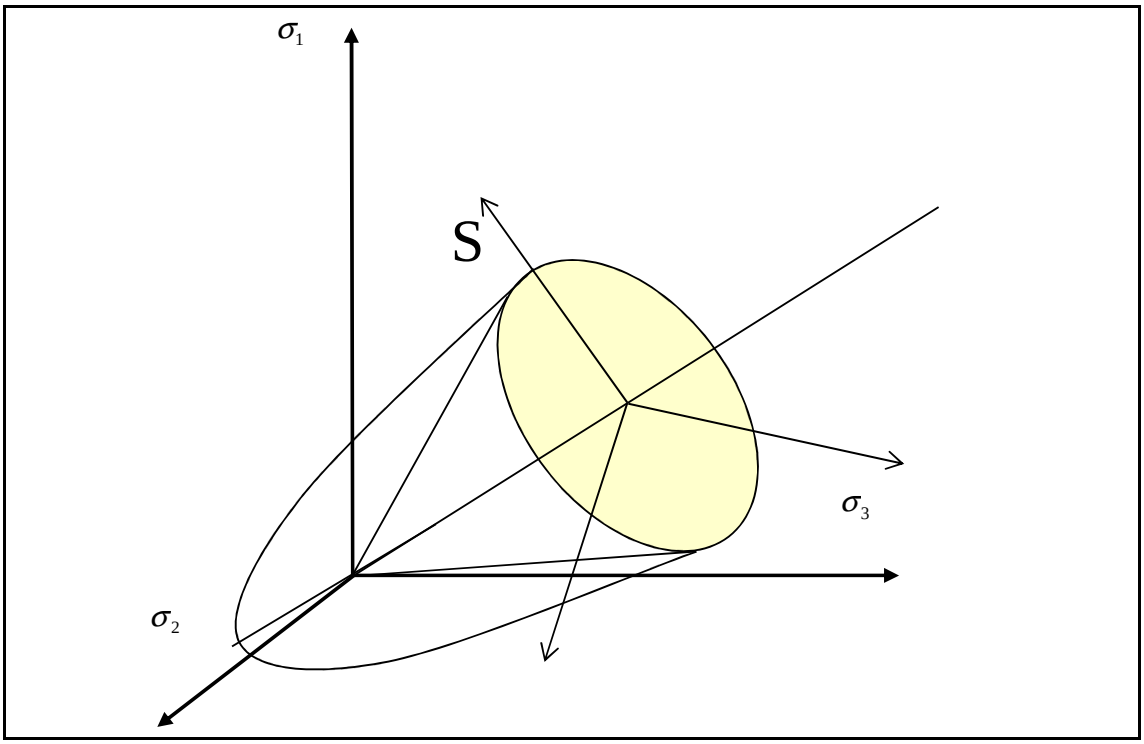

Figure 9.3.8 Material pressure variation in function of volumetric strain

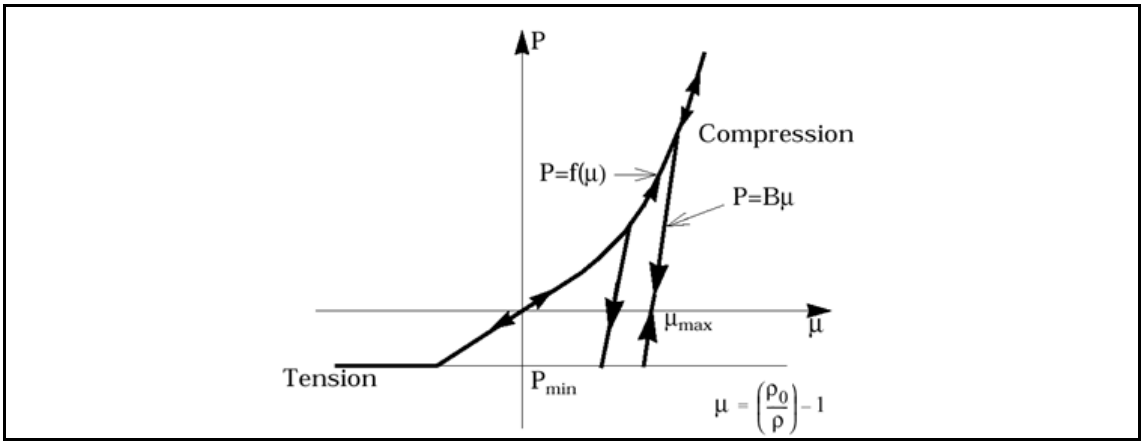

9.3.7 Brittle damage for Johnson-Cook plasticity model (law 27)

Johnson-Cook plasticity model is presented in section 9.3.1. For shell applications, a simple damage model can be associated to this law to take into account the brittle failure. The crack propagation occurs in the plan of shell in the case of mono-layer property and through the thickness if a multi-layer property is defined (Figure 9.3.9).

Figure 9.3.9 Damage Affected Material

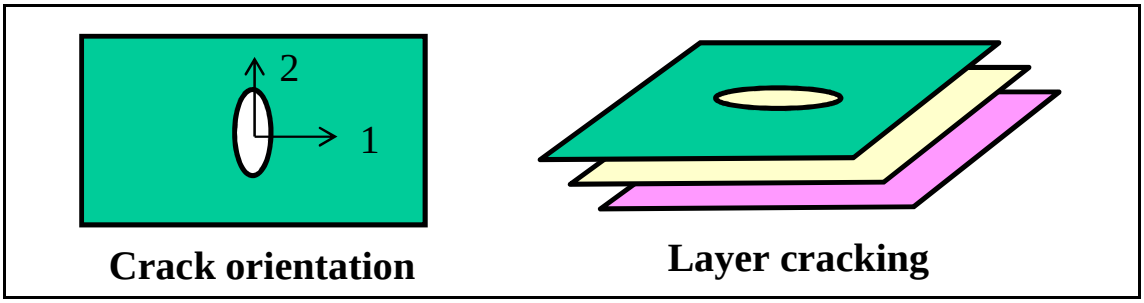

The elastic-plastic behavior of the material is defined by Johnson-Cook model. However, the stress-strain curve for the material incorporates a last part related to damage phase as shown in Figure 9.3.10. The damage parameters are:

ε_{t1} = Tensile rupture strain in direction 1

ε_{m1} = Maximum strain in direction 1

$d_{\max 1}$ = Maximum damage in direction 1

ε_{f1} = Maximum strain for element deletion in direction 1

The element is removed if one layer of element reaches the failure tensile strain, ε_{f1}. The nominal and effective stresses developed in an element are related by:

$$\sigma_n = \sigma_{eff}(1-d) \qquad \text{EQ. 9.3.7.1}$$

Where, $0 < d < 1$ is the damage factor.

The strains and the stresses in each direction are given by:

$$\varepsilon_1 = \frac{\sigma_1}{(1-d_1)E} - \frac{\nu\sigma_2}{E} \qquad \text{EQ. 9.3.7.2}$$

$$\varepsilon_2 = \frac{\sigma_2}{E} - \frac{\nu\sigma_1}{E} \qquad \text{EQ. 9.3.7.3}$$

$$\gamma_{12} = \frac{\sigma_{12}}{(1-d_1)G} \qquad \text{EQ. 9.3.7.4}$$

$$\sigma_1 = \frac{E(1-d_1)}{\left[1-(1-d_1)\nu^2\right]}\left(\varepsilon_1 + \nu\varepsilon_2\right) \qquad \text{EQ. 9.3.7.5}$$

$$\sigma_2 = \frac{E}{\left[1-(1-d_1)\nu^2\right]}\left(\varepsilon_2 + (1-d_1)\nu\varepsilon_1\right) \qquad \text{EQ. 9.3.7.6}$$

The conditions for these equations are:

$0 < d < 1$

$\varepsilon = \varepsilon_t$; d = 0

$\varepsilon = \varepsilon_m$; d = 1

A linear damage model is used to compute the damage factor in function of material strain.

$$d = \frac{\varepsilon - \varepsilon_t}{\varepsilon_m - \varepsilon_t} \qquad \text{EQ. 9.3.7.7}$$

The stress-strain curve is then modified to take into account the damage by EQ. 9.3.7.1. Therefore:

$$\sigma = E\frac{\varepsilon_m - \varepsilon}{\varepsilon_m - \varepsilon_t}\left(\varepsilon - \varepsilon_t^p\right) \qquad \text{EQ. 9.3.7.8}$$

The softening condition is given by:

$$\varepsilon_m - \varepsilon_t \le \varepsilon_t - \varepsilon_t^p \qquad \text{EQ. 9.3.7.9}$$

The mathematical approach described here can be applied to the modeling of rivets. Predit law in RADIOSS allows achievement of this end by a simple model where for the elastic-plastic behavior a Johnson-Cook model or a tabulated law (36) may be used.

Figure 9.3.10 Stress-strain curve for damage affected material

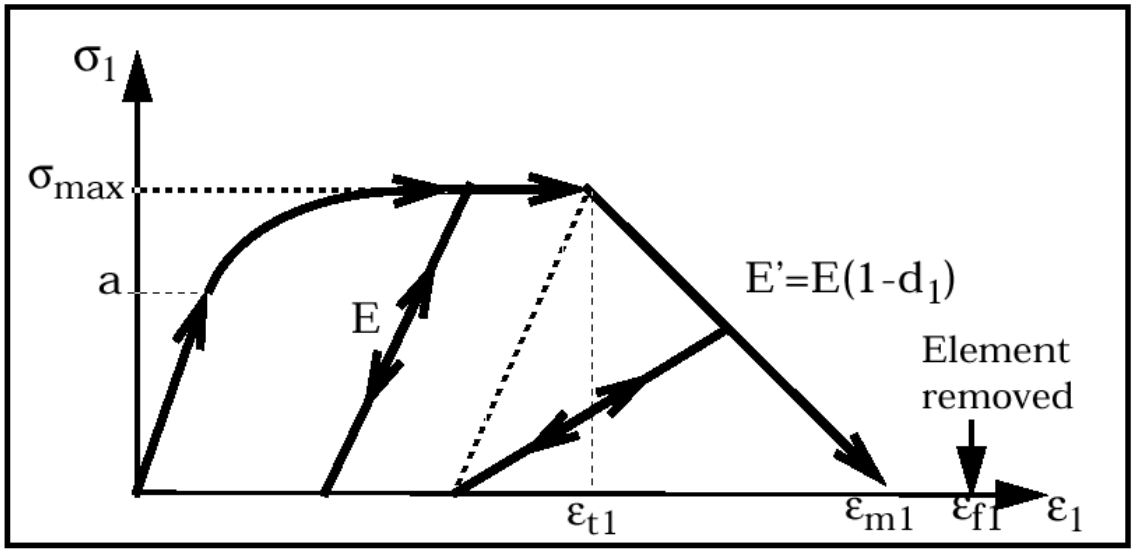

9.3.8 Brittle damage for reinforced concrete materials (law 24)

The model is a continuum, plasticity-based, damage model for concrete. It assumes that the main two failure mechanisms are tensile cracking and compressive crushing of the concrete material. The material law will enable to formulate the brittle elastic – plastic behavior of the reinforced concrete.

The input data for concrete are:

E_c Young's modulus (32000 MPa)

ν_c Poisson's ratio (0.2)

f_c Uniaxial compressive strength (32 MPa)

f_t/f_c Tensile strength ratio (default = 0.1)

f_b/f_c Biaxial strength ratio (default = 1.2)

f_2/f_c confined strength ratio (default = 4.0)

s_0/f_c confining stress ratio (default = 1.25)

Experimental results enable to determine the material parameters. This can be done by in-plane unidirectional and bi-axial tests as shown in Figure 9.3.11. The expression of the failure surface is in a general form as:

$$f(\sigma_m, J_2, f_c, f_b, \theta) - c = 0 \qquad \text{EQ. 9.3.8.1}$$

where:

J_2 = second invariant of stress

$\sigma_m = \frac{I_1}{3}$ = mean stress

θ = lode angle with $\cos 3\theta = \frac{3\sqrt{3}}{2}\frac{J_3}{J_2^{3/2}}$

A schematic representation of the failure surface in the principal stress space is given in Figure 9.3.12. The yield surface is derived from the failure envelope by introducing a scale factor k(σ_m, θ). The meridian planes are presented in Figure 9.3.13.

The steel directions are defined identically to material law 14 by a type 6 property set. If a property set is not given in the element input data, r ,s , Ψ are taken respectively as direction 1, 2, 3. For quad elements, direction 3 is taken as the Ψ direction.

Steel data properties are:

E = Young's modulus

σ_y = Yield strength

E_t = Tangent modulus

α_1 = Ratio of reinforcement in direction 1

α_2 = Ratio of reinforcement in direction 2

α_3 = Ratio of reinforcement in direction 3

Figure 9.3.11 Failure surface in plane stress

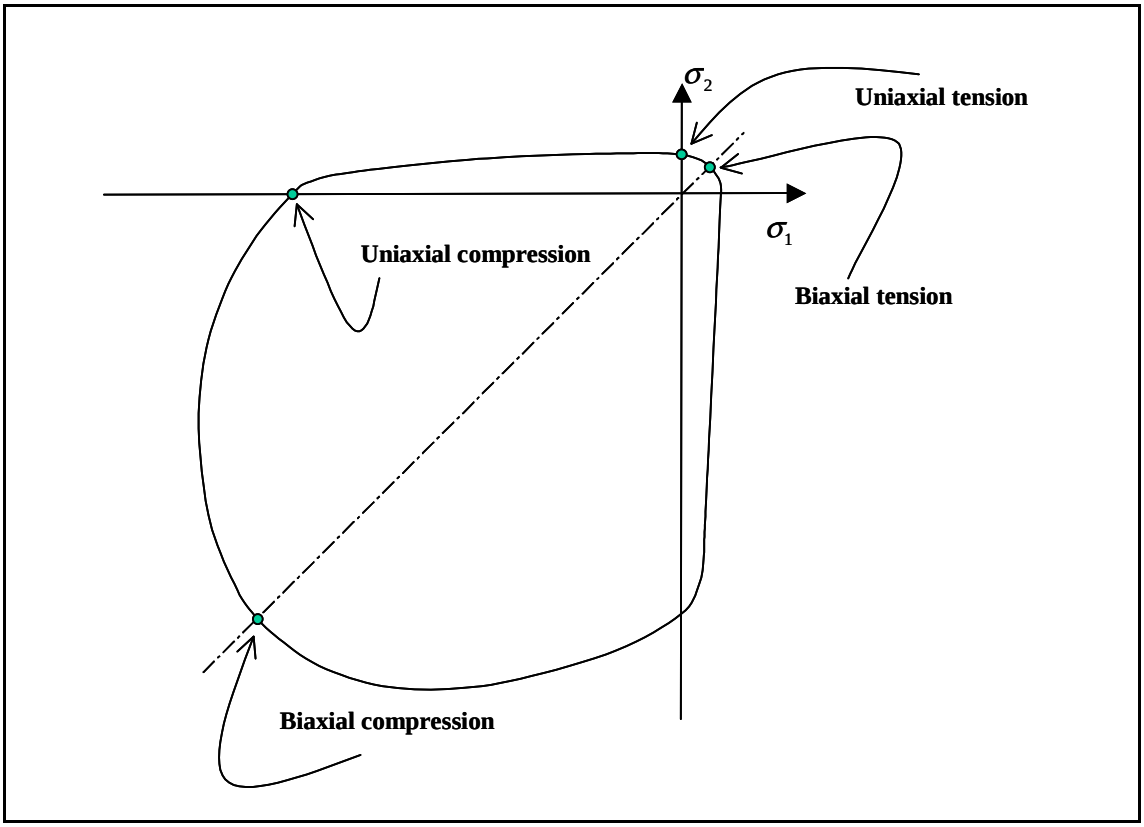

Figure 9.3.12 Failure surface in principal stress space

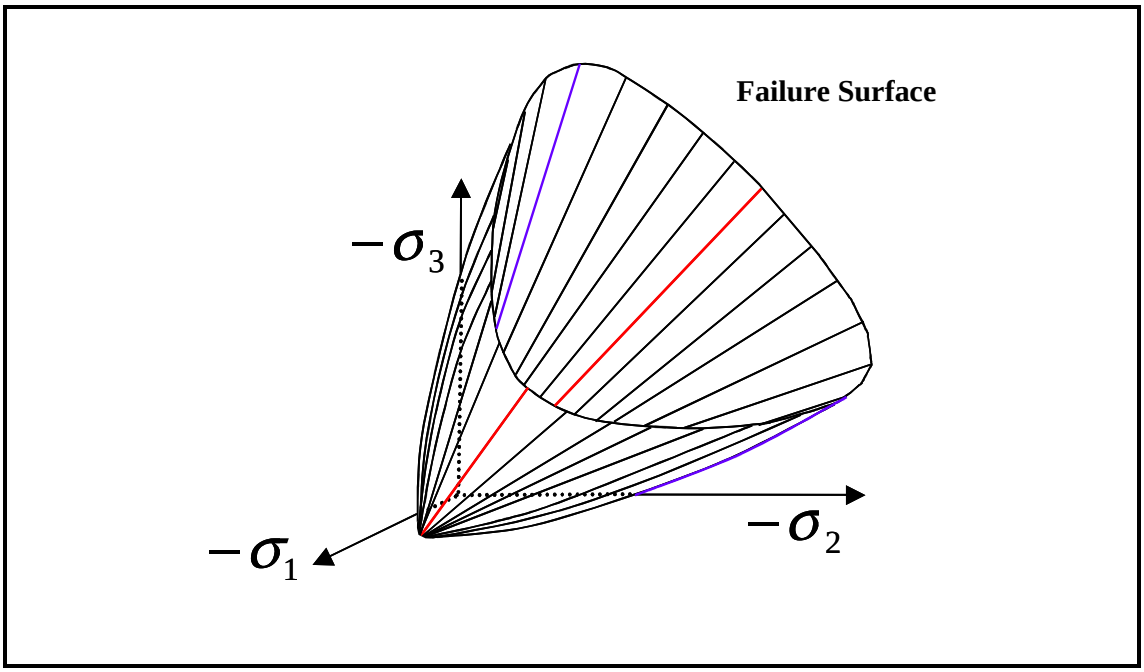

Figure 9.3.13 Meridians of failure and yield surfaces

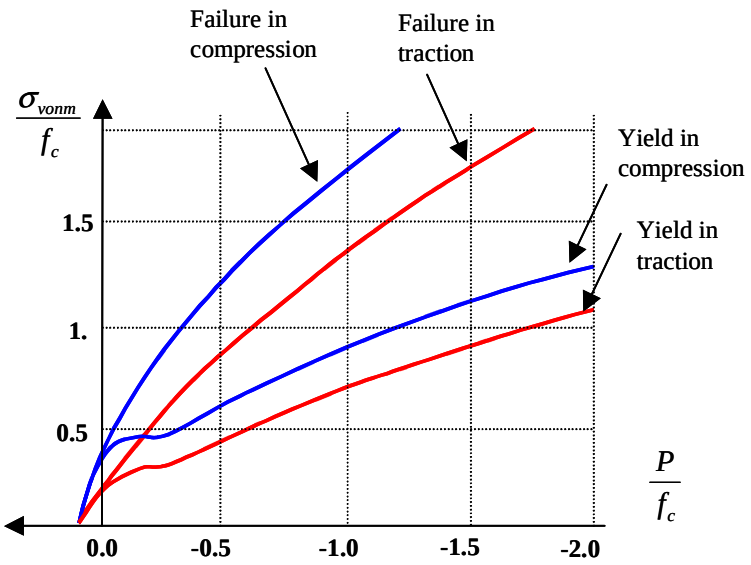

9.3.9 Ductile damage model

In section 9.3.7, a damage model for brittle materials is presented. It is used in RADIOSS law (27) valid for shell meshes. The damage is generated when the shell works in traction only. A generalized damage model for ductile materials is incorporated in RADIOSS laws (22), and (23). The damage is not only generated in traction but also in compression and shear. It is valid for solids and shells. The elastic-plastic behavior is formulated by Johnson-Cook model. The damage is introduced by the use of damage parameter, δ . The damage appears in the material when the strain is larger than a maximum value, ε_{dam} :

$$0 \le \delta \le 1$$

- If $\varepsilon < \varepsilon_{dam} \Rightarrow \delta = 0$ Law 22 is identical to law 2.
- If $\varepsilon \ge \varepsilon_{dam} \Rightarrow E_{dam} = (1-\delta)E$ and $\nu_{dam} = \frac{1}{2}\delta + (1-\delta)\nu$

This implies an isotropic damage with the same effects in tension and compression. The inputs of the model are the starting damage strain ε_{dam} and the slope of the softening curve E_t as shown in Figure 9.3.14.

For brick elements the damage law can be only applied to the deviatoric part of stress tensor s_{ij} and $G_{dam} = \frac{E_{dam}}{2(1+\nu_{dam})}$. This is the case of law (22) in RADIOSS. However, if the application of damage law to stress tensor σ_{ij} is expected, RADIOSS law (23) may be used.

Figure 9.3.14 Ductile damage model

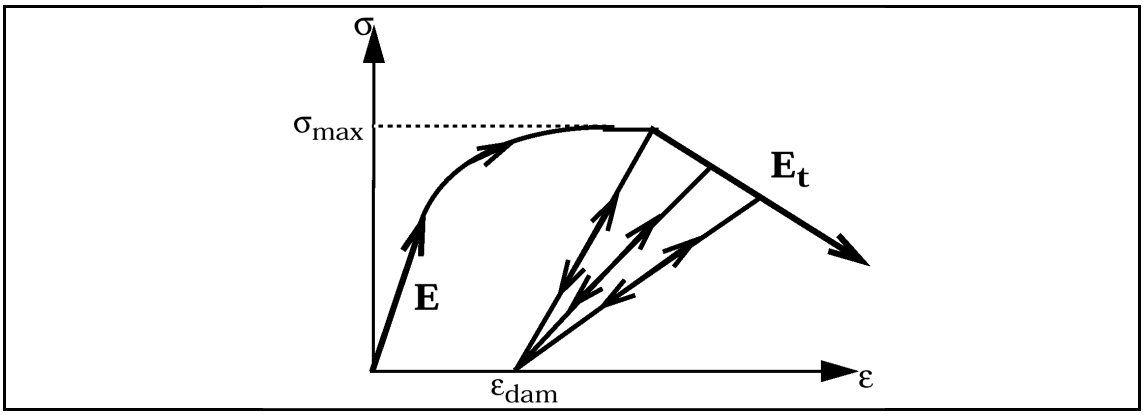

The strain rate definition and filtering for these laws are explained in section 9.3.1. The strain rate $\dot{\varepsilon}$ may or may not affect the maximum stress value σ_{max} according to the user's choice as shown in Figure 9.3.15.

Figure 9.3.15 Strain rate dependency

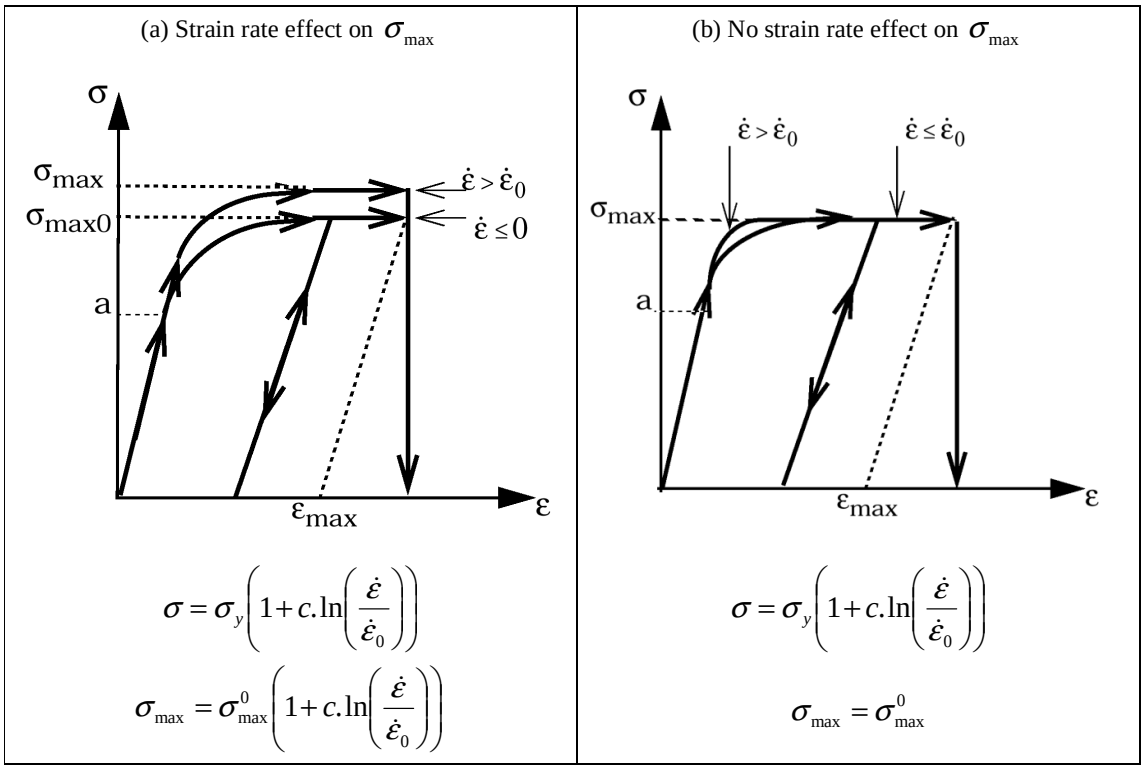

9.3.10 Ductile damage model for porous materials (Gurson law 52)

The Gurson constitutive law [64] models progressive microrupture through void nucleation and growth. It is dedicated to high strain rate elasto-viscoplastic porous metals. A coupled damage mechanical model for strain rate dependent voided material is used. The material undergoes several phases in the damage process as described in Figure 9.3.16.

Figure 9.3.16 Damage process for visco-elastic-plastic voided materials

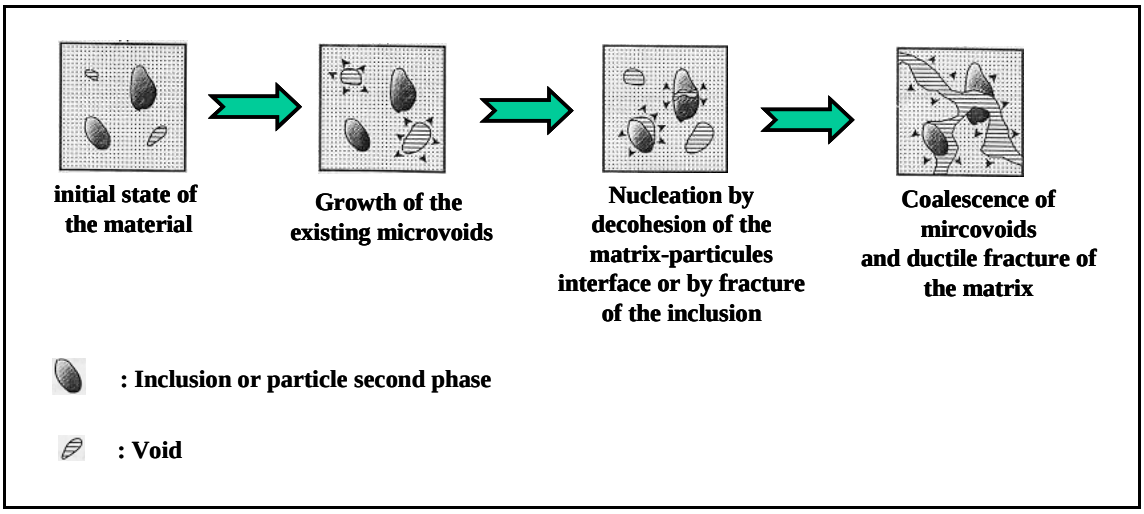

The constitutive law takes into account the void growth, nucleation and coalescence under dynamic loading. The evolution of the damage is represented by the void volume fraction, defined by:

$$f = \frac{V_a - V_m}{V_a} \qquad \text{EQ. 9.3.10.1}$$

Where V_a , V_m are respectively the elementary apparent volume of the material and the corresponding elementary volume of the matrix. The rate of increase of the void volume fraction is given by:

$$\dot{f} = \dot{f}_g + \dot{f}_n \qquad \text{EQ. 9.3.10.2}$$

The growth rate of voids is calculated by:

$$\dot{f}_g = (1-f)\,Trace\left[D^p\right] \qquad \text{EQ. 9.3.10.3}$$

Where *Trace[D^p]* is the trace of the macroscopic plastic strain rate tensor. The nucleation rate of voids is given by the following expression:

$$\dot{f}_n = \frac{f_N}{S_N\sqrt{2\pi}} e^{-\frac{1}{2}\left(\frac{\varepsilon_M - \varepsilon_N}{S_N}\right)^2} \dot{\varepsilon}_M \qquad \text{EQ. 9.3.10.4}$$

Where f_N is the nucleated void volume fraction, S_N is the Gaussian standard deviation, ε_N is the nucleated effective plastic strain and ε_M is the admissible plastic strain.

The viscoplastic flow of the porous material is described by:

$$\begin{cases} \Omega_{evp} = \dfrac{\sigma_{eq}^2}{\sigma_M^2} + 2q_1 f^* \cosh\left(\dfrac{3}{2} q_2 \dfrac{\sigma_m}{\sigma_M}\right) - \left(1 + q_3 f^{*2}\right) & if \quad \sigma_m > 0 \\ \Omega_{evp} = \dfrac{\sigma_{eq}^2}{\sigma_M^2} + 2q_1 f^* - \left(1 + q_3 f^{*2}\right) & if \quad \sigma_m \le 0 \end{cases} \qquad \text{EQ. 9.3.10.5}$$

Where σ_{eq} the von Mises is effective stress; σ_M is the admissible elasto-viscoplastic stress; σ_m is the hydrostatic stress and f^* is the specific coalescence function which can be written as:

$$\begin{cases} f^* = f & if \quad f \le f_c \\ f^* = f_c + \dfrac{f_u - f_c}{f_F - f_c}(f - f_c) & if \quad f > f_c \end{cases} \qquad \text{EQ. 9.3.10.6}$$

Where:

- f_c is the critical void volume fraction at coalescence,
- f_F is the critical void volume fraction at ductile fracture,
- f_u is the corresponding value of the coalescence function $f_u = \dfrac{1}{q_1}$, $f^*(f_F) = f_u$.

The variation of the specific coalescence function is shown in Figure 9.3.17.

Figure 9.3.17 Variation of specific coalescence function

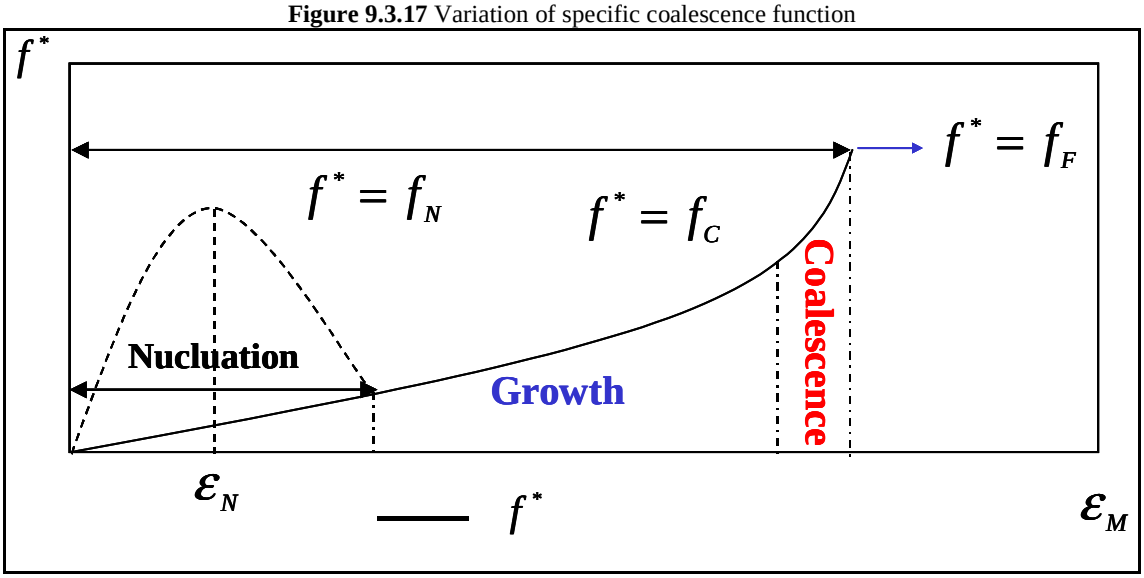

The admissible plastic strain rate is computed as follows:

$$\dot{\varepsilon}_M = \frac{\sigma : D^p}{(1-f)\sigma_M} \qquad \text{EQ. 9.3.10.7}$$

Where σ is the Cauchy stress tensor; σ_M is the admissible plastic stress and D^p is the macroscopic plastic strain rate tensor which can be written in the case of the associated plasticity as:

$$D^p = \dot{\lambda}\frac{\partial \Omega_{evp}}{\partial \sigma} \qquad \text{EQ. 9.3.10.8}$$

with Ω_{evp} the yield surface envelope. The viscoplastic multiplier is deduced from the consistency condition:

$$\Omega_{evp} = \dot{\Omega}_{evp} = 0 \qquad \text{EQ. 9.3.10.9}$$

From this last expression we deduce that:

$$\dot{\lambda} = \frac{\Omega_{evp}}{\frac{\partial \Omega_{evp}}{\partial \sigma} : C^e : \frac{\partial \Omega_{evp}}{\partial \sigma} - \frac{\partial \Omega_{evp}}{\partial \sigma_M}\frac{\partial \sigma_M}{\partial \varepsilon_M} A_2 - \frac{\partial \Omega_{evp}}{\partial f}\left[(1-f)\frac{\partial \Omega_{evp}}{\partial \sigma} : I + A_1 A_2\right]}$$ EQ. 9.3.10.10

where:

$$A_2 = \frac{\sigma : \frac{\partial \Omega_{evp}}{\partial \sigma}}{(1-f)\sigma_M}; \quad A_1 = \frac{f_N}{S_N\sqrt{2\pi}} e^{-\frac{1}{2}\left(\frac{\varepsilon_M - \varepsilon_N}{S_N}\right)^2}$$ EQ. 9.3.10.11

9.3.11 Connect materials (law 59)

For the moment /MAT/LAW59 is only compatible with /PROP/TYPE43 and /FAIL/CONNECT.

Solid connection element and material:

These materials and properties are only compatible with each other; /FAIL/CONNECT, and the designated failure model.

They are designed for spotweld, welding line or glue type connections.

The property is only compatible with standard 8 node brick elements. The element orientation with respect to the connected surfaces is important, and must be defined, as shown below:

Figure 9.3.18 solid connect element

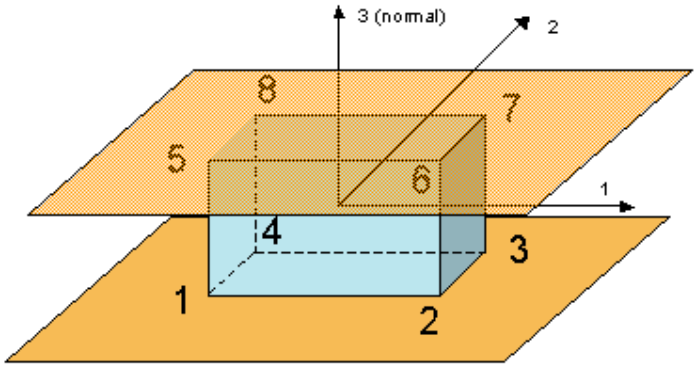

The main characteristic of CONNECT property is the time step is independent on the element height, only on the section surface area. Hence, it can be used for glue or spotweld connections, with null height distance.

Element definition:

The element local coordinate system is constructed in the mid-plane section between the bottom and top faces. The orientation is the same as in RADIOSS shell elements:

Figure 9.3.19 Points 1a, 2a, 3a and 4a are in the mid distance between bottom and top face nodes

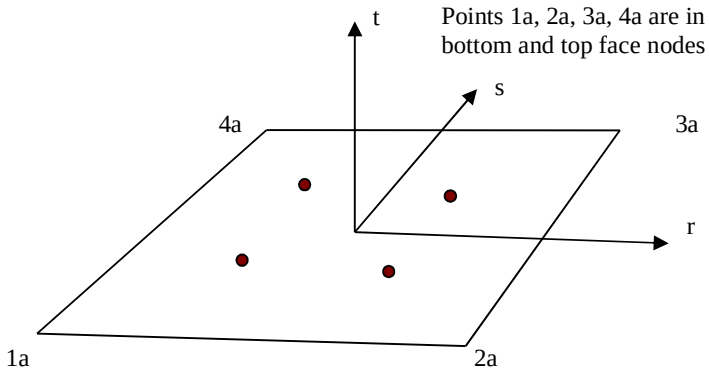

The local element system is fully corotational (not only convected), local deformations are thus independent on rigid element rotations.

The element has four Gauss integration points placed in the mid plane section. Element deformation in each point is constructed using nodal displacements and linear function forms in the following way:

Dzz = sum(Ni*Vzi)i=5,6,7,8 - sum(Nj*Vzj)j=1,2,3,4
Dxz = sum(Ni*Vxi)i=5,6,7,8 - sum(Nj*Vxj)j=1,2,3,4
Dyz = sum(Ni*Vyi)i=5,6,7,8 - sum(Nj*Vyj)j=1,2,3,4

Vx, Vy, and Vz being nodal velocities in local corotational system and Ni the function forms.

It's important to note that these independent variables are not deformations but relative displacements (velocities).

The element has only three "strain" components – traction/compression in normal (Z) direction and both transverse shears XZ and YZ. Actually, in-plane shear, as well as lateral tractions/compressions does not give any resistance forces. It's a pure "connection" element and is not intended to be used in independent way. Both upper and bottom faces have to be tied to different structural parts.

Material law:

The elastic-plastic behavior is modeled independently in normal and tangent (in-plane) directions in each Gauss integration points, using user-defined functions for work hardening curve. There is no coupling between normal and shear direction in the material law. The hardening model is purely isotropic. Different number of hardening curves may be defined in each direction, for different values of deformation rate.

For a given strain rate, a linear interpolation between corresponding curves is used to find the value of the yield stress for the actual plastic elongation.

Deformation rates may be optionally filtered. In this regard, the law is similar to the classical elastic-plastic tabulated approach.

Nodal forces are assembled using stress components calculated in each Gauss integration point, and additional treatment is performed to assure global force and moment balance at every time step.

Input parameters for material law:

The material stiffness parameters are input as total element rigidity per section area, which is equivalent to the Young and shear modulus per height unit [kg / (m^2 s^2)].

The hardening functions are expressed as engineering stress relative to plastic elongations.

Element stability:

The element does not have its own elementary time step. Corresponding nodal time step is calculated using nodal masses and stiffness to assure the numerical stability. In RADIOSS v12.0 the nodal time step is imposed to the whole model, in the next releases the elementary time step is option is maintained if chosen in the engine input file, only the connection material elements will use nodal time step.

9.4 Viscous materials

General case of viscous materials represents a time-dependent inelastic behavior. However, special attention is paid to the viscoelastic materials such as polymers exhibiting a rate- and time-dependent behavior. The viscoelasticity can be represented by a recoverable instantaneous elastic deformation and a non-recoverable viscous part occurring over the time. The characteristic feature of viscoelastic material is its fading memory. In a perfectly elastic material, the deformation is proportional to the applied load. In a perfectly viscous material, the rate of change of the deformation over time is proportional to the load. When an instantaneous constant tensile stress σ_0 is applied to a viscoelastic material, a slow continuous deformation of the material is observed. When the resulting time dependent strain $\varepsilon(t)$, is measured, the tensile creep compliance is defined as :

$$D(t) = \frac{\varepsilon(t)}{\sigma_0} \qquad \text{EQ. 9.4.0.1}$$

The creep behavior is mainly composed of three phases: (i) primary creep with fast decrease in creep strain rate, (ii) secondary creep with slow decrease in creep strain rate and (iii) tertiary creep with fast increase in creep strain rate. The creep strain rate is the slope of creep strain to time curve.

Another kind of loading concerns viscoelastic materials subjected to a constant tensile strain, ε_0. In this case, the stress, $\sigma(t)$ which is called stress relaxation, gradually decreases. The tensile relaxation modulus is then defined as:

$$E(t) = \frac{\sigma(t)}{\varepsilon_0} \qquad \text{EQ. 9.4.0.2}$$

Because viscoelastic response is a combination of elastic and viscous responses, the creep compliance and the relaxation modulus are often modeled by combinations of springs and dashpots. A simple schematic model of viscoelastic material is given by the Maxwell model shown in Figure 9.4.1. The model is composed of an elastic spring with the stiffness *E* and a dashpot assigned a viscosity μ. It is assumed that the total strain is the sum of the elastic and viscous strains:

$$\varepsilon = \varepsilon^e + \varepsilon^v \qquad \text{EQ. 9.4.0.3}$$

Figure 9.4.1 Maxwell model

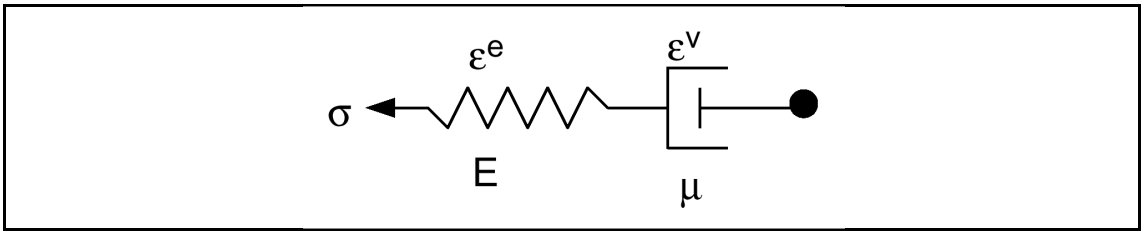

The time derivation of the last expression gives the expression of the total strain rate:

$$\dot{\varepsilon} = \dot{\varepsilon}^e + \dot{\varepsilon}^v$$ EQ. 9.4.0.4

As the dashpot and the spring are in series, the stress is the same in the two parts:

$$\sigma^e = \sigma^v = \sigma$$ EQ. 9.4.0.5

The constitutive relations for linear spring and dashpot are written as:

$$\sigma = E\varepsilon^e \quad \text{then} \quad \dot{\sigma} = E\dot{\varepsilon}^e$$ EQ. 9.4.0.6

$$\sigma = \mu\dot{\varepsilon}^v$$ EQ. 9.4.0.7

Combining EQ. 9.4.0.4, EQ. 9.4.0.6 and EQ. 9.4.0.7, an ordinary differential equation for stress is obtained:

$$\dot{\sigma} = E\left(\dot{\varepsilon} - \frac{\sigma}{\mu}\right) \quad \text{or} \quad \dot{\sigma} = E\dot{\varepsilon} - \frac{\sigma}{\tau}$$ EQ. 9.4.0.8

where $\tau = \frac{\mu}{E}$ is the relaxation time. A solution to the differential equation is given by the convolution integral:

$$\sigma(t) = \int_{-\infty}^{t} E\, e^{[-(t-t')/\tau]} \frac{d\varepsilon(t')}{dt'} dt' = \int_{-\infty}^{t} R(t-t') \frac{d\varepsilon(t')}{dt'} dt'$$ EQ. 9.4.0.9

where *R(t)* is the relaxation modulus. The last equation is valid for the special case of Maxwell one-dimensional model. It can be extended to the multi-axial case by:

$$\sigma(t) = \int_{-\infty}^{t} \mathbf{C}_{ijkl}(t-t') \frac{d\varepsilon(t')}{dt'} dt'$$ EQ. 9.4.0.10

where $\mathbf{C}_{ijkl}$ are the relaxation moduli. The Maxwell model represents reasonably the material relaxation. But it is only accurate for secondary creep as the viscous strains after unloading are not taken into account.

Another simple schematic model for viscoelastic materials is given by Kelvin-Voigt solid. The model is represented by a simple spring-dashpot system working in parallel as shown in Figure 9.4.2.

Figure 9.4.2 Kelvin-Voigt model

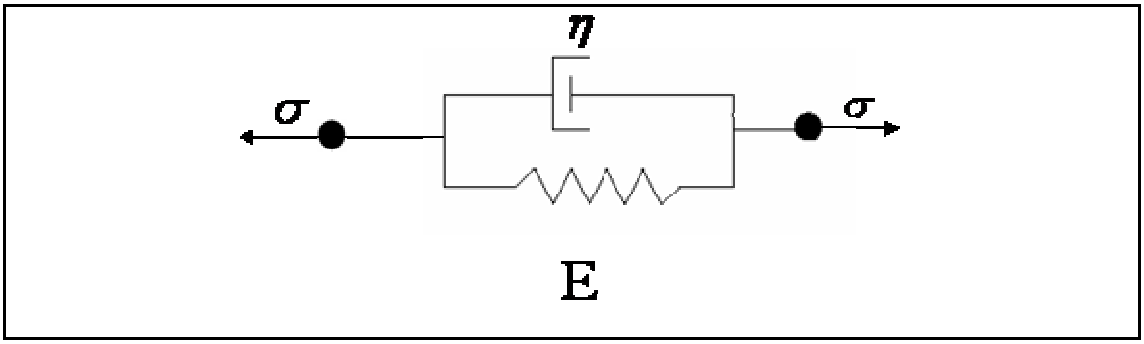

The mathematical relation of Kelvin-Voigt solid is written as:

$$\sigma = E\varepsilon + \eta\dot{\varepsilon}$$ EQ. 9.4.0.11

When $\eta = 0$ (no dashpot), the system is a linearly elastic system. When E=0 (no spring), the material behavior is expressed by Newton's equation for viscous fluids. In the above relation, a one-dimensional model is considered. For multiaxial situations, the equations can be generalized and rewritten in tensor form.

The Maxwell and Kelvin-Voigt models are appropriate for ideal stress relaxation and creep behaviors. They are not adequate for most of physical materials. A generalization of these laws can be obtained by adding other springs to the initial models as shown in Figures 9.4.3 and 9.4.4. The equations related to the generalized Maxwell model are given as:

$$\sigma = \sigma_i + \sigma_1$$ EQ. 9.4.0.12

$$\varepsilon = \frac{\sigma_i}{E_i}$$ EQ. 9.4.0.13

$$\dot{\varepsilon} = \frac{\dot{\sigma}_1}{E_1} + \frac{\sigma_1}{\eta_1}$$ EQ. 9.4.0.14

The mathematical relations which hold the generalized Kelvin-Voigt model are:

$$\varepsilon = \varepsilon^e + \varepsilon^k$$ EQ. 9.4.0.15

$$\sigma = \sigma^e + \sigma^k$$

$$\varepsilon^e = \frac{\sigma}{E} \;; \qquad \varepsilon^k = \frac{\sigma^V}{E_t} \;; \qquad \dot{\varepsilon}^k = \frac{\sigma^V}{\eta}$$

The combination of these equations enables to obtain the expression of stress and strain rates:

$$\dot{\varepsilon} = \dot{\varepsilon}^e + \dot{\varepsilon}^k = \frac{\dot{\sigma}}{E} + \dot{\varepsilon}^k$$ EQ. 9.4.0.16

$$\sigma = \eta\dot{\varepsilon}^k + E_t\varepsilon^k$$ EQ. 9.4.0.17

$$\dot{\sigma} = E\dot{\varepsilon} - \frac{(E + E_t)\sigma}{\eta} + \frac{EE_t\varepsilon}{\eta}$$ EQ. 9.4.0.18

Figure 9.4.3 Generalized Maxwell model

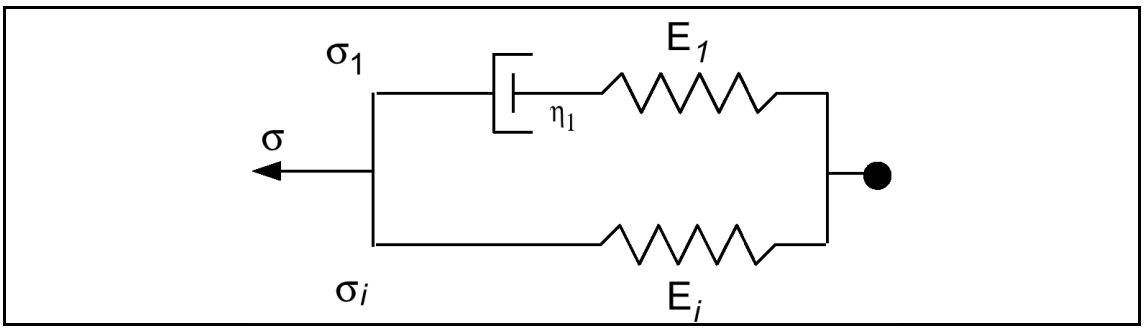

Figure 9.4.4 Generalized Kelvin-Voigt model

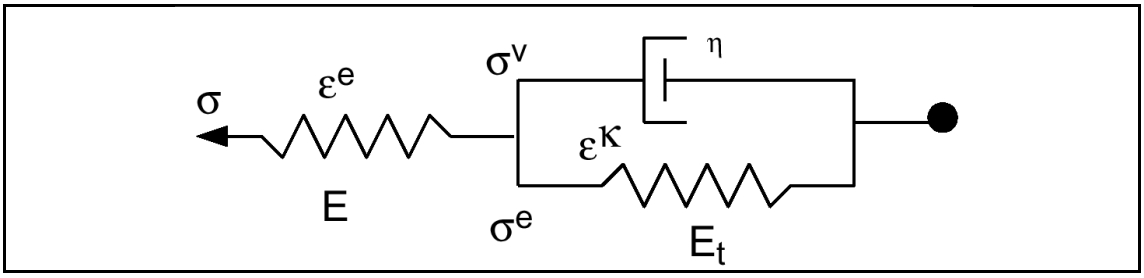

The models described above concern the viscoelastic materials. The plasticity can be introduced in the models by using a plastic spring. The plastic element is inactive when the stress is less than the yield value. The modified model is able to reproduce creep and plasticity behaviors. The viscoplasticity law (33) in RADIOSS will enable to implement very general constitutive laws useful for a large range of applications as low density closed cells polyurethane foam, honeycomb, impactors and impact limiters.

The behavior of viscoelastic materials can be generalized to three dimensions by separating the stress and strain tensors into deviatoric and pressure components:

$$s_{ij} = \int_0^t 2\Psi(t-\tau)\frac{\partial e_{ij}}{\partial \tau} d\tau \qquad \text{EQ. 9.4.0.19}$$

$$\sigma_{kk}(t) = \int_0^t 3K(t-\tau)\frac{\partial \varepsilon_{kk}}{\partial \tau} d\tau \qquad \text{EQ. 9.4.0.20}$$

where s_{ij} and e_{ij} are the stress and strain deviators. ε_{kk}, Ψ (t) and K (t) are respectively the dilatation and the shear and bulk relaxation moduli.

9.4.1 Boltzmann Viscoelastic model (law 34)

This law valid for solid elements can be used for viscoelastic materials like polymers, elastomers, glass and fluids. Elastic bulk behavior is assumed. Air pressure may be taken into account for closed cell foams:

$$P = -K\varepsilon_{kk} + P_{air} \qquad \text{EQ. 9.4.1.1}$$

with:

$$P_{air} = -\frac{P_0\gamma}{1+\gamma-\Phi} \quad ; \qquad \gamma = \frac{V}{V_0} - 1 + \gamma_0 \qquad \text{EQ. 9.4.1.2}$$

and:

$$\varepsilon_{kk} = \ln\left(\frac{V}{V_0}\right) \qquad \text{EQ. 9.4.1.3}$$

Where, γ is the volumetric strain, Φ is the porosity, P_0 is the initial air pressure, γ_0 is the initial volumetric strain and *K* is the bulk modulus. For deviatoric behavior, the generalized Maxwell model is used. The shear relaxation moduli in EQ. 9.4.0.19 is then defined as:

$$\Psi(t) = G_l + G_s \cdot e^{-\beta t} \qquad \text{EQ. 9.4.1.4}$$

$$G_s = G_0 - G_l \qquad \text{EQ. 9.4.1.5}$$

where G_0 is the short time shear modulus, G_l is the long time shear modulus and β is the decay constant, defined as the inverse of relaxation time τ_s:

$$\beta = \frac{1}{\tau_s} \quad ; \qquad \text{with } \tau_s = \frac{\eta_s}{G_s} \qquad \text{EQ. 9.4.1.6}$$

The coefficients η_s, G_s and G_l are defined for the generalized Maxwell model as shown in Figure 9.4.5.

Figure 9.4.5 Generalized Maxwell Model for Boltzmann law

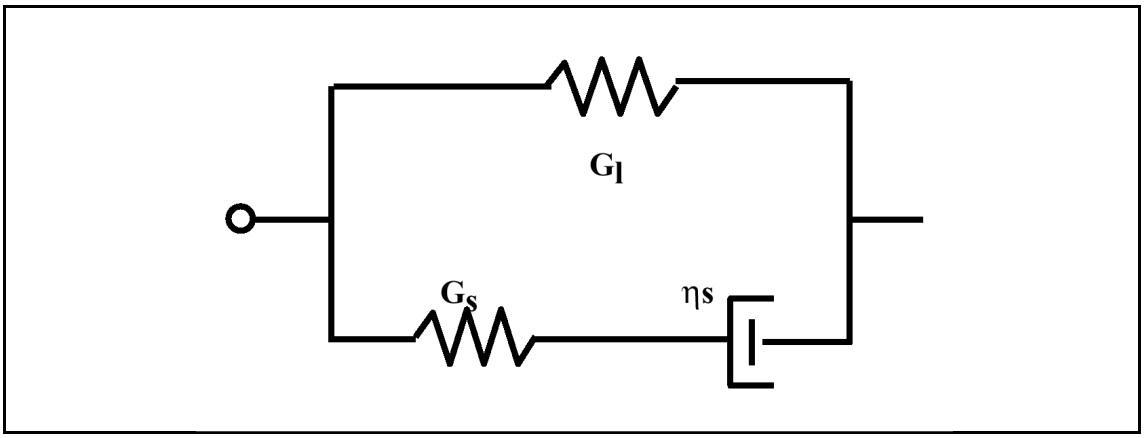

From EQ. 9.4.1.4, the value of β governs the transition from the initial modulus G_0 to the final modulus G_l. For t=0, we obtain $\Psi(t) = G_0$ and when $t \to \infty$ then $\Psi(t) \to G_l$. For a linear response, we put $G_0 = G_I$.

9.4.2 Generalized Kelvin-Voigt model (law 35)

This law uses a generalized viscoelastic Kelvin-Voigt model whereas the viscosity is based on the Navier equations. The effect of the enclosed air is taken into account via a separate pressure versus compression function. For open cell foam, this function may be replaced by an equivalent "removed air pressure" function. The model takes into account the relaxation (zero strain rate), creep (zero stress rate), and unloading. It may be used for open cell foams, polymers, elastomers, seat cushions, dummy paddings, etc. In RADIOSS the law is compatible with shell and solid meshes.

The simple schematic model in Figure 9.4.6 describes the generalized Kelvin-Voigt material model where a time-dependent spring working in parallel with a Navier dashpot is put in series with a nonlinear rate-dependent spring.

If $\sigma_m = \frac{I_1}{3}$ is the mean stress, the deviatoric stresses s_{ij} at steps *n* and *n+1* are computed by the expressions:

$$s_{ij}^n = \sigma_{ij}^n - \delta_{ij}\sigma_m^n \qquad \delta = 1 \quad for \quad i = j \quad else \quad \delta = 0 \qquad \text{EQ. 9.4.2.1}$$

$$s_{ij}^{n+1} = s_{ij}^n + \dot{s}_{ij}dt \qquad \text{EQ. 9.4.2.2}$$

with:

$$\dot{s}_{ij} = 2G\dot{e}_{ij} - \left(\frac{G+G_t}{\eta_0}s_{ij}(t)\right) + \frac{2G.G_t}{\eta_0}e_{ij} \qquad (for\ i \neq j) \qquad \text{EQ. 9.4.2.3}$$

$$\dot{s}_{ij} = G\dot{e}_{ii} - \left(\frac{G+G_t}{\eta_0}s_{ii}(t)\right) + \frac{G.G_t}{\eta_0}e_{ii} \qquad (for\ i = j) \qquad \text{EQ. 9.4.2.4}$$

where G and G_t are defined as:

$$G = Min\left(\frac{E}{2(1+\nu)}, \frac{A\dot{e}+B}{2(1+\nu)}\right) \qquad \text{EQ. 9.4.2.5}$$

$$G_t = \frac{E_t}{2(1+\nu_t)} \qquad \text{EQ. 9.4.2.6}$$

In EQ. 9.4.2.5 the coefficients *A* and *B* are defined for Young's modulus updates ($E = E_1\dot{\varepsilon} + E_2$).

Figure 9.4.6 Generalized Kelvin-Voigt model for RADIOSS law 35

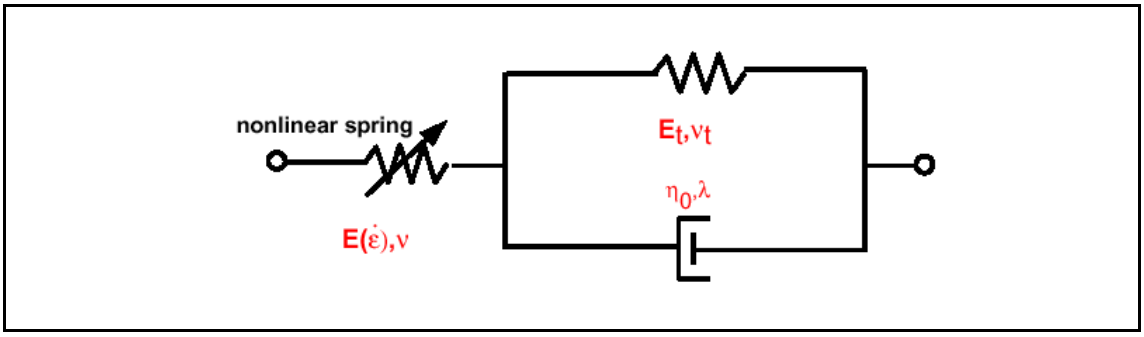

The expressions used by default to compute the pressure is:

$$\frac{dP}{dt} = C_1 K\dot{\varepsilon}_{kk} - C_2\left[\frac{K+K_t}{3\lambda+2\eta_0}\sigma_{kk}\right] + C_3\left[\frac{KK_t}{3\lambda+2\eta_0}\varepsilon_{kk}\right] \qquad \text{EQ. 9.4.2.7}$$

where:

$$K = \frac{E}{3(1-2\nu)} \qquad \text{EQ. 9.4.2.8}$$

$$K_t = \frac{E_t}{3(1-2\nu_t)} \qquad \text{EQ. 9.4.2.9}$$

$$P = -\frac{1}{3}\sigma_{kk} \qquad \text{EQ. 9.4.2.10}$$

$$\varepsilon_{kk} = \ln\left(\frac{V}{V_0}\right) \qquad \text{EQ. 9.4.2.11}$$

λ and η_0 are the Navier Stokes viscosity coefficients which can be compared to Lame constants in elasticity. $\left(\lambda + \frac{2\eta_0}{3}\right)$ is called the volumetric coefficient of viscosity. For incompressible model, $\varepsilon_{kk}^V = 0$ and $\lambda \to \infty$ and $\mu_0 = \frac{\mu}{3}$. In EQ. 9.4.2.11, C_1, C_2 and C_3 are Boolean multipliers used to define different responses. For example, C_1=1, C_2= C_3=0 refers to a linear bulk model. Similarly, C_1=C_2=C_3=1 corresponds to a visco-elastic bulk model.

For polyurethane foams with closed cells, the skeletal spherical stresses may be increased by:

$$P_{air} = -\frac{P_0 \cdot \gamma}{1 + \gamma - \Phi} \qquad \text{EQ. 9.4.2.12}$$

where γ is the volumetric strain, Φ the porosity, P_0 the initial air pressure. In RADIOSS, the pressure may also be computed with the *P* versus $\mu = \frac{\rho_0}{\rho} - 1$, by a user-defined function. Air pressure may be assumed as an "equivalent air pressure" vs. μ. You can define this function used for open cell foams or for closed cell by defining a model identical to material law FOAM_PLAS (33) (see following sections).

9.4.3 Tabulated strain rate dependent law for viscoelastic materials (law 38)

The law incorporated in RADIOSS can only be used with solid elements. It can be used to model:

- polymers,
- elastomers,
- foam seat cushions,
- dummy paddings,
- hyperfoams,
- hypoelastic materials.

In compression, the nominal stress-strain curves for different strain rates are defined by you (Figure 9.4.7). Up to 5 curves may be input. The curves represent nominal stresses versus engineering strains.

Figure 9.4.7 Nominal stress-strain curves defined by user input functions

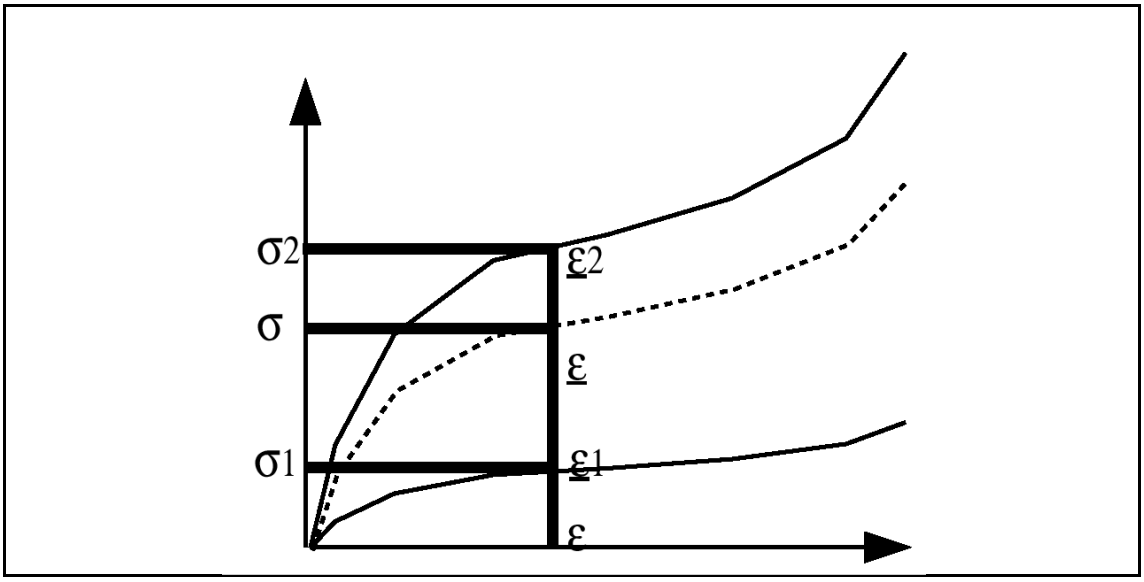

The first curve is considered to represent the static loading. All values of the strain rate lower than the assumed static curve are replaced by the strain rate of the static curve. It is reasonable to set the strain rate corresponding to the first curve equal to zero. For strain rates higher than the last curve, values of the last curve are used. For a given value of $\dot{\varepsilon}$, two values of function at ε for the two immediately lower $\dot{\varepsilon}_1$ and higher $\dot{\varepsilon}_2$ strain rates are read. The related stress is then computed as:

$$\sigma = \sigma_2 + (\sigma_1 - \sigma_2)\left(1 - \left(\frac{\dot{\varepsilon} - \dot{\varepsilon}_1}{\dot{\varepsilon}_2 - \dot{\varepsilon}_1}\right)^a\right)^b \qquad \text{EQ. 9.4.3.1}$$

Parameters *a* and *b* define the shape of the interpolation functions. If $a = b = 1$, then the interpolation is linear.

Figure 9.4.8 shows the influence of *a* and *b* parameters.

Figure 9.4.8 Influence of a and b parameters

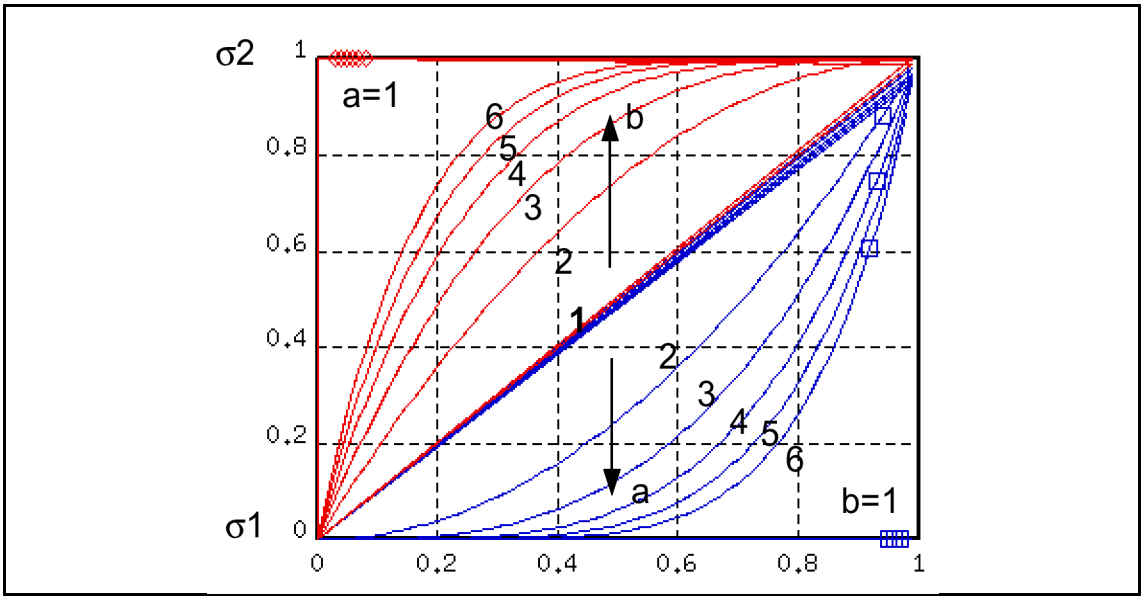

The coupling between the principal nominal stresses in tension is computed using anisotropic Poisson's Ratio:

$$\nu_{ij} = \nu_c + (\nu_t - \nu_c)\left(1 - \exp\left(-R_\nu \left|\varepsilon_{ij}\right|\right)\right) \qquad \text{EQ. 9.4.3.2}$$

Where, ν_t is the maximum Poisson's ratio in tension, ν_c being the maximum Poisson's ratio in compression, and R_ν, the exponent for the Poisson's ratio computation (in compression, Poisson's ratio is always equal to ν_c).

In compression, material behavior is given by nominal stress vs nominal strain curves as defined by you for different strain rates. Up to 5 curves may be input.

The algorithm of the formulation follows several steps:

1. Compute principal nominal strains and strain rates.
2. Find corresponding stress value from the curve network for each principal direction.
3. Compute principal Cauchy stress.
4. Compute global Cauchy stress.
5. Compute instantaneous modulus, viscosity and stable time step.

Stress, strain and strain rates must be positive in compression. Unloading may be either defined with an unloading curve, or else computed using the "static" curve, corresponding to the lowest strain rate (Figures 9.4.9 and 9.4.10).

Figure 9.4.9 Unloading behavior (no unloading curve defined)

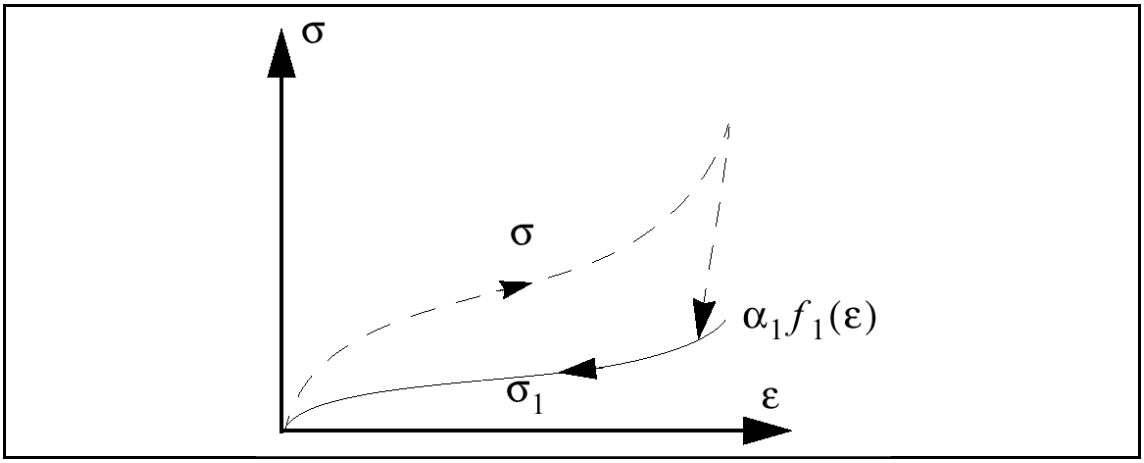

Figure 9.4.10 Unloading behavior (unloading curve defined)

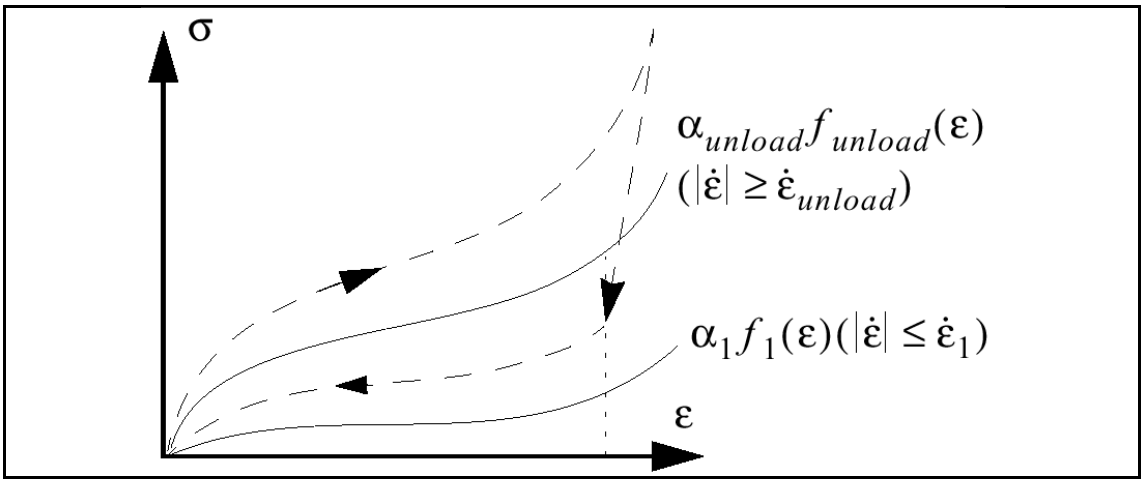

It should be noted that for stability reasons, damping is applied to strain rates with a damping factor:

$$\dot{\varepsilon}^{n-1} + R_D\left(\dot{\varepsilon}^n - \dot{\varepsilon}^{n-1}\right) \qquad \text{EQ. 9.4.3.3}$$

The stress recovery may be applied to the model in order to ensure that the stress tensor is equal to zero, in an undeformed state.

An hysteresis decay may be applied when loading, unloading or in both phases by:

$$\sigma = \sigma \cdot H \cdot \min\left(1, \left(1 - e^{-\beta\varepsilon(t)}\right)\right) \qquad \text{EQ. 9.4.3.4}$$

Where, *H* is the hysteresis coefficient, and β is the relaxation parameter.

Confined air content may be taken into account, either by using a user-defined function, or using the following relation:

$$P_{air} = P_0 \frac{\left(1 - \frac{V}{V_0}\right)}{\left(\frac{V}{V_0} - \Phi\right)} \qquad \text{EQ. 9.4.3.5}$$

The relaxation may be applied to air pressure: $P_{air} = Min(P_{air}, P_{\max})\exp(-R_p t)$.

9.4.4 Generalized Maxwell-Kelvin model for viscoelastic materials (law 40)

This law may only be applied to solid elements.

Bulk behavior is assumed to be linear:

$$\frac{dp}{dt} = K\dot{\varepsilon}_{kk} \qquad \text{EQ. 9.4.4.1}$$

Shear behavior is computed using a shear factor as follows:

$$G(t) = G_\infty + \sum_1^3 G_i e^{-\beta_i t} \qquad \text{EQ. 9.4.4.2}$$

Figure 9.4.11 Maxwell-Kelvin Model

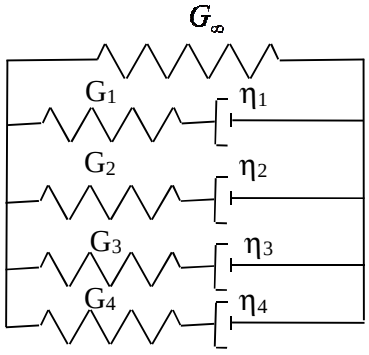

β_i are time decays, $\beta_i = \frac{G_i}{\eta_i} = \frac{1}{\tau_i}$ with τ_i being relaxation time.

9.4.5 Visco-elasto-plastic materials for foams (law 33)

This material law can be used to model low density closed cell polyurethane foams, impactors, impact limiters. It can only be used with solid elements.

The main assumptions in this law are the following:

- The components of the stress tensor are uncoupled until full volumetric compaction is achieved (Poisson's ration = 0.0).
- The material has no directionality.
- The effect of enclosed air is considered via a separate Pressure vs Volumetric Strain relation:

$$P_{air} = -\frac{P_0 \cdot \gamma}{1 + \gamma - \Phi} \qquad \text{EQ. 9.4.5.1}$$

with: $\gamma = \frac{V}{V_0} - 1 + \gamma_0$ EQ. 9.4.5.2

Where, γ is the volumetric strain, Φ is the porosity, P_0 is the initial air pressure, and γ_0 is the initial volumetric strain.

- The skeletal stresses $\left(\sigma^s\right)$ before yield follow the Maxwell-Kelvin-Voight viscoelastic model (see Figure 9.4.12):

Figure 9.4.12 Maxwell-Kelvin-Voight Model

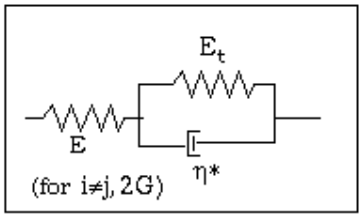

$$\sigma_{ij}^s\left(t+\Delta t\right)=\sigma_{ij}^s\left(t\right)+\left(E\dot{\varepsilon}_{ij}-\left(\frac{E+E_t}{\eta}\cdot\sigma_{ij}^s\left(t\right)\right)+\frac{EE_t}{\eta}\cdot\varepsilon_{ij}\right)\cdot\Delta t \qquad \text{EQ. 9.4.5.3}$$

- The Young's Modulus used in the calculation is: $E=\max\left(E,E_1\dot{\varepsilon}+E_2\right)$
- Plasticity is defined by a user-defined curve vs volumetric strain, γ, or $\sigma_y=A+B\left(1+C\gamma\right)$
- Plasticity is applied to the principal skeletal stresses.
- The full stress tensor is obtained by adding air pressure to the skeletal stresses:

$$\sigma_{ij}\left(t\right)=\sigma_{ij}^s\left(t\right)-\left(P_{air}\cdot\delta_{ij}\right) \qquad \text{EQ. 9.4.5.4}$$

9.4.6 Hyper visco-elastic law for foams (law 62)

Experimental tests on foam specimens working in compression illustrate that the material behavior is highly nonlinear. The general behavior can be subdivided into three parts related to particular deformation modes of material cells. When the strain is small, the cells working in compression deform in membrane without causing buckling in its lateral thin-walls. In the second step, the lateral thin-walls of the cells buckle while the material undergoes large deformation. Finally, in the last step the cells are completely collapsed and the contact between the lateral thin-walled cells increases the global stiffness of the material.

As the viscous behavior of foams is demonstrated by various tests, it is worthwhile to elaborate a material law including the viscous and hyper elasticity effects. This is developed in [101] where a decoupling between viscous and elastic parts is introduced by using finite transformations. Only the deviatoric part of the stress tensor is concerned by viscous effects.

Material law 62 corresponds to a hyper-elastic solid material using the Ogden formulation for rubber material. The strain energy functional is given by [34]:

$$W\left(\mathbf{C}\right)=\sum_{i=1}^{N}\frac{2\mu_i}{\alpha_i^{\,2}}\left(\lambda_1^{\alpha_i}+\lambda_2^{\alpha_i}+\lambda_3^{\alpha_i}-3+\frac{1}{\beta}\left(J^{-\alpha_i\beta}-1\right)\right) \qquad \text{EQ. 9.4.6.1}$$

Where, $\mathbf{C}$ is the right Cauchy Green Tensor, $C=F^tF$ with F the deformation gradient matrix, λ_i are the eigenvalues of **F,** J = det **F**,

$$\beta=\frac{\nu}{(1-2\nu)},\ \nu\neq 0 \text{ and } \nu\neq\frac{1}{2}$$

Note that for rubber materials which are almost incompressible: the bulk modulus is very large compared to the shear modulus.

The ground shear modulus is given by:

$$\mu = \sum_{i=1}^{N} \mu_i$$ EQ. 9.4.6.2

W can be written as:

$$W(C) = \overline{W}(\overline{C}) + U(J)$$ EQ. 9.4.6.3

Where $\overline{C} = \overline{F}^t \overline{F}$, $\overline{F} = J^{-1/3} F$

$\overline{C}$ is the deviatoric part of the right Cauchy Green Tensor

U and $\overline{W}$ are the volumetric and deviatoric parts of the stored energy functions and S_0 the second Piola-Kirchhoff stress tensor given by:

$$S_0 = \frac{\partial W}{\partial E} = 2\frac{\partial W}{\partial C} = 2\frac{\partial \overline{W}}{\partial C} + 2\frac{\partial U}{\partial C} = S_0^{dev} + S_0^{vol}$$ EQ. 9.4.6.4

With $E = \frac{1}{2}(C - I)$

The Green-Lagrange strain tensor:

$S_0^{dev} = 2\frac{\partial \overline{W}}{\partial C}$ and $S_0^{vol} = 2\frac{\partial U}{\partial C}$ are the deviatoric and volumetric parts of the second Piola-Kirchhoff stress tensor S_0.

Rate effects are modeled through visco-elasticity using a convolution integral using Prony series. This corresponds to an extension of small strain theory or finite deformation to large strain. The rate effect is applied only to the deviatoric stress. The deviatoric stress is computed as:

$$S^{dev}(t) = \gamma_\infty S_0^{dev}(t) - J^{-2/3} DEV[\sum_{i=1}^{M_i} Q_i(t)]$$ EQ. 9.4.6.5

Q_i is the internal variable given by the following rate equations:

$$\dot{Q}_i(t) + \frac{1}{\tau_i} Q_i(t) = \frac{\gamma_i}{\tau_i} DEV[2\frac{\partial \overline{W}}{\partial \overline{C}}(t)]$$ EQ. 9.4.6.6

$\lim Q_i(t) = 0$, $t \to -\infty$

$\gamma_i \in [0,1]$, $\tau_i > 0$

Q_i is given by the following convolution integral:

$$Q_i(t) = \frac{\gamma_i}{\tau_i} \int_{-\infty}^{t} \exp\left[-(t-s)/\tau_i\right] \frac{d\left[DEV\{2\partial_{\overline{C}} \overline{W}^0[\overline{C}(s)]\}\right]}{ds} ds$$ EQ. 9.4.6.7

Where:

$\gamma_\infty = G_\infty / G_0$ $\qquad$ $1 = \gamma_\infty + \sum_{i=1}^{M_i} \gamma_i$

$\gamma_i = G_i / G_0$ $\qquad$ $G_0 = G_\infty + \sum_{i=1}^{M_i} G_i$

$dev(\bullet) = \bullet - \frac{1}{3}(\bullet : C)C^{-1}$

G_0 is the initial shear modulus; G_0 should be exactly the same as the ground shear modulus μ. G_∞ is the long-term shear modulus that can be obtained from long-term material testing. τ_i are the relaxation times.

The relation between the second Piola-Kirchhoff stress tensor $S = S^{dev} + S_0^{vol}$ and Cauchy stress tensor σ is:

$$\sigma = \frac{1}{\det F} FSF^t \qquad \text{EQ. 9.4.6.8}$$

The reader is invited to consult references [101], [102], and [118] for more details.

9.5 Materials for Hydrodynamic Analysis

The following material laws are commonly used for fluid simulations:

- Johnson-Cook model for strain rate and temperature dependence on yield stress (law 4),
- Hydrodynamic viscous material for Newtonian or turbulent fluids (law 6),
- Elasto-plastic hydrodynamic materials with von Mises isotropic hardening and polynomial pressure (law 3),
- Steinberg-Guinan elasto-plastic hydrodynamic law with thermal softening (law 49),
- Boundary element materials (law 11),
- Purely thermal materials (law 18)

RADIOSS provides a material database incorporated in the installation. Many parameters are already defined by default and give accurate results. Some of them are described in the following sections:

energy and pressure equations are solved simultaneously.

9.5.1 Johnson Cook Law for Hydrodynamics (law 4)

This law enables to model hydrodynamic behavior of an elastic-plastic material using Johnson-Cook Yield criteria and any equation of state available with /EOS card. It based on law3 (/MAT/LAW3) and adds strain rate and temperature dependency. The advantage of material law04 regarding classical law02 (/MAT/JCOOK) is that you can choose any available EOS from /EOS card.

The equation describing yield stress (scale value) is:

$$\sigma_y = \left(A + B\ \varepsilon_p^{\,n}\right)\left(1 + C \ln\frac{\dot{\varepsilon}}{\dot{\varepsilon}_0}\right)\left(1 - T^{*m}\right) \qquad \text{EQ. 9.5.1.1}$$

where $T^* = \left(\frac{T - T_0}{T_{melt} - T_0}\right)$

The pressure and energy values are obtained by solving equation of state P(μ,E) related to the material (/EOS).

Material parameters are the same as in law 3.

The parameters are:

C = Strain rate coefficient

$\dot{\varepsilon}_0$ = Reference strain rate.

m = Temperature exponent

T_{melt} = Melting temperature

T_{max} = Maximum Temperature. For T > T_{max} : m=1 is used.

$p_0 C_p$ = specific heat per unit volume

For an explanation about strain rate filtering, refer to Chapter 9.3.1.2.

9.5.2 Hydrodynamic Viscous Fluid Law (law 6)

This law is specifically designed to model liquids and gases.

The equations used to describe the material are:

$$S_{ij} = 2\rho\nu\dot{e}_{ij} \quad \text{EQ. 9.5.2.1}$$

$$p = C_0 + C_1\mu + C_2\mu^2 + C_3\mu^3 + (C_4 + C_5\mu)E_n \quad \text{EQ. 9.5.2.2}$$

Where, S_{ij} is the deviatoric stress tensor, ν is the kinematic viscosity, and $\dot{e}_{ij}$ is the deviatoric strain rate tensor.

The kinematic viscosity ν is related to the dynamic viscosity, η by:

$$\nu = \frac{\eta}{\rho} \quad \text{EQ. 9.5.2.3}$$

9.5.2.1 Modeling a perfect gas

To model a perfect gas, all coefficients C_0, C_1, C_2, C_3 must be set to equal zero. Also:

$$C_4 = C_5 = \gamma - 1 \quad \text{EQ. 9.5.2.4}$$

$$E_{n0} = \frac{P_0}{\gamma - 1} \quad \text{EQ. 9.5.2.5}$$

A perfect gas allows compressibility and expansion and contraction with a rise in temperature. However, for many situations, especially very slow subsonic flows, an incompressible gas gives accurate and reliable results with less computation.

9.5.2.2 Modeling an incompressible gas

To model an incompressible gas, the coefficients should be set to:

$$C_0 = C_2 = C_3 = C_4 = C_5 = E_0 = 0 \quad \text{EQ. 9.5.2.6}$$

$$C_1 = \rho_0 \cdot c^2 \quad \text{EQ. 9.5.2.7}$$

where, *c* is the speed of sound.

Incompressibility is achieved via a penalty method. The sound speed is set to at least 10 times the maximum velocity.

This classical assumption is not valid when fluid and structures are coupled. In this case, set the sound speed in the fluid so that the first eigen frequency is at least 10 times higher in the fluid than in the structure.

9.5.3 Elasto-plastic Hydrodynamic Material (law 3)

This law is only used with solid brick and quadrilateral elements. It models the elastic and plastic regions, similar to law 2, with a non-linear behavior of pressure and without strain rate effect. The law is designed to simulate materials in compression.

The stress - strain relationship for the material under tension is:

$$\sigma = \left(A + B\varepsilon_p^n\right) \qquad \text{EQ. 9.5.3.1}$$

The pressure and energy values are obtained by solving equation of state P(μ,E) related to the material (see /EOS).

Input requires Young's or the elastic modulus, *E*, and Poisson's ratio, υ. These quantities are used only for the deviatoric part. The plasticity material parameters are:

A = Yield Stress

B = Hardening Modulus

n = Hardening Exponent

σ_{max} = Maximum flow stress

ε_{max} = Plastic strain at rupture

A pressure cut off, p_{min}, can be given to limit the pressure in tension. The pressure cut off must be lower or equal to zero. Figure 9.5.1 shows a typical curve of the hydrodynamic pressure.

Figure 9.5.1 Hydrodynamic Pressure Relationship

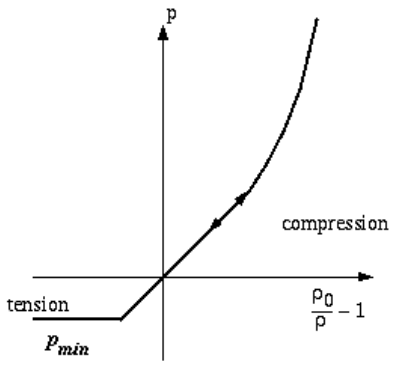

9.5.4 Steinberg-Guinan material (law 49)

This law defines as elastic-plastic material with thermal softening. When material approaches meting point, the yield strength and shear modulus reduces to zero. The melting energy is defined as:

$$E_m = E_c + \rho c_p T_m \qquad \text{EQ. 9.5.4.1}$$

Where, E_c is cold compression energy and T_m melting temperature is supposed to be constant. If the internal energy E is less than E_m, the shear modulus and the yield strength are defined by the following equations:

$$G = G_0\left[1 + b_1 pV^{1/3} - h\left(T - T_0\right)\right] e^{-\frac{fE}{E - E_m}} \qquad \text{EQ. 9.5.4.2}$$

$$\sigma_y = \sigma_0'\left[1 + b_2 pV^{1/3} - h\left(T - T_0\right)\right] e^{-\frac{fE}{E - E_m}} \qquad \text{EQ. 9.5.4.3}$$

Where b_1, b_2, h and f are the material parameters. σ_0' is given by a hardening rule:

$$\sigma_0' = \sigma_0\left[1 + \beta\varepsilon_p\right]^n \qquad \text{EQ. 9.5.4.4}$$

The value of σ_0' is limited by $\sigma_{\max}$.

The material pressure p is obtained by solving equation of state P(μ,E) related to the material (/EOS) as in law 3.

9.6 Void Material (law 0)

This material can be used to define elements to act as a void, or empty space.

9.7 Failure model

In addition to the possibility to define user's material failure models, RADIOSS integrates several failure models. These models use generally a global notion of cumulative damage to compute failure. They are mostly independent to constitutive law and the hardening model and can be linked to several available material laws. A compatibility table is given in the RADIOSS Reference Guide. The following table gives a brief description of available models.

Table 9.0.2 FAILURE MODEL DESCRIPTION

Failure Model	Type	Description
CHANG	Chang-Chang model	Failure criteria for composites
CONNECT	Failure	Normal and Tangential failure model
EMC	Extended Mohr Coulomb failure model	Failure dependent on effective plastic strain
ENERGY	Energy isotrop	Specific energy
FLD	Forming limit diagram	Introduction of the experimental failure data in the simulation
HASHIN[128][129]	Composite model	Hashin model
JOHNSON	Ductile failure model	Cumulative damage law based on the plastic strain accumulation
LAD_DAMA	Composite delamination	Ladeveze delamination model
NXT	NXT failure criteria	Similar to FLD, but based on stresses
PUCK	Composite model	Puck model
SNCONNECT	Failure	Failure criteria for plastic strain

Failure Model	Type	Description
SPALLING	Ductile + Spalling	Johnson Cook failure model with Spalling effect
TAB1	Strain failure model	Based on damage accumulation using user-defined functions
TBUTCHER	Failure due to fatigue	Fracture appears when time integration of a stress expression becomes true
TENSSTRAIN	Traction	Strain failure
WIERZBICKI	Ductile material	3-D failure model for solid and shells
WILKINS	Ductile Failure model	Cumulative damage law

9.7.1 Johnson-Cook failure model

High-rate tests in both compression and tension using the Hopkinson bar generally demonstrate the stress-strain response is highly isotropic for a large scale of metallic materials. The Johnson-Cook model is very popular as it includes a simple form of the constitutive equations. In addition, it also has a cumulative damage law that can be accesses failure:

$$d = \sum \frac{\Delta \varepsilon}{\varepsilon_f} \qquad \text{EQ. 9.7.1.1}$$

with: $\varepsilon_f = \left[D_1 + D_2 \exp\left(D_3 \sigma^*\right)\right]\left[1 + D_4 \ln\left(\frac{\dot{\varepsilon}}{\dot{\varepsilon}_0}\right)\right]\left[1 + D_5 T^*\right]$ EQ. 9.7.1.2

Where $\Delta\varepsilon$ is the increment of plastic strain during a loading increment, $\sigma^* = \frac{\sigma_m}{\sigma_{VM}}$ the normalized mean stress and the parameters D_i the material constants. Failure is assumed to occur when d=1.

9.7.2 Wilkins failure criteria

An early continuum model for void nucleation is presented in [98]. The model proposes that the decohesion (failure) stress σ_c is a critical combination of the hydrostatic stress σ_m and the equivalent von Mises stress σ_{VM} :

$$\sigma_c = \sigma_m + \sigma_{VM} \qquad \text{EQ. 9.7.2.1}$$

In a similar approach, a failure criteria based on a cumulative equivalent plastic strain was proposed by Wilkins. Two weight functions are introduced to control the combination of damage due to the hydrostatic and deviatoric loading components. The failure is assumed when the cumulative reaches a critical value d_c. The cumulative damage is obtained by:

$$d_c = \int_0^t W_1 W_2 \, d\varepsilon_p \approx \sum_{i=1}^{n} W_1 W_2 \, \Delta\varepsilon_p^i \qquad \text{EQ. 9.7.2.2}$$

with: $W_1 = \left(\frac{1}{1+aP}\right)^{\alpha}$, $P = \frac{1}{3}\sum_{j=1}^{3} \sigma_{jj}$, $W_2 = \left(2 - A\right)^{\beta}$, $A = Max\left(\frac{s_2}{s_3}, \frac{s_2}{s_1}\right)$, $s_1 \geq s_2 \geq s_3$

where:

$\Delta\varepsilon_p$ is an increment of the equivalent plastic strain,

W_1 is the hydrostatic pressure weighting factor,

W_2 is the deviatoric weighting factor,

s_i are the deviatoric principal stresses,

a, α and β are the material constants.

9.7.3 Tuler-Butcher failure criteria

A solid may break owning to fatigue due to Tuler-Butcher criteria [99]:

$$d = \int_0^t (\sigma - \sigma_r)^{\lambda} dt \qquad \text{EQ. 9.7.3.1}$$

Where σ_r is the fracture stress, σ is the maximum principal stress, λ is material constant, *t* is the time when solid cracks and *d* is another material constant called damage integral.

9.7.4 Forming Limit Diagram for failure (FLD)

In this method the failure zone is defined in the plane of principal strains (Fig. 9.7.1). The method usable for shell elements allows introducing the experimental results in the simulation.

Figure 9.7.1 Generic forming limit diagram (FLD)

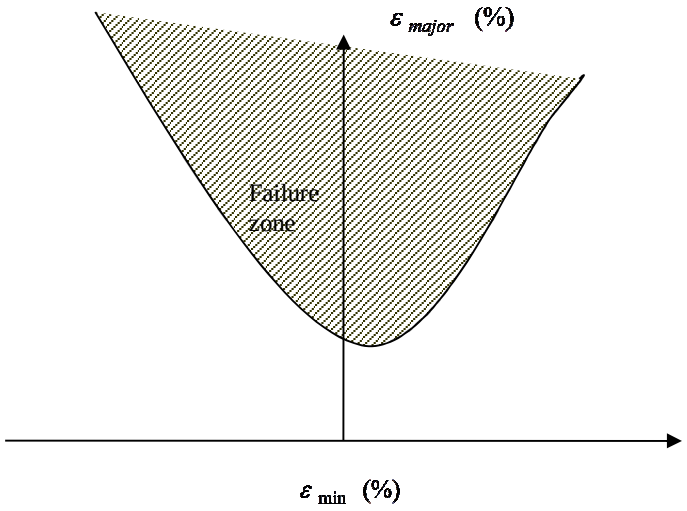

9.7.5 Spalling with Johnson-Cook Failure model

In this model, the Johnson-Cook failure model is combined to a Spalling model where we take into account the spall of the material when the pressure achieves a minimum value p_{min}. The deviatoric stresses are set to zero for compressive pressure. If the hydrostatic tension is computed, then the pressure is set to zero. The failure equations are the same as in Johnson-Cook model.

9.7.6 Bao-Xue-Wierzbicki Failure model

Bao-Xue-Wierzbicki model [115] represents a 3-D fracture criterion which can be expressed by the following equations:

$$\bar{\varepsilon}_f^n = \bar{\varepsilon}_{\max}^n - \left[\bar{\varepsilon}_{\max}^n - \bar{\varepsilon}_{\min}^n\right]\left(1-\xi^m\right)^{1/m} \qquad \text{EQ. 9.7.6.1}$$

$$\bar{\varepsilon}_{\max} = C_1 e^{-C_2\eta}$$

$$\bar{\varepsilon}_{\min} = C_3 e^{-C_4\eta}$$

Where C_1, C_2, C_3, C_4, γ and m are the material constants, n the hardening parameter and η and ξ are defined as following:

- for solids: $\eta = \dfrac{\sigma_m}{\sigma_{VM}}$; $\xi = \dfrac{27}{2}\dfrac{J_3}{{\sigma_{VM}}^3}$
- for shells: $\eta = \dfrac{\sigma_m}{\sigma_{VM}}$; $\xi = -\dfrac{27}{2}\eta\left(\eta^2 - \dfrac{1}{3}\right)$

Where, σ_m is the hydrostatic stress, σ_{VM} is the von Mises stress, and $J_3 = s_1 s_2 s_3$ are third invariant of principal deviatoric stresses.

Figure 9.7.2 Graphical representation of Bao-Xue-Wierzbicki failure criteria

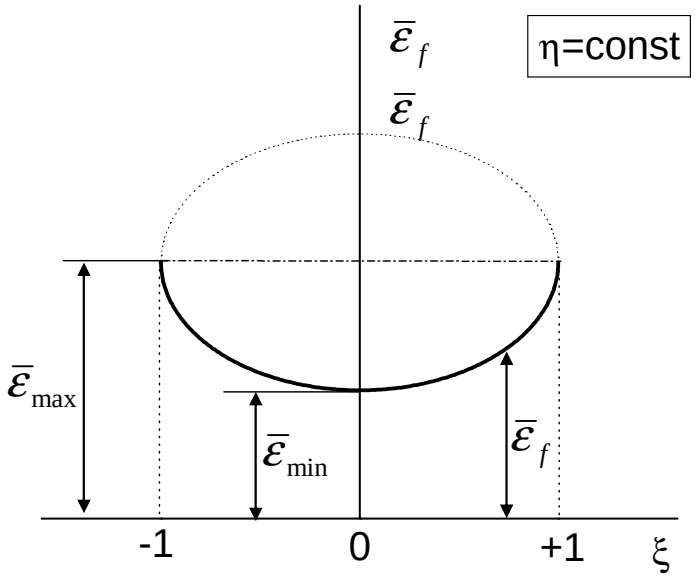

9.7.7 Strain Failure Model

This failure model can be compared to the damage model in law 27. When the principal tension strain ε_1 reaches ε_{t1}, a damage factor *D* is applied to reduce the stress as shown in Fig. 9.7.3. The element is ruptured when D=1. In addition, the maximum strains ε_{t1} and ε_{t2} may depend on the strain rate by defining a scale function.

Figure 9.7.3 Strain failure model

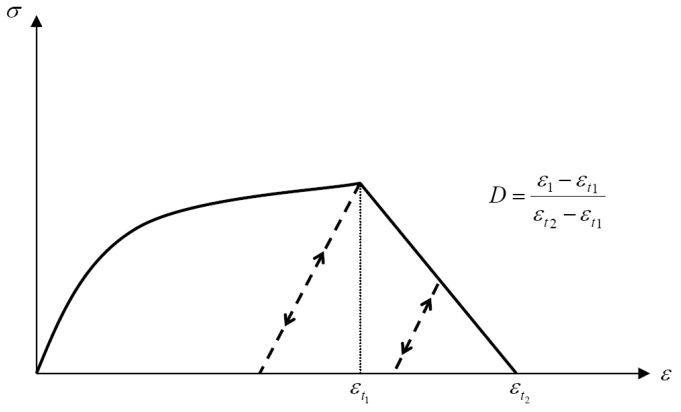

9.7.8 Specific Energy Failure Model

When the energy per unit volume achieves the value E_1, then the damage factor D is introduced to reduce the stress. For the limit value E_2, the element is ruptured. In addition, the energy values E_1 and E_2 may depend on the strain rate by defining a scale function.

Figure 9.7.4 Strain failure model

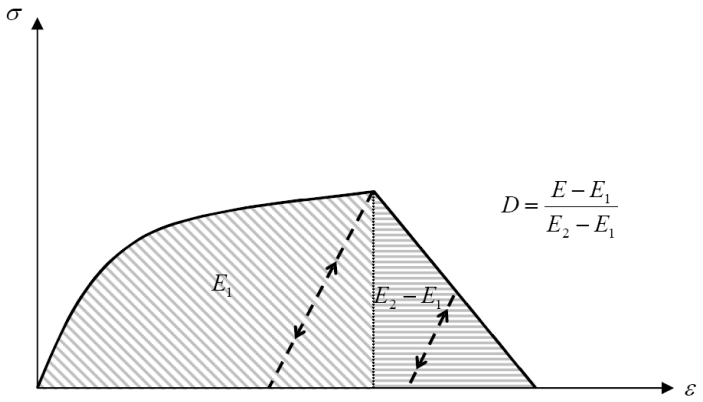

9.7.9 XFEM Crack Initialization Failure Model

This failure model is available for Shell only.

The failure mode criteria are written as:

For ductile materials, the cumulative damage parameter is:

$$D = \int_0^t (\sigma - \sigma_r)^{\lambda} \, dt$$

Where,

σ_r is the fracture stress

σ is the maximum principal stress

λ is the material constant

t is the time when shell cracks for initiation of a new crack within the structure

D is another material constant called damage integral

For brittle materials, the damage parameter is:

$$\dot{D} = \frac{1}{K}(\sigma - \sigma_r)^a$$

$\sigma_r = \sigma_0 (1 - D)^b$

$$D = D + \dot{D}\,\Delta t$$